

Electronic Supplementary Information

Catalytic Enantioselective Hosomi–Sakurai Reaction of α -Ketoesters Promoted by Chiral Copper(II) Complexes

Yutaro Niwa, Mayu Miyake, Ichiro Hayakawa, Akira Sakakura*

*Graduate School of Natural Science and Technology, Okayama University, 3-1-1, Tsushima-naka, Kita-ku, Okayama,
Japan*

Table of Contents

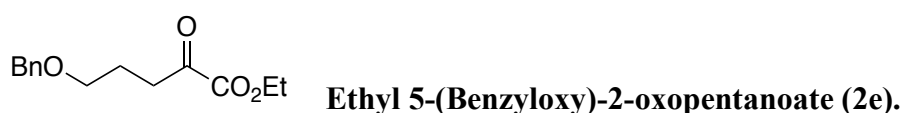
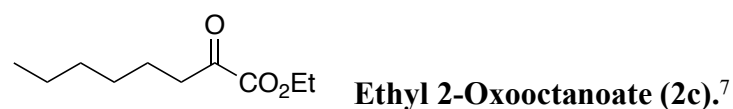
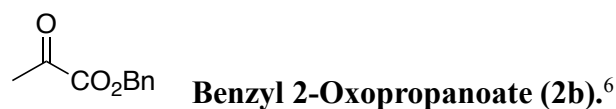
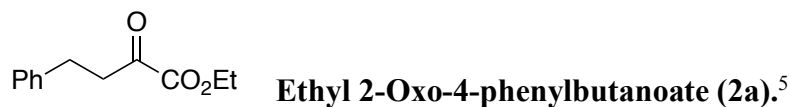
Table of Contents	S1
General Methods	S2
Synthesis of α -Keto Esters 2	S3–S4
Typical Procedure of Nucleophilic Addition of Allyltrimethylsilane	S5–S8
Typical Procedure of Nucleophilic Addition of Methallyltrimethylsilane	S9–S15
Examination Solvents for the Nucleophilic Addition of Allyltrimethylsilane with 2a	S16
Catalytic Activities of Chiral Copper(II) Complexes in the Enantioselective Addition of 2a with Methallyltrimethylsilane	S17
Transformation of 3d and 4d	S18–S19
Proposed Mechanism of Generation of Silyl Ether 3	S19
References	S20
¹ H and ¹³ C NMR Charts of New Compounds	S21–S66
Chiral HPLC Charts of New Compounds	S67–S88

General Methods.

IR spectra were recorded on a SHIMADZU FTIR-8400 spectrometer. ^1H NMR spectra were measured on a Varian NMR System 600 PS600 spectrometer (600 MHz), a Varian 400-MR ASW spectrometer (400 MHz), and a Varian Mercury-300 spectrometer (300 MHz) at ambient temperature. Data were recorded as follows: chemical shift in ppm from the solvent resonance employed as the internal standard (CHCl_3 at 7.26 ppm) on the δ scale, multiplicity (s = singlet; d = doublet; t = triplet; m = multiplet), coupling constant (Hz), and integration. ^{13}C NMR spectra were measured on a Varian NMR System 600 PS600 spectrometer (150 MHz) and a Varian 400-MR ASW spectrometer (100 MHz) at ambient temperature. Chemical shifts were recorded in ppm from the solvent resonance employed as the internal standard (CDCl_3 at 77.0 ppm). Analytical HPLC was performed on a JASCO model PU-980 intelligent HPLC pump, a JASCO model UV-970 intelligent UV-vis detector (254 nm), and a JASCO model MD-2018 Plus photodiode array detector using a column of Daicel CHIRALPAK AD-H (4.6×250 mm), YMC CHIRAL Amylose-SA (4.6×250 mm), and YMC CHIRAL Cellose-SB (4.6×250 mm). Optical rotations were measured on a digital polarimeter Horiba SEPA-300 using a $3.5 \text{ mm} \times 0.5 \text{ dm}$ pyrex cell. For TLC analysis, Merck precoated TLC plates (silica gel 60 F₂₅₄ 0.25 mm) were used. For preparative column chromatography, Kanto Chemical Co., Inc. silica gel 60 N (spherical, neutral), Fuji Silysia Chemical PSQ100B, and Kanto Chemical Co., Inc. silica gel 60 (spherical) NH_2 were used. High resolution mass spectral analysis (HRMS) was measured on a JEOL JMS-700 Mstation (FAB) and a Bruker micrOTOF II (ESI) at Chemical Instrument Facility, Okayama University.

Dry tetrahydrofuran, dichloromethane, isopropyl alcohol, and acetonitrile were purchased from Kanto Chemical Co., Inc. or Wako Pure Chemical Industries Ltd. as the “anhydrous” and stored under nitrogen. Nitroethane was freshly distilled from calcium hydride. Allyltrimethylsilanes (Aldrich or TCI), methallyltrimethylsilane (TCI), allyltriisopropylsilane (TCI), copper(II) triflate [$\text{Cu}(\text{OTf})_2$] (Aldrich), (*S,S*)-*t*-Bu-bis(oxazoline) (**1c**, TCI), methyl 2-oxo-2-phenylacetate (**2h**, TCI) and other materials were obtained from commercial supplies and used without further purification. Copper(II) trifluoromethanesulfonimide [$\text{Cu}(\text{NTf}_2)_2$],¹ **1a**,² **1b**,² **1d**,³ **1e**,⁴ and **1f**⁴ were reported previously.

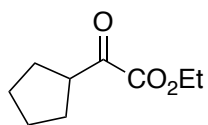
Synthesis of α -Keto Esters 2.



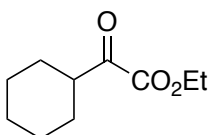
An oven-dried two-necked flask was charged with magnesium turnings (191 mg, 7.84 mmol). The flask was heated by heat gun under reduced pressure for 15 min with vigorous stirring. The resultant activated magnesium was suspended in THF (3.0 mL). To a stirred suspension of activated magnesium in THF were added 3-bromotoluene (0.67 mL, 5.5 mmol) in THF (3.0 mL) and a trace amount of iodine at ambient temperature. The mixture was stirred at ambient temperature for 30 min to give a THF solution of Grignard reagent.

To a stirred solution of diethyl oxalate (0.80 mL, 5.9 mmol) in THF (18 mL) was slowly added above-mentioned THF solution of Grignard reagent via syringe at -78 °C. After being stirred -78 °C for 1.5 h, the mixture was warmed to 0 °C and diluted with saturated aqueous NH_4Cl (10 mL). The resultant mixture was extracted with Et_2O (3×10 mL). The combined extracts were dried (MgSO_4), filtered, and concentrated. The crude product was purified by column chromatography on silica gel (35 g, hexane– EtOAc 10 : 1) to give **2e** (606 mg, 41%) as a yellow oil.

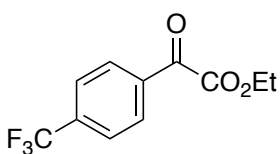
IR (film) 2932, 2862, 1724, 1452, 1273, 1103 cm^{-1} ; ^1H NMR (400 MHz, CDCl_3) δ 7.36–7.27 (m, 5H), 4.46 (s, 2H), 4.27 (q, $J = 7.2$ Hz, 2H), 3.51 (t, $J = 6.0$ Hz, 2H), 2.95 (t, $J = 7.2$ Hz, 2H), 2.02–1.97 (m, 2H), (t, $J = 7.2$ Hz, 3H); ^{13}C NMR (150 MHz, CDCl_3) δ 194.0, 167.8, 138.0, 128.2 (2C), 127.4 (2C), 127.4, 72.6, 68.7, 62.1, 36.1, 23.8, 13.8; HRMS (ESI) calcd for $\text{C}_{14}\text{H}_{18}\text{NaO}_4$ $[\text{M}+\text{Na}]^+$ 273.1103, found 273.1109.



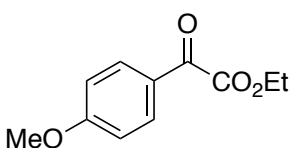
Ethyl 2-Cyclopentyl-2-oxoacetate (2f).⁹



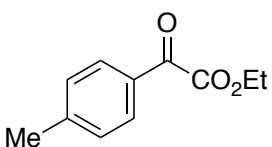
Ethyl 2-Cyclohexyl-2-oxoacetate (2g).¹⁰



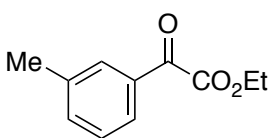
Ethyl 2-Oxo-2-(4-(trifluoromethyl)phenyl)acetate (2i).¹¹



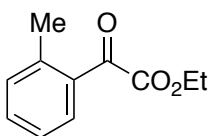
Ethyl 2-(4-Methoxyphenyl)-2-oxoacetate (2j).¹¹



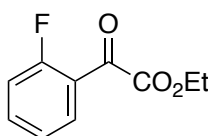
Ethyl 2-Oxo-2-(*p*-tolyl)acetate (2k).¹²



Ethyl 2-Oxo-2-(*m*-tolyl)acetate (2l).¹⁰



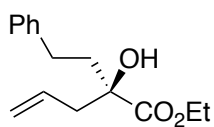
Ethyl 2-Oxo-2-(*o*-tolyl)acetate (2m).¹²



Ethyl 2-(2-Fluorophenyl)-2-oxoacetate (2n).¹³

Typical Procedure of Nucleophilic Addition of Allyltrimethylsilane with α -Keto Ester **2a** promoted by **1a**•Cu(NTf₂)₂ (Table 1, entry 1).

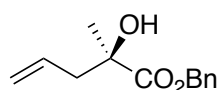
Copper(II) trifluoromethanesulfonimide (6.2 mg, 0.010 mmol) and ligand **1a** (4.2 mg, 0.010 mmol) were combined in an argon atmosphere glove box. The sealed flask was then removed from the box and connected to a nitrogen balloon. Anhydrous EtNO₂ (1.0 mL) was added, whereupon a blue solution was formed within 5 minutes. The solution was stirred for 2 h at ambient temperature. α -Keto ester **2a** (41.2 mg, 0.200 mmol) was added at ambient temperature. After allyltrimethylsilane (0.10 mL, 0.30 mmol) was added to the mixture, the resulting solution was stirred at ambient temperature for 2 h. The reaction was quenched by the addition of saturated aqueous NaHCO₃ (1 mL), and the mixture was extracted with Et₂O (3 × 10 mL). The combined extracts were dried (MgSO₄) and concentrated. After the resultant residue was dissolved in THF (2 mL), the mixture was cooled to 0 °C. Tetrabutylammonium fluoride (1.0 M solution in THF, 0.20 mL, 0.20 mmol) was added to the mixture. After being stirred at 0 °C for 1 h, the reaction mixture was diluted with saturated aqueous NH₄Cl (1 mL) and extracted with EtOAc (3 × 10 mL). The combined extracts were dried (MgSO₄) and concentrated. The resultant residue was purified by column chromatography on silica gel using hexane–EtOAc (20:1) to give **3a** (78% yield, 74% ee) as a colorless oil. The enantiomeric excess (ee) was determined through chiral HPLC analysis.



Ethyl (*R*)-2-Hydroxy-2-phenethylpent-4-enoate (3a**).** Colorless oil; [α]_D²⁰

–25.9 (*c* 0.92, CHCl₃) (74% ee); IR (film) 3522, 1730, 1224, 1182, 920 cm⁻¹; ¹H NMR (400 MHz, CDCl₃) δ 7.30–7.24 (m, 2H), 7.20–7.15 (m, 3H), 5.78 (tdd, *J* = 7.2, 11.2, 16.0 Hz, 1H), 5.13–5.08 (m, 2H), 4.24–4.14 (m, 2H), 3.32 (s, 1H), 2.81 (ddd, *J* = 5.2, 11.2, 13.2 Hz, 1H), 2.52–2.39 (m, 3H), 2.12–1.95 (m, 2H), 1.29 (t, *J* = 6.8 Hz, 3H); ¹³C NMR (100 MHz, CDCl₃) δ 175.9, 141.6, 132.2, 128.4 (3C), 128.3, 125.9, 119.0, 76.8, 61.9, 44.1, 40.5, 30.0, 14.3; HRMS (FAB) calcd for C₁₅H₂₁O₃ [M+H]⁺ 249.1491, found 249.1508.

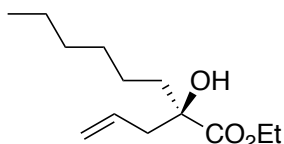
Enantiomeric excess was determined by chiral HPLC analysis: YMC CHIRAL Amylose-SA; hexane–*i*-PrOH 100:1; flow rate 0.3 mL/min; *t*_R = 25.5 min (major enantiomer), 23.4 min (minor enantiomer); λ = 215 nm. Absolute configuration (*R*) was assigned by analogy with **3b**.



Benzyl (*R*)-2-Hydroxy-2-methylpent-4-enoate (3b**).** Colorless oil; [α]_D¹⁹

–3.9 (*c* 1.04, MeOH) (65% ee); IR (film) 3522, 1732, 1456, 1267, 1217, 1166, 920 cm^{-1} ; ^1H NMR (400 MHz, CDCl_3) δ 7.42–7.32 (m, 5H), 5.73 (tdd, $J = 7.2, 10.0, 17.2$ Hz, 1H), 5.19 (s, 2H), 5.08 (m, 1H), 5.03 (m, 1H), 3.13 (s, 1H), 2.51 (dd, $J = 7.2, 13.6$ Hz, 1H), 2.39 (tdd, $J = 1.2, 7.2, 13.6$ Hz, 1H), 1.44 (s, 3H); ^{13}C NMR (100 MHz, CDCl_3) δ 176.3, 135.3, 132.2, 128.6 (2C), 128.5, 128.3 (2C), 119.2, 74.4, 67.5, 44.6, 25.5; HRMS (FAB) calcd for $\text{C}_{13}\text{H}_{17}\text{O}_3$ $[\text{M}+\text{H}]^+$ 221.1178, found 221.1182.

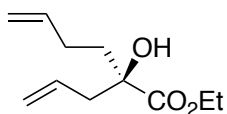
Enantiomeric excess was determined by chiral HPLC analysis: YMC CHIRAL Amylose-SA; hexane–*i*-PrOH 100:1; flow rate 0.3 mL/min; $t_{\text{R}} = 46.6$ min (major enantiomer), $t_{\text{R}} = 50.7$ min (minor enantiomer); $\lambda = 215$ nm. Absolute configuration was assigned to be *R* from the sign of measured optical rotation: Lit¹⁴ 95% ee (*S* isomer), $[\alpha]_{\text{D}}^{28} +5.8$ (*c* 1.09, EtOH).



Ethyl (*R*)-2-Allyl-2-hydroxyoctanoate (3c). Colorless oil; $[\alpha]_{\text{D}}^{25} -9.3$ (*c*

1.13, CHCl_3) (74% ee); IR (film) 3524, 2957, 2928, 1730, 1557, 1223 cm^{-1} ; ^1H NMR (600 MHz, CDCl_3) δ 5.77 (m, 1H), 5.10 (m, 1H), 5.08 (m, 1H), 4.23 (dq, $J = 2.4, 7.2$ Hz, 2H), 3.19 (s, 1H), 2.46 (q, $J = 7.2$ Hz, 1H), 2.40 (ddt, $J = 1.2, 7.2, 13.8$ Hz, 1H), 1.74 (ddd, $J = 4.8, 12.0, 13.8$ Hz, 1H), 1.64 (ddd, $J = 4.8, 12.0, 13.8$ Hz, 1H), 1.47 (m, 1H), 1.29 (t, $J = 7.2$ Hz, 3H), 1.28–1.24 (m, 6H), 1.07 (m, 1H), 0.87 (t, $J = 7.2$ Hz, 3H); ^{13}C NMR (150 MHz, CDCl_3) δ 176.2, 132.5, 118.7, 77.2, 61.8, 43.9, 38.8, 31.6, 29.3, 23.4, 22.5, 14.3, 14.0; HRMS (ESI) calcd for $\text{C}_{13}\text{H}_{24}\text{NaO}_3$ $[\text{M}+\text{Na}]^+$ 251.16231, found 251.1619.

Enantiomeric excess was determined by chiral HPLC analysis after the transformation of **3c** into the corresponding 3,5-dinitrobenzoate: YMC CHIRAL Cellulose-SB; hexane–*i*-PrOH 9:1; flow rate 1.0 mL/min; $t_{\text{R}} = 9.4$ min (major enantiomer), 26.6 min (minor enantiomer); $\lambda = 254$ nm. Absolute configuration (*R*) was assigned by analogy with **3b**.

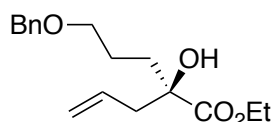


Ethyl (*R*)-2-Allyl-2-hydroxyhex-5-enoate (3d). Colorless oil; $[\alpha]_{\text{D}}^{25} -9.4$ (*c*

0.53, CHCl_3) (74% ee); IR (film) 3624, 3078, 2980, 1730, 1641, 1447, 1223 cm^{-1} ; ^1H NMR (400 MHz, CDCl_3) δ 5.83–5.71 (m, 2H), 5.12 (m, 1H), 5.08 (m, 1H), 5.01 (dq, $J = 1.6, 17.2$ Hz, 1H),

4.94 (m, 1H), 4.23 (dq, $J = 2.4, 7.2$ Hz, 2H), 3.24, (s, 1H), 2.50–2.39 (m, 2H), 2.23 (m, 1H), 1.90 (m, 1H), 1.86–1.73 (m, 2H), 2.30 (t, $J = 7.2$ Hz, 3H); ^{13}C NMR (150 MHz, CDCl_3) δ 175.9, 137.9, 132.3, 118.9, 114.8, 76.8, 61.8, 44.0, 37.9, 27.9, 14.3; HRMS (ESI) calcd for $\text{C}_{11}\text{H}_{18}\text{NaO}_3$ $[\text{M}+\text{Na}]^+$ 221.1154, found 221.1144.

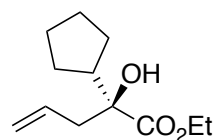
Enantiomeric excess was determined by chiral HPLC analysis after the transformation of **3d** into the corresponding 3,5-dinitrobenzoate: YMC CHIRAL Cellulose-SB; hexane-*i*-PrOH 20:1; flow rate 1.0 mL/min; $t_{\text{R}} = 23.3$ min (major enantiomer), $t_{\text{R}} = 40.8$ min (minor enantiomer); $\lambda = 254$ nm. Absolute configuration (*R*) was assigned by analogy with **3b**.



Ethyl (*R*)-2-(3-(Benzyloxy)propyl)-2-hydroxypent-4-enoate (3e).

Colorless oil; $[\alpha]_{\text{D}}^{25} -11.5$ (c 0.64, CHCl_3) (73% ee); IR (film) 3524, 2932, 2859, 1728, 1225, 1098 cm^{-1} ; ^1H NMR (400 MHz, CDCl_3) δ 7.36–7.26 (m, 5H), 5.77 (m, 1H), 5.12–5.07 (m, 2H), 4.49 (s, 2H), 4.25–4.18 (m, 2H), 3.49–3.45 (m, 2H), 2.51–2.36 (m, 2H), 1.91 (m, 1H), 1.79–1.70 (m, 2H), 1.51 (m, 1H), 1.28 (t, $J = 7.2$ Hz, 3H). A signals due to one proton (OH) was not observed; ^{13}C NMR (100 MHz, CDCl_3) δ 175.9, 138.3, 132.4, 128.3 (2C), 127.5 (2C), 127.5, 118.8, 76.9, 72.7, 70.1, 61.8, 43.9, 35.6, 23.9, 14.3; HRMS (ESI) calcd for $\text{C}_{17}\text{H}_{24}\text{NaO}_4$ $[\text{M}+\text{Na}]^+$ 315.1572, found 315.1570.

Enantiomeric excess was determined by chiral HPLC analysis: YMC CHIRAL Amylose-SA; hexane-*i*-PrOH 100:1; flow rate 0.3 mL/min; $t_{\text{R}} = 27.1$ min (major enantiomer), $t_{\text{R}} = 29.4$ min (minor enantiomer), $\lambda = 215$ nm. Absolute configuration (*R*) was assigned by analogy with **3b**.

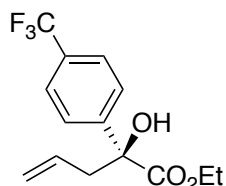


Ethyl (*S*)-2-Cyclopentyl-2-hydroxypent-4-enoate (3f).

Colorless oil; $[\alpha]_{\text{D}}^{26} -22.7$ (c 0.95, CHCl_3) (69% ee); IR (film) 3524, 2957, 2870, 1726, 1223, 1179 cm^{-1} ; ^1H NMR (600 MHz, CDCl_3) δ 5.76 (m, 1H), 5.10–5.06 (m, 2H), 4.22 (q, $J = 7.2$ Hz, 2H), 2.50–2.41 (m, 2H), 2.23 (m, 1H), 1.74–1.35 (m, 8H), 1.29 (t, $J = 7.2$ Hz, 3H). A signals due to one proton (OH) was not observed; ^{13}C NMR (150 MHz, CDCl_3) δ 176.4, 133.0, 118.4, 78.2, 61.7, 46.9, 42.7, 26.6, 26.0, 25.7, 25.6, 14.3; HRMS (ESI) calcd for $\text{C}_{12}\text{H}_{20}\text{NaO}_3$ $[\text{M}+\text{Na}]^+$ 235.1310, found 235.1315.

Enantiomeric excess was determined by chiral HPLC analysis after the transformation of **3f** into the

corresponding 3,5-dinitrobenzoate: YMC CHIRAL Cellulose-SB; hexane-*i*-PrOH 9:1; flow rate 1.0 mL/min; $t_R = 10.5$ min (major enantiomer), $t_R = 45.1$ min (minor enantiomer); $\lambda = 254$ nm. Absolute configuration (*S*) was assigned by analogy with methyl (*R*)-2-cyclohexyl-2-hydroxypent-4-enoate {91% ee, $[\alpha]^{25}_D +8.3$ (*c* 1.2, CHCl₃)}.¹⁵



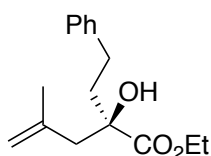
Benzyl (*S*)-2-Hydroxy-2-(4-(trifluoromethyl)phenyl)pent-4-enoate (3i**).**

Colorless oil; $[\alpha]^{20}_D +16.1$ (*c* 1.30, CHCl₃) (79% ee); IR (film) 3508, 1730, 1618, 1411, 1329, 1230, 1166, 1126, 1070 cm⁻¹; ¹H NMR (400 MHz, CDCl₃) δ 7.76 (d, $J = 8.8$ Hz, 2H), 7.61 (d, $J = 8.8$ Hz, 2H), 5.77 (dddd, $J = 6.8, 7.6, 10.4, 17.2$ Hz, 1H), 5.21–5.13 (m, 2H), 4.29 (qd, $J = 7.2, 10.8$ Hz, 1H), 4.21 (qd, $J = 7.2, 10.8$ Hz, 1H), 3.84 (s, 1H), 2.96 (dd, $J = 7.6, 14.0$ Hz, 1H), 2.74 (ddt, $J = 1.2, 6.8, 14.0$ Hz, 1H), 1.28 (t, $J = 7.2$ Hz, 3H); ¹³C NMR (100 MHz, CDCl₃) δ 174.0, 145.2, 131.7, 130.0 (q, ² $J_{CF} = 32.3$ Hz), 126.2 (2C), 125.2 (q, ³ $J_{CF} = 3.8$ Hz, 2C), 124.1 (q, ¹ $J_{CF} = 270.7$ Hz), 119.8, 77.7, 62.8, 44.3, 14.0; HRMS (ESI) calcd for C₁₄H₁₅F₃O₃Na [M+Na]⁺ 311.0871, found 311.0870.

Enantiomeric excess was determined by chiral HPLC analysis: Daicel CHIRALPAK AD-H; hexane-*i*-PrOH 100:1; flow rate 0.3 mL/min; $t_R = 27.5$ min (major enantiomer), $t_R = 29.8$ min (minor enantiomer); $\lambda = 254$ nm). Absolute configuration (*S*) was assigned by analogy with methyl (*S*)-2-hydroxy-2-phenylhex-5-enoate {95% ee, $[\alpha]^{24}_D +78.5$ (*c* 1.0, CHCl₃)}.¹⁶

Typical Procedure of Nucleophilic Addition of Methallyltrimethylsilane with α -Keto Ester **2a** promoted by **1a**•Cu(NTf₂)₂ (Table 3, entry 1).

Copper(II) trifluoromethanesulfonimide (6.2 mg, 0.010 mmol) and ligand **1a** (4.2 mg, 0.010 mmol) were combined in an argon atmosphere glove box. The sealed flask was then removed from the box and connected to a nitrogen balloon. Anhydrous EtNO₂ (1.0 mL) was added, whereupon a blue solution was formed within 5 minutes. The solution was stirred for 2 h at ambient temperature. After α -keto ester **2a** (41.2 mg, 0.200 mmol) was added at ambient temperature, the solution was cooled to -30 °C. To this mixture was added methallyltrimethylsilane (0.10 mL, 0.60 mmol), and the resulting solution was stirred at -30 °C for 1 h, and then at ambient temperature for 2 h. The reaction was quenched by the addition of saturated aqueous NaHCO₃ (1 mL), extracted with Et₂O (3 × 10 mL). The combined extracts were dried (MgSO₄) and concentrated. The residue was dissolved in THF (2 mL). After the solution was cooled to 0 °C, tetrabutylammonium fluoride (1.0 M solution in THF, 0.20 mL, 0.20 mmol) was added to the mixture. After being stirred at 0 °C for 1 h, the reaction mixture was diluted with saturated aqueous NH₄Cl (1 mL) and extracted with EtOAc (3 × 10 mL). The combined extracts were dried (MgSO₄) and concentrated. The resultant residue was purified by column chromatography on silica gel using hexane–EtOAc (20:1) to give **4a** (90% yield, 96% ee) as a colorless oil. The enantiomeric excess (ee) was determined through chiral HPLC analysis.

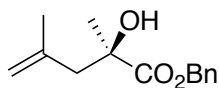


Ethyl (*R*)-2-Hydroxy-4-methyl-2-phenethylpent-4-enoate (4a**).** Colorless

oil; $[\alpha]_D^{20}$ +19.7 (*c* 1.31, CHCl₃) (96% ee); IR (film) 3520, 1728, 1454, 1373, 1253, 1207, 1114, 1060, 1020 cm⁻¹; ¹H NMR (400 MHz, CDCl₃) δ 7.65–7.29 (m, 2H), 7.20–7.16 (m, 3H), 4.88 (qd, *J* = 1.2, 1.6 Hz, 1H), 4.75 (qd, *J* = 0.8, 1.6 Hz, 1H), 4.21 (qd, *J* = 7.2, 10.8 Hz, 1H), 4.18 (qd, *J* = 7.2, 10.8 Hz, 1H), 3.35 (s, 1H), 2.83 (ddd, *J* = 5.2, 12.0, 13.6 Hz, 1H), 2.53 (d, *J* = 13.6 Hz, 1H), 2.420 (dd, *J* = 0.8, 13.6 Hz, 1H), 2.419 (ddd, *J* = 5.2, 12.0, 13.6 Hz, 1H), 2.10 (dddd, *J* = 0.8, 5.2, 12.0, 13.6 Hz, 1H), 1.99 (ddd, *J* = 5.2, 12.0, 13.6 Hz, 1H), 1.77 (dd, *J* = 0.8, 1.2 Hz, 3H), 1.31 (t, *J* = 7.2 Hz, 3H); ¹³C NMR (100 MHz, CDCl₃) δ 176.1, 141.6, 141.1, 128.40 (2C), 128.35 (2C), 125.9, 115.0, 77.3, 61.8, 47.3, 41.4, 30.0, 24.0, 14.2; HRMS (FAB) calcd for C₁₆H₂₃O₃ [M+H]⁺ 263.1647, found 263.1660.

Enantiomeric excess was determined by chiral HPLC analysis: YMC CHIRAL Amylose-SA;

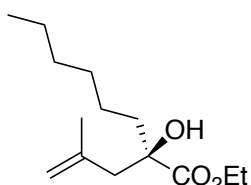
hexane-*i*-PrOH 100:1; flow rate 0.3 mL/min; $t_R = 19.2$ min (major enantiomer), $t_R = 18.4$ min (minor enantiomer), $\lambda = 215$ nm. Absolute configuration (*R*) was assigned by analogy with **3b**.



Benzyl (*R*)-2-Hydroxy-2,4-dimethylpent-4-enoate (4b). Colorless oil;

$[\alpha]_D^{20} +16.1$ (c 1.03, CHCl_3) (94% ee); IR (film) 3526, 1734, 1456, 1375, 1263, 1198, 1111 cm^{-1} ; ^1H NMR (400 MHz, CDCl_3) δ 7.41–7.30 (m, 5H), 5.21 (d, $J = 12.0$ Hz, 1H), 5.13 (d, $J = 12.0$ Hz, 1H), 4.85 (qd, $J = 1.6, 2.4$ Hz, 1H), 4.70 (qd, $J = 1.2, 2.4$ Hz, 1H), 3.14 (s, 1H), 2.54 (d, $J = 14.0$ Hz, 1H), 2.38 (dd, $J = 0.8, 14.0$ Hz, 1H), 1.72 (dd, $J = 1.2, 1.6$ Hz, 3H), 1.45 (s, 3H); ^{13}C NMR (100 MHz, CDCl_3) δ 176.6, 141.1, 135.2, 128.6, 128.6, 128.5, 128.3, 128.3, 115.1, 74.6, 67.5, 47.8, 26.4, 23.8; HRMS (FAB) calcd for $\text{C}_{14}\text{H}_{19}\text{O}_3$ $[\text{M}+\text{H}]^+$ 235.1334, found 235.1346.

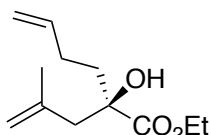
Enantiomeric excess was determined by chiral HPLC analysis: YMC CHIRAL Amylose-SA; hexane-*i*-PrOH 100:1; flow rate 0.3 mL/min; $t_R = 25.2$ min (major enantiomer), $t_R = 23.5$ min (minor enantiomer), $\lambda = 215$ nm. Absolute configuration (*R*) was assigned by analogy with **3b**.



Ethyl (*R*)-2-Hydroxy-2-(2-methylallyl)octanoate (4c). Colorless oil;

$[\alpha]_D^{19} -11.0$ (c 1.03, CHCl_3) (94% ee); IR (film) 3528, 1730, 1456, 1205, 1139, 1097, 1022, 1070 cm^{-1} ; ^1H NMR (400 MHz, CDCl_3) δ 4.85 (qd, $J = 2.0, 2.4$ Hz, 1H), 4.73 (qd, $J = 0.8, 2.4$ Hz, 1H), 4.25 (qd, $J = 7.2, 10.8$ Hz, 1H), 4.19 (qd, $J = 7.2, 10.8$ Hz, 1H), 3.19 (s, 1H), 2.49 (d, $J = 13.6$ Hz, 1H), 2.36 (d, $J = 13.6$ Hz, 1H), 1.75 (m, 1H), 1.75 (s, 3H), 1.63 (ddd, $J = 4.4, 12.0, 13.2$ Hz, 1H), 1.46 (m, 1H), 1.30 (t, $J = 7.2$ Hz, 3H), 1.26–1.22 (m, 6H), 1.04 (m, 1H), 0.87 (t, $J = 7.2$ Hz, 3H); ^{13}C NMR (100 MHz, CDCl_3) δ 176.4, 141.4, 114.7, 77.5, 61.7, 47.2, 39.7, 31.6, 29.3, 24.0, 23.3, 22.5, 14.2, 14.0; HRMS (FAB) m/z $\text{C}_{14}\text{H}_{27}\text{O}_3$ $[\text{M}+\text{H}]^+$ 243.1960, found 243.1962.

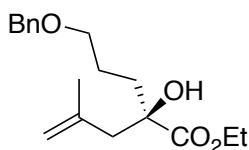
Enantiomeric excess was determined by chiral HPLC analysis: Daicel CHIRALPAK AD-H; hexane-*i*-PrOH 100:1; flow rate 0.3 mL/min; $t_R = 13.8$ min (major enantiomer), $t_R = 14.6$ min (minor enantiomer), $\lambda = 215$ nm. Absolute configuration (*R*) was assigned by analogy with **3b**.



Ethyl (*R*)-2-Hydroxy-2-(2-methylallyl)hex-5-enoate (4d). Colorless oil;

$[\alpha]^{23}_D -98.6$ (*c* 2.09, CHCl_3) (96% ee); IR (film) 3516, 3078, 2980, 1730, 1641, 1449, 1221 cm^{-1} ; ^1H NMR (600 MHz, CDCl_3) δ 5.77 (m, 1H), 4.99 (dq, $J = 1.8, 17.4$ Hz, 1H), 4.93 (m, 1H), 4.86 (dt, $J = 1.8, 4.2$ Hz, 1H), 4.73 (dt, $J = 1.8, 4.2$ Hz, 1H), 4.27–4.17 (m, 2H), 3.24 (s, 1H), 2.50 (dd, $J = 1.2, 13.2$ Hz, 1H), 2.38 (dd, $J = 1.2, 13.2$ Hz, 1H), 2.22 (m, 1H), 1.92–1.84 (m, 2H), 1.75 (m, 1H), 1.75 (dd, $J = 1.2, 1.2$ Hz, 3H), 1.31 (t, $J = 7.2$ Hz, 3H); ^{13}C NMR (150 MHz, CDCl_3) δ 176.1, 141.2, 137.9, 114.8, 114.8, 77.2, 61.7, 47.2, 38.7, 27.9, 24.0, 14.2; HRMS (ESI) calcd for $\text{C}_{12}\text{H}_{20}\text{NaO}_3$ $[\text{M}+\text{Na}]^+$ 235.1310, found 235.1311.

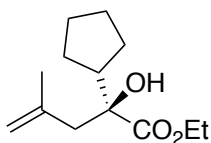
Enantiomeric excess was determined by chiral HPLC analysis: YMC CHIRAL Amylose-SA; hexane–EtOH 200:1; flow rate 0.5 mL/min; $t_R = 10.9$ min (major enantiomer), $t_R = 11.6$ min (minor enantiomer); $\lambda = 215$ nm). Absolute configuration (*R*) was assigned by analogy with **3b**.



Ethyl (*R*)-2-(3-(Benzyloxy)propyl)-2-hydroxy-4-methylpent-4-enoate (4e).

Colorless oil; $[\alpha]^{25}_D -9.55$ (*c* 0.77, CHCl_3) (98% ee); IR (film) 3518, 2959, 2926, 2857, 1728, 1454, 1209, 1099 cm^{-1} ; ^1H NMR (400 MHz, CDCl_3) δ 7.35–7.32 (m, 4H), 7.28 (m, 1H), 4.86 (m, 1H), 4.73 (m, 1H), 4.50 (s, 2H), 4.25–4.17 (m, 2H), 3.49–3.45 (m, 2H), 3.37 (s, 1H), 2.51 (d, $J = 13.8$ Hz, 1H), 2.38 (d, $J = 13.8$ Hz, 1H), 1.90 (ddd, $J = 4.8, 10.2, 13.2$ Hz, 1H), 1.79 (m, 1H), 1.75 (s, 3H), 1.72 (ddd, $J = 4.8, 10.2, 13.2$ Hz, 1H), 1.47 (m, 1H), 1.29 (t, $J = 7.2$ Hz, 3H); ^{13}C NMR (100 MHz, CDCl_3) δ 176.1, 141.3, 138.4, 128.3 (2C), 127.5 (2C), 127.5, 114.8, 77.3, 72.7, 70.1, 61.7, 47.1, 36.5, 24.0, 23.9, 14.2; HRMS (ESI) calcd for $\text{C}_{18}\text{H}_{26}\text{NaO}_4$ $[\text{M}+\text{Na}]^+$ 329.1723, found 329.1721.

Enantiomeric excess was determined by chiral HPLC analysis: YMC CHIRAL Amylose-SA; hexane–*i*-PrOH 9:1; flow rate 0.3 mL/min; $t_R = 22.3$ min (major enantiomer), $t_R = 24.2$ min (minor enantiomer), $\lambda = 254$ nm. Absolute configuration (*R*) was assigned by analogy with **3b**.

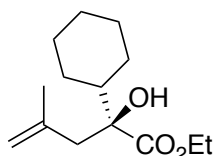


Ethyl (*S*)-2-Cyclopentyl-2-hydroxy-4-methylpent-4-enoate (4f). Colorless

oil; $[\alpha]^{26}_D -20.3$ (*c* 0.46, CHCl_3) (88% ee); IR (film) 3522, 2955, 2870, 1726, 1204 cm^{-1} ; ^1H NMR

(400 MHz, CDCl₃) δ 4.82 (m, 1H), 4.71 (m, 1H), 4.26–4.16 (m, 2H), 3.14 (s, 1H), 2.46 (dd, J = 9.6, 14.0 Hz, 2H), 2.24 (quin, J = 8.4 Hz, 1H), 1.75 (s, 3H), 1.73–1.36 (m, 8H), 1.30 (t, J = 7.2 Hz, 3H); ¹³C NMR (100 MHz, CDCl₃) δ 176.6, 141.9, 114.2, 78.6, 61.6, 47.7, 45.7, 26.6, 26.1, 25.7, 25.7, 24.0, 14.2; HRMS (ESI) calcd for C₁₃H₂₂NaO₃ [M+Na]⁺ 249.1467, found 249.1461.

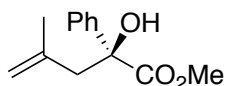
Enantiomeric excess was determined by chiral HPLC analysis after the transformation of **4f** into the corresponding 3,5-dinitrobenzoate: YMC CHIRAL Amylose-SA; hexane–*i*-PrOH 9:1; flow rate 0.3 mL/min; t_R = 18.1 min (major enantiomer), t_R = 17.0 min (minor enantiomer), λ = 254 nm. Absolute configuration (*S*) was assigned by analogy with methyl (*R*)-2-cyclohexyl-2-hydroxypent-4-enoate {91% ee, $[\alpha]^{25}_D$ +8.3 (*c* 1.2, CHCl₃)}.¹⁵



Ethyl (*S*)-2-Cyclohexyl-2-hydroxy-4-methylpent-4-enoate (4g**).** Colorless

oil; $[\alpha]^{20}_D$ –14.1 (*c* 0.86, CHCl₃) (78% ee); IR (film) 3524, 1726, 1449, 1265, 1236, 1204, 1152, 1111 cm^{–1}; ¹H NMR (400 MHz, CDCl₃) δ 4.82 (qd, J = 1.6, 2.0 Hz, 1H), 4.71 (qd, J = 0.8, 2.0 Hz, 1H), 4.23 (qd, J = 7.2, 10.8 Hz, 1H), 4.18 (qd, J = 7.2, 10.8 Hz, 1H), 3.13 (s, 1H), 2.50 (d, J = 13.2 Hz, 1H), 2.40 (d, J = 13.2 Hz, 1H), 1.90–1.60 (m, 5H), 1.74 (s, 3H), 1.40–1.05 (m, 6H), 1.30 (t, J = 7.2 Hz, 3H); ¹³C NMR (100 MHz, CDCl₃) δ 176.4, 142.1, 114.3, 80.2, 61.6, 45.9, 44.1, 27.4, 26.3 (2C), 26.2, 25.8, 24.1, 14.2; HRMS (FAB) calcd for C₁₄H₂₅O₃ [M+H]⁺ 241.1804, found 241.1819.

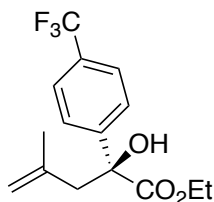
Enantiomeric excess was determined by chiral HPLC analysis: YMC CHIRAL Amylose-SA; hexane–*i*-PrOH 100:1; flow rate 0.3 mL/min; t_R = 16.0 min (major enantiomer), t_R = 17.1 min (minor enantiomer), λ = 215 nm. Absolute configuration (*S*) was assigned by analogy with methyl (*R*)-2-cyclohexyl-2-hydroxypent-4-enoate {91% ee, $[\alpha]^{25}_D$ +8.3 (*c* 1.2, CHCl₃)}.¹⁵



Methyl (*S*)-2-Hydroxy-4-methyl-2-phenylpent-4-enoate (4h**).** Colorless

oil; $[\alpha]^{20}_D$ +24.2 (*c* 1.25, CHCl₃) (98% ee); IR (film) 3509, 1732, 1449, 1437, 1246, 1213, 1119 cm^{–1}; ¹H NMR (400 MHz, CDCl₃) δ 7.64–7.61 (m, 2H), 7.38–7.33 (m, 2H), 7.29 (m, 1H), 4.90 (qd, J = 1.6, 2.0 Hz, 1H), 4.79 (qd, J = 1.2, 2.0 Hz, 1H), 3.77 (s, 3H), 3.72 (s, 1H), 3.05 (d, J = 14.0 Hz, 1H), 2.70 (dd, J = 0.8, 14.0 Hz, 1H), 1.73 (d, J = 0.8 Hz, 3H); ¹³C NMR (100 MHz, CDCl₃) δ 175.3, 141.8, 141.1, 128.2 (2C), 127.8, 125.5 (2C), 115.3, 78.2, 53.1, 47.2, 24.0; HRMS (FAB) calcd for C₁₃H₁₇O₃ [M+H]⁺ 221.1178, found 221.1169.

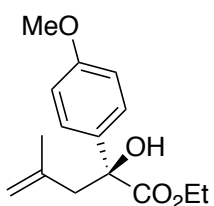
Enantiomeric excess was determined by chiral HPLC analysis: YMC CHIRAL Amylose-SA; hexane-*i*-PrOH 100:1; flow rate 0.3 mL/min; $t_R = 22.9$ min (major enantiomer), $t_R = 25.0$ min (minor enantiomer), $\lambda = 200$ nm. Absolute configuration (*S*) was assigned by analogy with methyl (*S*)-2-hydroxy-2-phenylhex-5-enoate {95% ee, $[\alpha]^{24}_D +78.5$ (*c* 1.0, CHCl₃)}.¹⁶



Ethyl (*S*)-2-Hydroxy-4-methyl-2-(4-(trifluoromethyl)phenyl)pent-4-enoate

(4i). Colorless oil; $[\alpha]^{21}_D +16.1$ (*c* 0.64, CHCl₃) (97% ee); IR (film) 3501, 1728, 1618, 1412, 1329, 1260, 1211, 1167, 1128, 1101, 1071 cm⁻¹; ¹H NMR (300 MHz, CDCl₃) δ 7.78 (d, $J = 8.4$ Hz, 2H), 7.61 (d, $J = 8.4$ Hz, 2H), 4.90 (m, 1H), 4.79 (m, 1H), 4.27 (qd, $J = 7.2, 10.8$ Hz, 1H), 4.22 (qd, $J = 7.2, 10.8$ Hz, 1H), 3.85 (s, 1H), 3.02 (d, $J = 13.8$, 1H), 2.68 (d, $J = 13.8$ Hz, 1H), 1.74 (s, 3H), 1.29 (t, $J = 7.2$ Hz, 3H); ¹³C NMR (100 MHz, CDCl₃) δ 174.2, 145.8, 140.6, 129.9 (q, $^2J_{CF} = 32.3$ Hz), 126.2 (2C), 125.1 (q, $^3J_{CF} = 3.8$ Hz, 2C), 124.1 (q, $^1J_{CF} = 270.5$ Hz), 115.7, 78.0, 62.8, 47.4, 24.1, 14.0; HRMS (FAB) calcd for C₁₅H₁₈F₃O₃ [M+H]⁺ 303.1208, found 303.1216.

Enantiomeric excess was determined by chiral HPLC analysis: Daicel CHIRALPAK AD-H; hexane-*i*-PrOH 9:1; flow rate 0.3 mL/min; $t_R = 17.6$ min (major enantiomer), $t_R = 16.8$ min (minor enantiomer), $\lambda = 254$ nm. Absolute configuration (*S*) was assigned by analogy with methyl (*S*)-2-hydroxy-2-phenylhex-5-enoate {95% ee, $[\alpha]^{24}_D +78.5$ (*c* 1.0, CHCl₃)}.¹⁶

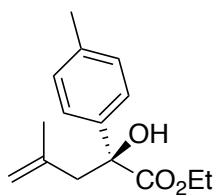


Ethyl (*S*)-2-Hydroxy-2-(4-methoxyphenyl)-4-methylpent-4-enoate (4j).

Colorless oil; $[\alpha]^{21}_D +22.7$ (*c* 1.62, CHCl₃) (93% ee); IR (film) 3501, 1724, 1609, 1510, 1456, 1300, 1250, 1207, 1179, 1099, 1034 cm⁻¹; ¹H NMR (300 MHz, CDCl₃) δ 7.54 (d, $J = 9.0$ Hz, 2H), 6.87 (d, $J = 9.0$ Hz, 2H), 4.89 (m, 1H), 4.80 (m, 1H), 4.24 (qd, $J = 6.9, 10.5$ Hz, 1H), 4.19 (qd, $J = 6.9, 10.5$ Hz, 1H), 3.80 (s, 3H), 3.73 (s, 1H), 3.01 (d, $J = 13.8$ Hz, 1H), 2.67 (d, $J = 13.8$ Hz, 1H), 1.74 (s, 3H), 1.27 (t, $J = 6.9$ Hz, 3H); ¹³C NMR (100 MHz, CDCl₃) δ 175.0, 159.1, 141.3, 134.2, 126.8 (2C), 115.1, 113.4 (2C), 77.7, 62.3, 55.2, 47.2, 24.1, 14.0; HRMS (ESI) calcd for C₁₅H₂₀NaO₄ [M+Na]⁺ 287.1259, found 287.1252.

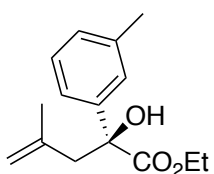
Enantiomeric excess was determined by chiral HPLC analysis: Daicel CHIRALPAK AD-H;

hexane-*i*-PrOH 9:1; flow rate 0.3 mL/min; $t_R = 33.6$ min (major enantiomer), $t_R = 36.1$ min (minor enantiomer), $\lambda = 254$ nm. Absolute configuration (*S*) was assigned by analogy with methyl (*S*)-2-hydroxy-2-phenylhex-5-enoate {95% ee, $[\alpha]^{24}_D +78.5$ (*c* 1.0, CHCl₃)}.¹⁶



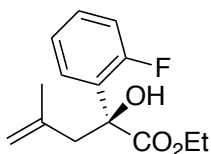
Ethyl (*S*)-2-Hydroxy-4-methyl-2-(*p*-tolyl)pent-4-enoate (4k). Colorless oil;

$[\alpha]^{25}_D +17.8$ (*c* 1.34, CHCl₃) (96% ee); IR (film) 3503, 2982, 2922, 1724, 1207 cm⁻¹; ¹H NMR (400 MHz, CDCl₃) δ 7.51 (d, *J* = 8.4 Hz, 2H), 7.16 (d, *J* = 8.4 Hz, 2H), 4.89 (m, 1H), 4.80 (m, 1H), 4.26–4.17 (m, 2H), 3.73 (s, 1H), 3.02 (d, *J* = 14 Hz, 1H), 2.68 (d, *J* = 14 Hz, 1H), 2.34 (s, 3H), 1.74 (s, 3H), 1.28 (t, *J* = 7.2 Hz, 3H); ¹³C NMR (100 MHz, CDCl₃) δ 175.0, 141.3, 139.1, 137.3, 128.8 (2C), 125.4 (2C), 115.1, 77.9, 62.3, 47.2, 24.1, 21.0, 14.0; HRMS (ESI) calcd for C₁₅H₂₀NaO₃ [M+Na]⁺ 271.1310, found 271.1306. Enantiomeric excess was determined by chiral HPLC analysis: Daicel CHIRALPAK AD-H; hexane- *i*-PrOH 100:1; flow rate 0.5 mL/min; $t_R = 36.2$ min (major enantiomer), $t_R = 31.5$ min (minor enantiomer), $\lambda = 215$ nm. Absolute configuration (*S*) was assigned by analogy with methyl (*R*)-2-hydroxy-2-(*p*-tolyl)pent-4-enoate {91% ee, $[\alpha]^{28}_D -16.1$ (*c* 0.38, CH₂Cl₂)}.⁸



Ethyl (*S*)-2-Hydroxy-4-methyl-2-(*m*-tolyl)pent-4-enoate (4l). Colorless oil;

$[\alpha]^{25}_D +14.6$ (*c* 1.03, CHCl₃) (95% ee); IR (film) 3505, 3077, 2980, 2924, 1724, 1447, 1209 cm⁻¹; ¹H NMR (400 MHz, CDCl₃) δ 7.46 (s, 1H), 7.42 (dd, *J* = 0.4, 8.0 Hz, 1H), 7.24 (t, *J* = 8.0 Hz, 1H), 7.10 (m, 1H), 4.90 (m, 1H), 4.81 (m, 1H), 4.22 (tq, *J* = 6.0, 16.2 Hz, 2H), 3.73 (s, 1H), 3.04 (d, *J* = 14.0 Hz, 1H), 2.68 (d, *J* = 14.0 Hz, 1H), 2.36 (s, 3H), 1.75 (s, 3H), 1.28 (t, *J* = 7.2 Hz, 3H); ¹³C NMR (100 MHz, CDCl₃) δ 174.9, 142.0, 141.3, 137.8, 128.4, 128.0, 126.1, 122.6, 115.1, 78.0, 62.3, 47.2, 24.1, 21.6, 14.0; HRMS (ESI) calcd for C₁₅H₂₀NaO₃ [M+Na]⁺ 271.1310, found 271.1301. Enantiomeric excess was determined by chiral HPLC analysis: YMC CHIRAL Amylose-SA; hexane-EtOH 100:1; flow rate 0.3 mL/min; $t_R = 16.0$ min (major enantiomer), $t_R = 17.0$ min (minor enantiomer), $\lambda = 220$ nm. Absolute configuration (*S*) was assigned by analogy with methyl (*R*)-2-hydroxy-2-(*m*-tolyl)pent-4-enoate {90% ee, $[\alpha]^{28}_D -15.2$ (*c* 0.39, CH₂Cl₂)}.¹⁷



Ethyl (S)-2-(2-Fluorophenyl)-2-hydroxy-4-methylpent-4-enoate (4n).

Colorless oil; $[\alpha]_D^{22} +10.3$ (*c* 0.86, CHCl₃) (97% ee); IR (film) 3509, 1734, 1487, 1456, 1373, 1256, 1229, 1209, 1095, 1022 cm⁻¹; ¹H NMR (400 MHz, CDCl₃) δ 7.58 (dd, *J* = 1.2, 8.0 Hz, 1H), 7.15 (m, 1H), 7.15 (dd, *J* = 1.2, 8.0 Hz, 1H), 7.03 (dd, *J* = 1.2, 8.0 Hz, 1H), 4.90 (m, 1H), 4.79 (m, 1H), 4.22 (q, *J* = 7.2 Hz, 2H), 3.80 (s, 1H), 3.03 (d, *J* = 13.2 Hz, 1H), 2.96 (d, *J* = 13.2 Hz, 1H), 1.75 (dd, *J* = 1.2, 0.8 Hz, 3H), 1.24 (t, *J* = 7.2 Hz, 3H); ¹³C NMR (100 MHz, CDCl₃) δ 174.2, 160.2 (d, ¹*J*_{CF} = 246.9 Hz), 140.9, 129.8 (d, ³*J*_{CF} = 8.7 Hz), 129.3 (d, ³*J*_{CF} = 12.0 Hz), 127.5 (d, ²*J*_{CF} = 3.8 Hz), 123.9 (d, ⁴*J*_{CF} = 3.4 Hz), 116.1 (d, ²*J*_{CF} = 23.0 Hz), 115.7, 76.2, 62.3, 44.5, 24.1, 13.9; HRMS (FAB) calcd for C₁₄H₁₈FO₃ [M+H]⁺ 253.1240, found 253.1255.

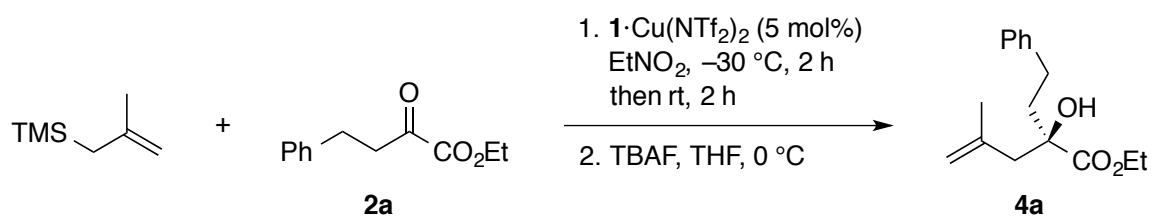
Enantiomeric excess was determined by chiral HPLC analysis: YMC CHIRAL Amylose-SA; hexane-*i*-PrOH 100:1; flow rate 0.3 mL/min; *t*_R = 26.3 min (major enantiomer), *t*_R = 29.2 min (minor enantiomer), λ = 260 nm. Absolute configuration (*S*) was assigned by analogy with methyl (*S*)-2-hydroxy-2-phenylhex-5-enoate {95% ee, $[\alpha]_D^{24} +78.5$ (*c* 1.0, CHCl₃)}.¹⁶

Examination of Solvents in the $1\mathbf{a}\cdot\text{Cu}(\text{NTf}_2)_2$ -catalyzed Addition of $2\mathbf{a}$ with Allyltrimethylsilane

Solvent	Conditions	Results
CH_2Cl_2	40 °C, 22 h	0% yield
THF	50 °C, 5 h	0% yield
CH_3CN	50 °C, 5 h	0% yield
<i>i</i> -PrOH	50 °C, 5 h	0% yield
EtNO_2	rt, 21 h	78% yield, 74% ee

The reaction of $2\mathbf{a}$ (0.2 mmol) with allyltrimethylsilane (3 equiv) was conducted in the presence of $1\mathbf{a}\cdot\text{Cu}(\text{NTf}_2)_2$ (5 mol%) under the indicated conditions. The crude product was treated with TBAF (1 equiv) in THF at 0 °C for 0.5 h.

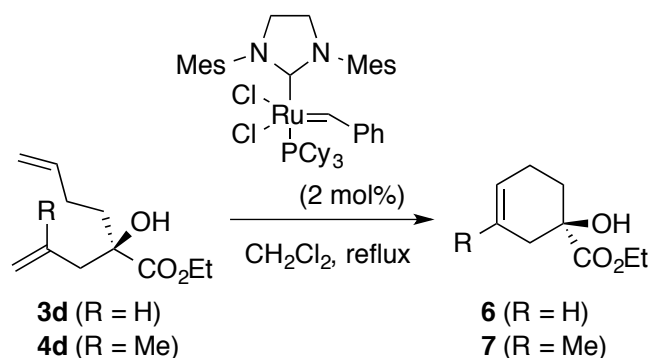
Catalytic Activities of Chiral Copper(II) Complexes in the Enantioselective Addition of **2a** with Methallyltrimethylsilane



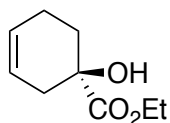
Ligand (1)	Yield (%)	Ee (%)
1a	90	96
1b	75	74
1c	71	-71
1d	62	-35
1e	68	52
1f	84	66

The reaction of **2a** (0.2 mmol) with methallyltrimethylsilane (3 equiv) was conducted in the presence of **1**·Cu(NTf₂)₂ (5 mol%) in EtNO₂ at -30 °C for 2 h, then at ambient temperature for 2 h. The crude product was treated with TBAF (1 equiv) in THF at 0 °C for 0.5 h.

Transformation of 3d and 4d



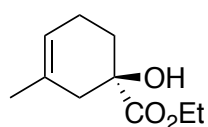
Grubbs 2nd generation (1.0 mg, 1.1 μmol , 2 mol%) was placed in an oven-dried two-necked flask. Adduct **4d** (12 mg, 0.056 mmol) in CH_2Cl_2 (2.0 mL) was added to the above-mentioned flask. After being stirred at 35 $^\circ\text{C}$ for 3h, the reaction mixture was concentrated. The residual oil was purified by column chromatography on silica gel (3 g, hexane–EtOAc 15 : 1) to give cyclohexene **9** (8.7 mg, 84%) as a yellow oil.



Ethyl (*R*)-1-Hydroxycyclohex-3-ene-1-carboxylate (6). Colorless oil; $[\alpha]^{24}_{\text{D}}$

-29.3 (c 0.30, CHCl_3) (75% ee); IR (film) 3503, 2978, 2930, 1728, 1437, 1221, 1098 cm^{-1} ; ^1H NMR (400 MHz, CDCl_3) δ 5.76 (m, 1H), 5.61 (m, 1H), 4.21 (q, $J = 7.2$ Hz, 2H), 3.10 (s, 1H), 2.57 (m, 1H), 2.28 (m, 1H), 2.10–2.05 (m, 2H), 1.91 (m, 1H), 1.74 (m, 1H), 1.27 (t, $J = 7.2$ Hz, 3H); ^{13}C NMR (100 MHz, CDCl_3) δ 176.8, 126.3, 122.8, 72.1, 61.8, 34.9, 30.6, 21.3, 14.1; HRMS (ESI) calcd for $\text{C}_9\text{H}_{14}\text{NaO}_3$ $[\text{M}+\text{Na}]^+$ 193.0841, found 193.0833.

Enantiomeric excess was determined by chiral HPLC analysis after the transformation of **6** into the corresponding 3,5-dinitrobenzoate: Daicel CHIRALPAK AD-H; hexane–*i*-PrOH 20:1; flow rate 1.0 mL/min; $t_{\text{R}} = 22.1$ min (major enantiomer), $t_{\text{R}} = 20.8$ min (minor enantiomer); $\lambda = 254$ nm. Absolute configuration (*R*) was assigned by analogy with methyl (*S*)-1-hydroxycyclohex-3-ene-1-carboxylate {92% ee, $[\alpha]^{20.9}_{\text{D}} +32.7$ (c 0.660, CH_2Cl_2)}.¹⁸



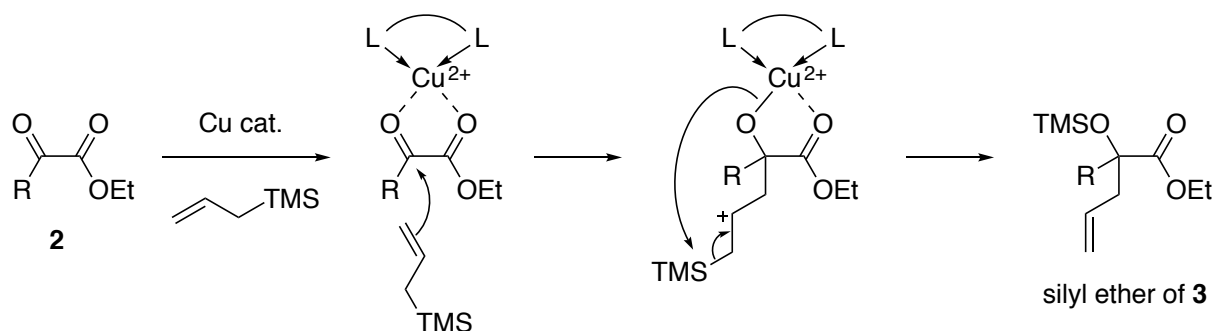
Ethyl (*R*)-1-Hydroxy-3-methylcyclohex-3-ene-1-carboxylate (7). Yellow oil;

$[\alpha]^{20}_{\text{D}} -36.5$ (c 1.17, CHCl_3) (95% ee); IR (film) 3495, 2967, 2928, 1728, 1447, 1246, 1099 cm^{-1} ;

^1H NMR (600 MHz, CDCl_3) δ 5.49 (m, 1H), 4.24 (q, $J = 7.2$ Hz, 2H), 3.05 (s, 1H), 2.53 (m, 1H), 2.27 (m, 1H), 2.06 (m, 1H), 1.95 (m, 1H), 1.84 (m, 1H), 1.71 (m, 1H), 1.68 (s, 3H), 1.29 (t, $J = 7.2$ Hz, 3H); ^{13}C NMR (150 MHz, CDCl_3) δ 176.9, 130.0, 120.1, 72.8, 61.8, 39.5, 30.5, 23.6, 21.4, 14.1; HRMS (ESI) calcd for $\text{C}_{10}\text{H}_{16}\text{NaO}_3$ $[\text{M}+\text{Na}]^+$ 207.0997, found 207.0987.

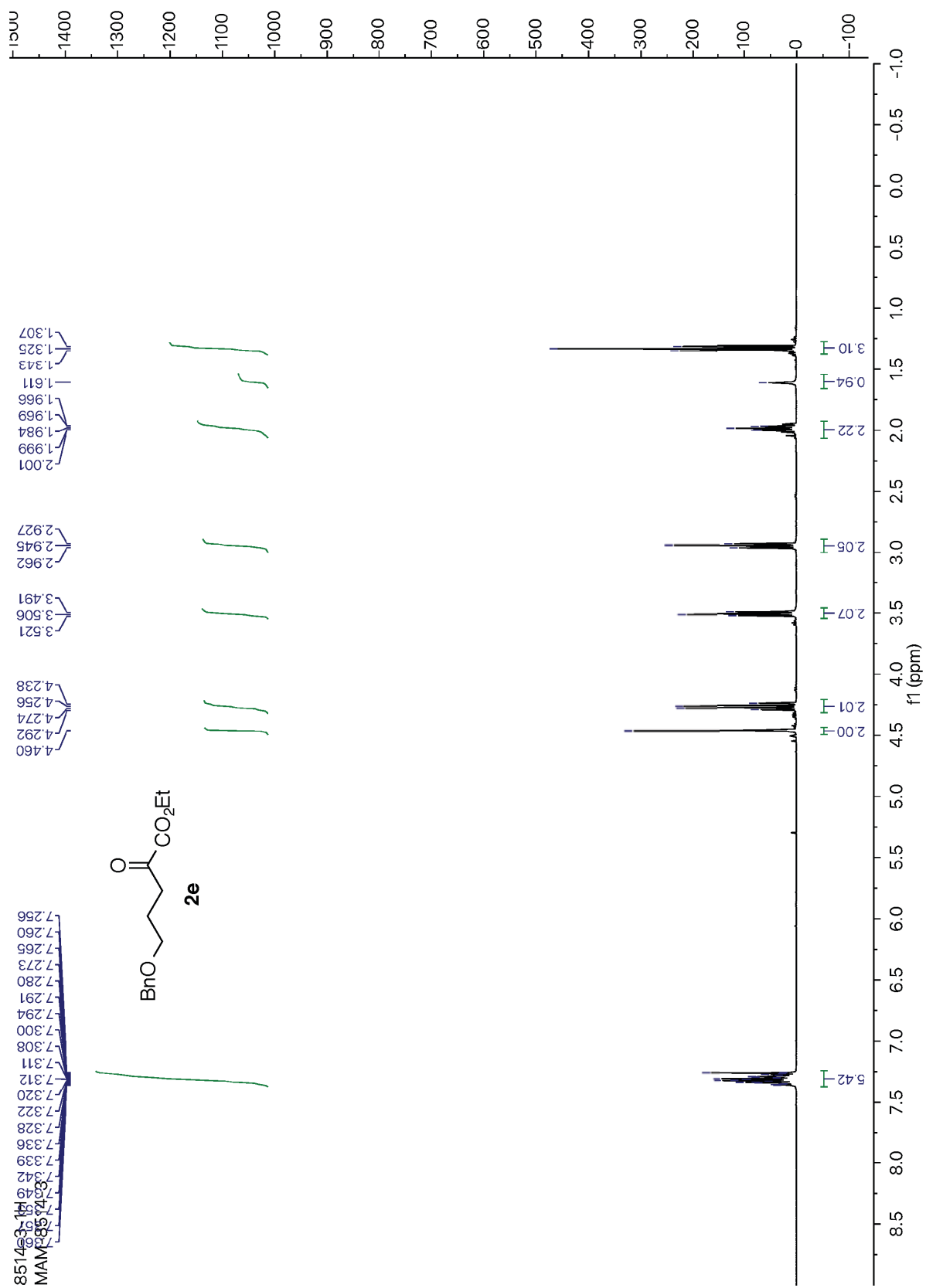
Enantiomeric excess was determined by chiral HPLC analysis: YMC CHIRAL Cellulose-SB; hexane-*i*-PrOH 9:1; flow rate 0.3 mL/min; $t_{\text{R}} = 17.0$ min (major enantiomer), $t_{\text{R}} = 15.8$ min (minor enantiomer); $\lambda = 215$ nm. Absolute configuration (*R*) was assigned by analogy with methyl (*S*)-1-hydroxycyclohex-3-ene-1-carboxylate {92% ee, $[\alpha]_{\text{D}}^{20.9} +32.7$ (c 0.660, CH_2Cl_2)}.¹⁸

Proposed Mechanism of Generation of Silyl Ether 3

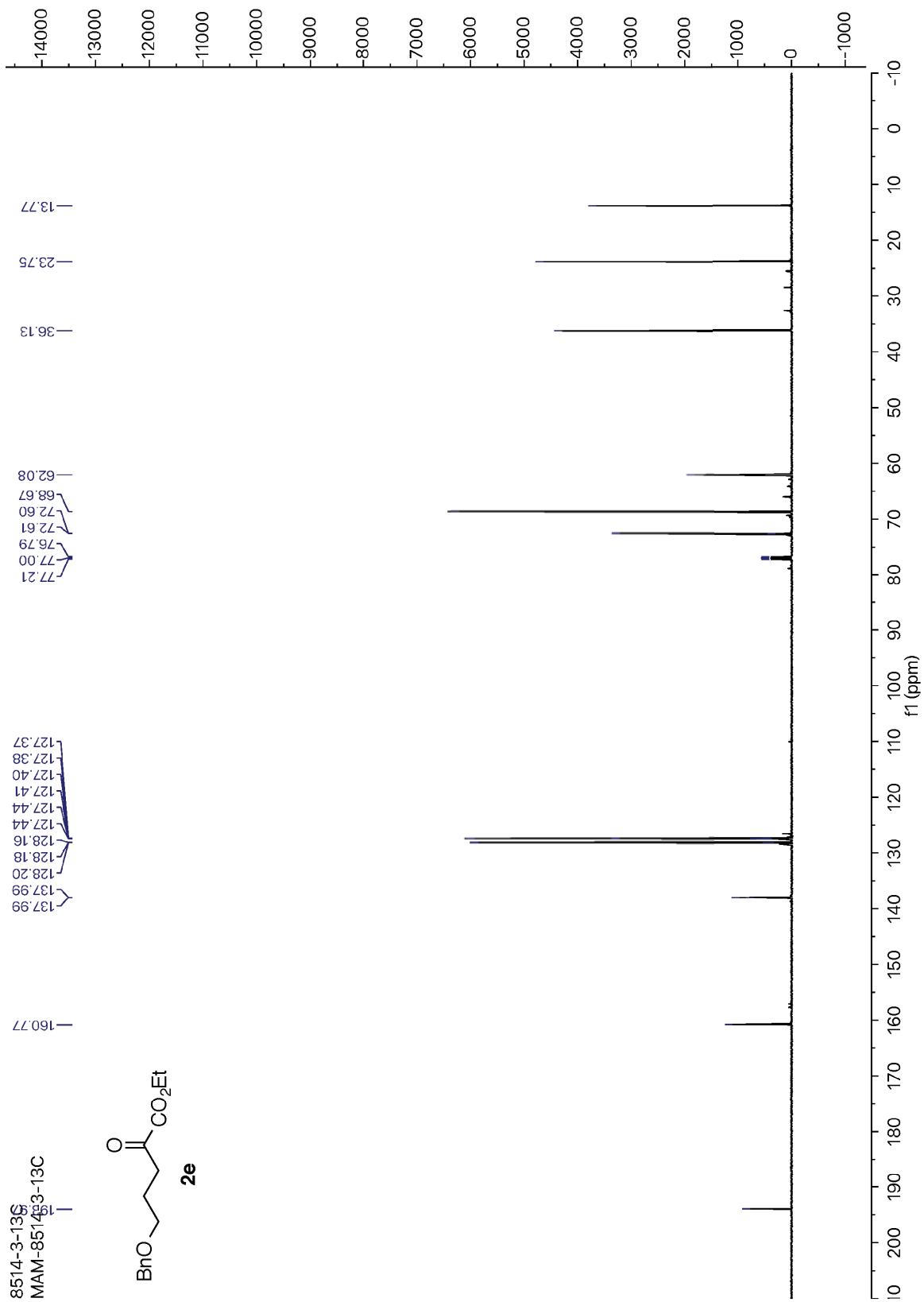


References

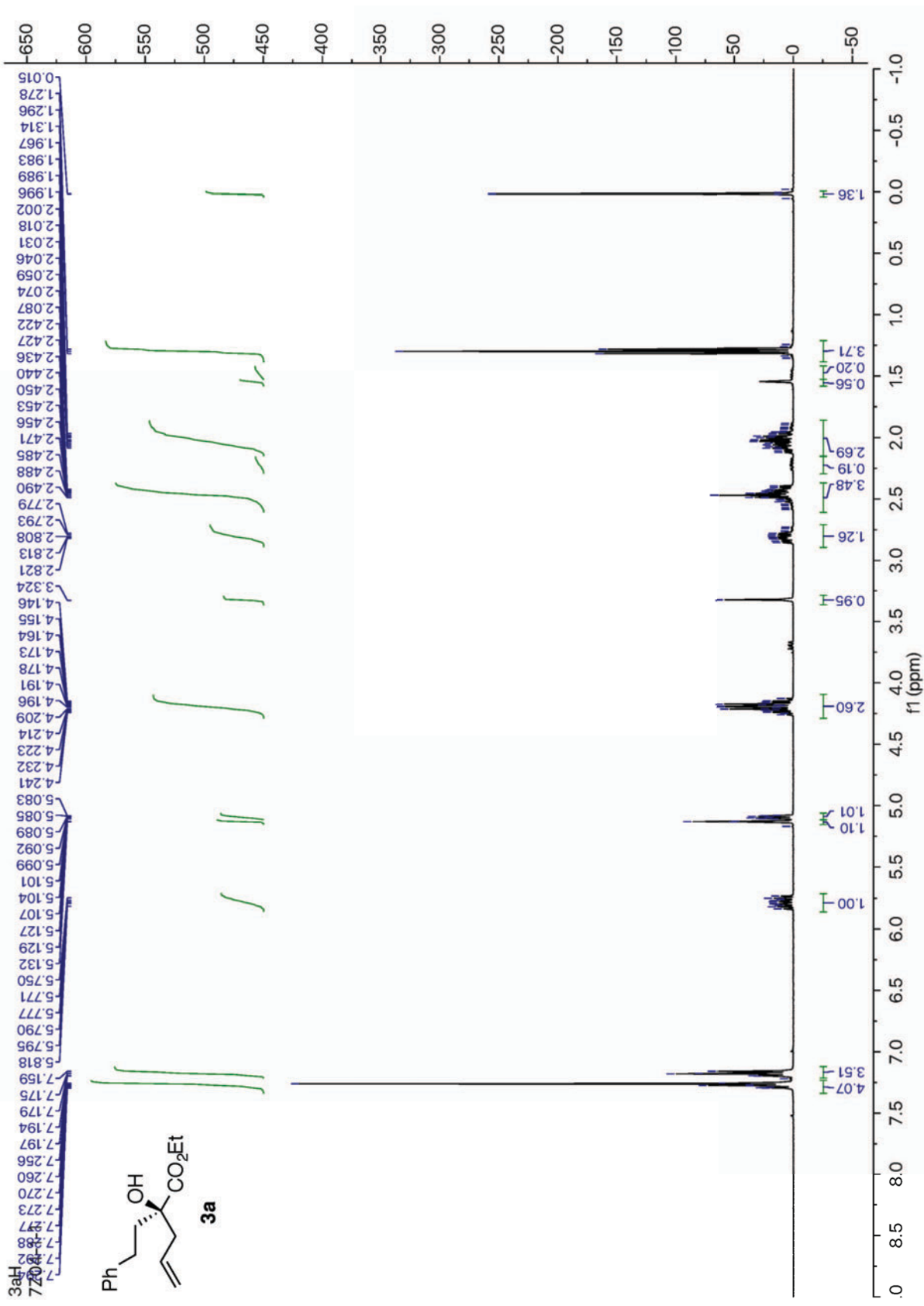
- (1) K. Murase, K. Nitta, T. Hirato, Y. Awakura, *J. Appl. Electrochem.*, 2001, **31**, 1089.
- (2) A. Sakakura, R. Kondo, Y. Matsumura, M. Akakura, K. Ishihara, *J. Am. Chem. Soc.*, 2009, **131**, 17762.
- (3) J. Mao, F. Liu, M. Wang, L. Wu, B. Zheng, S. Liu, J. Zhong, *J. Am. Chem. Soc.*, 2014, **136**, 17662.
- (4) G. Desimoni, G. Faita, M. Mella, *Tetrahedron*, 1996, **52**, 13649.
- (5) Z.-W. Mei, T. Omote, M. Mansour, H. Kawafuchi, Y. Takaguchi, A. Jutand, S. Tsuboi, T. Inokuchi, *Tetrahedron*, 2008, **64**, 10761.
- (6) Y. Fan, Y. Jiang, D. An, D. Sha, J. Antilla, S. Zhang, *Org. Lett.*, 2014, **16**, 6112.
- (7) V. Roznyatovskiy, V. Lynch, L. Sessler, *Org. Lett.*, 2010, **12**, 4424.
- (8) J. A. Macritchie, A. Silcock, C. L. Willis, *Tetrahedron: Asymmetry*, 1997, **8**, 3895.
- (9) M. A. de las Heras, J. J. Vaquero, J. L. García-Navio, J. Alvarez-Builla, *J. Org. Chem.*, 1996, **61**, 9009.
- (10) M. Hayashi, S. Nakamura, *Angew. Chem. Int. Ed.*, 2011, **50**, 2249.
- (11) A. Metz, C. Kozlowski, *J. Org. Chem.*, 2013, **78**, 717.
- (12) R. Infante, X. Tang, J. Xi, W. Xu, J. Gong, *Angew Chem. Int. Ed.*, 2013, **52**, 14021.
- (13) A. Pena, D. Monge, E. Martin, E. Alvarez, *J. Am. Chem. Soc.*, 2012, **134**, 12912.
- (14) K. Yamada, T. Tozawa, M. Nishida, T. Mukaiyama, *Bull. Chem. Soc. Jpn.*, 1997, **70**, 2301.
- (15) D. W. Robbins, K. Lee, D. L. Silverio, A. Volkov, S. Torker, A. H. Hoveyda, *Angew. Chem. Int. Ed.*, 2016, **55**, 9610.
- (16) T. Ooi, K. Fukumoto, K. Maruoka, *Angew. Chem. Int. Ed.*, 2006, **45**, 3839.
- (17) K. Zeng, B. Qin, X. Liu, X. Feng, *J. Org. Chem.*, 2007, **72**, 8478.
- (18) M. Seto, J. L. Roizen, B. M. Stoltz, *Angew. Chem. Int. Ed.*, 2008, **47**, 6873.



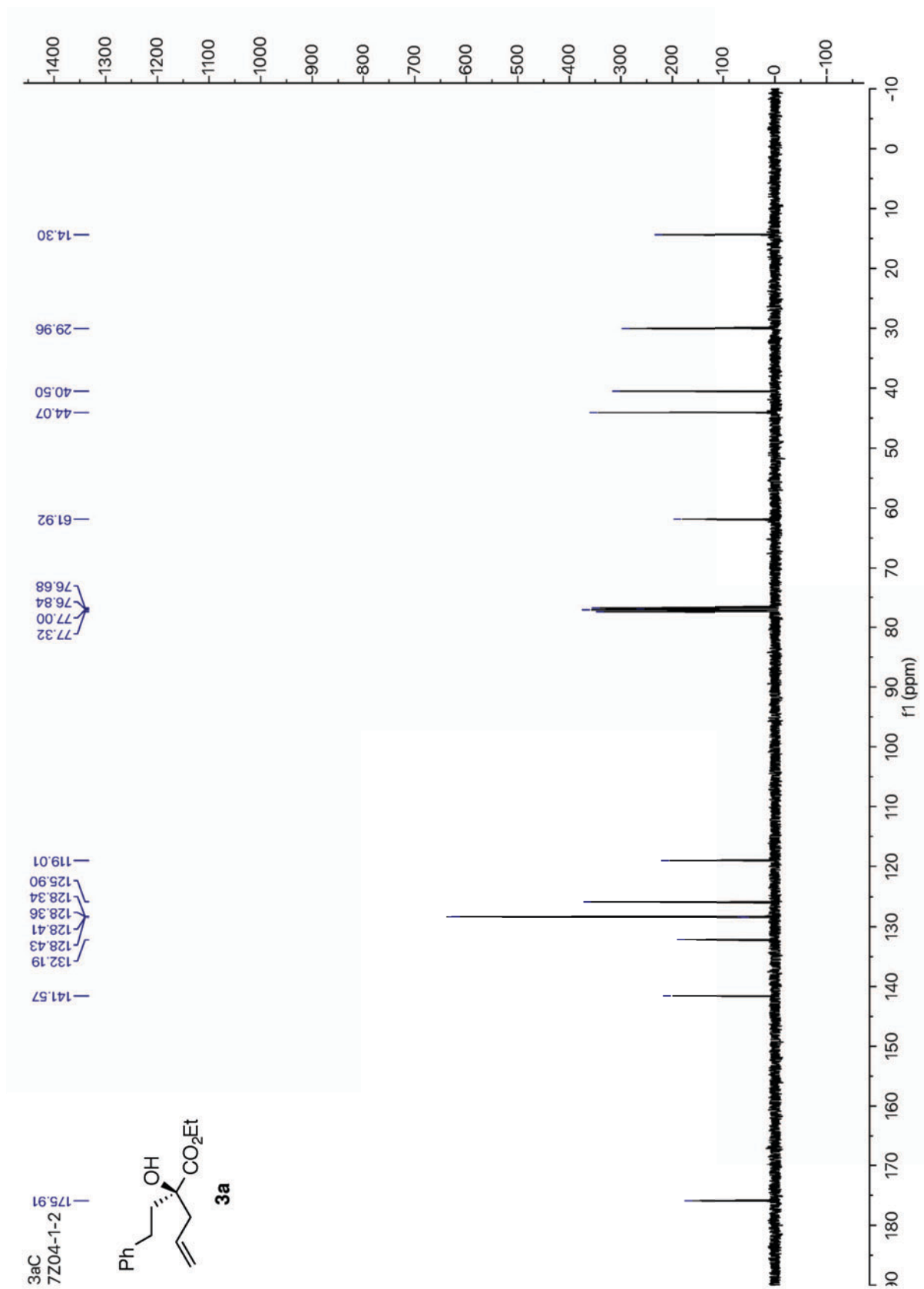
¹H NMR spectra of compound **2e** (400 MHz, CDCl₃)



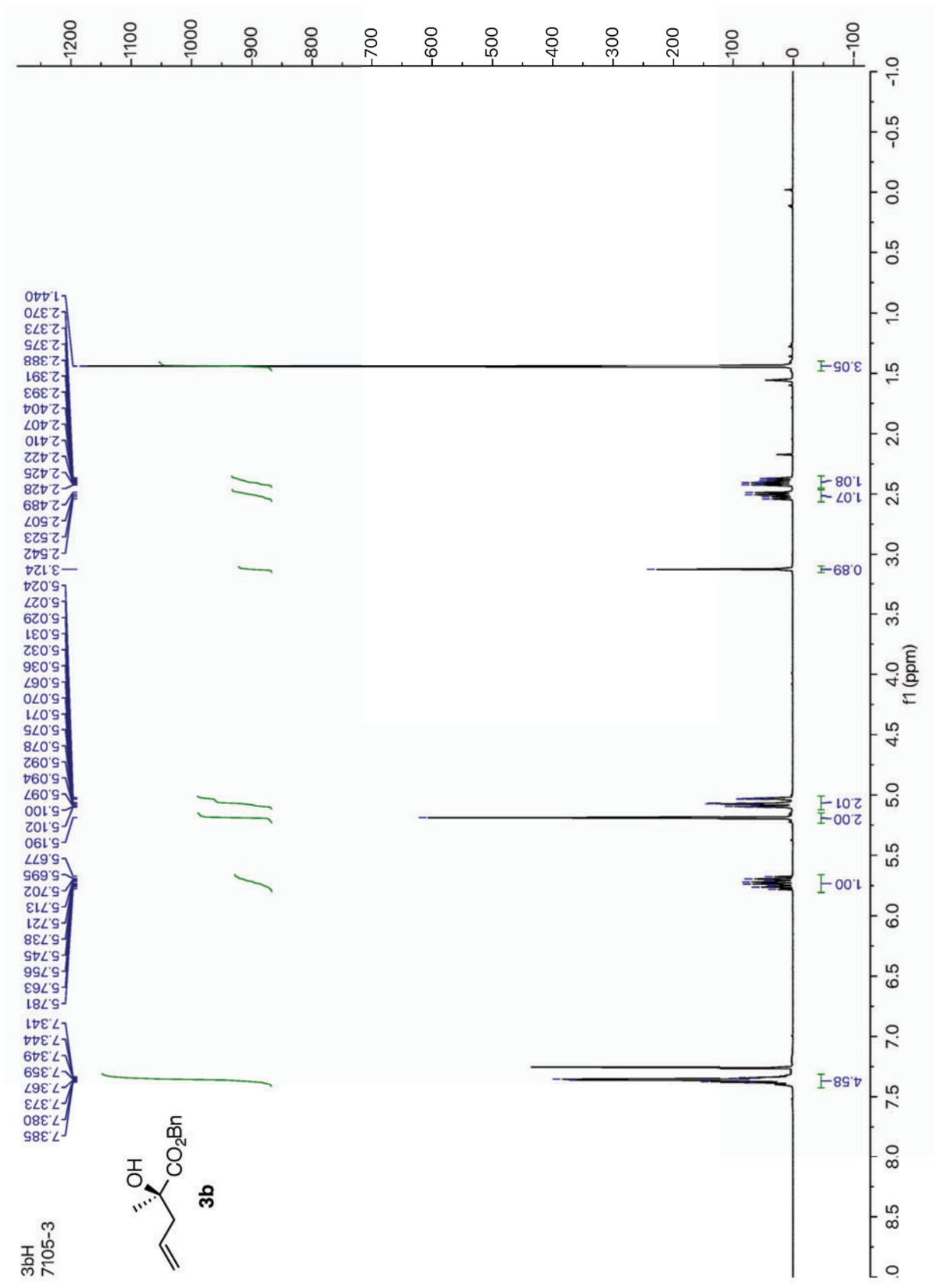
^{13}C NMR spectra of compound **2e** (150 MHz, CDCl_3)



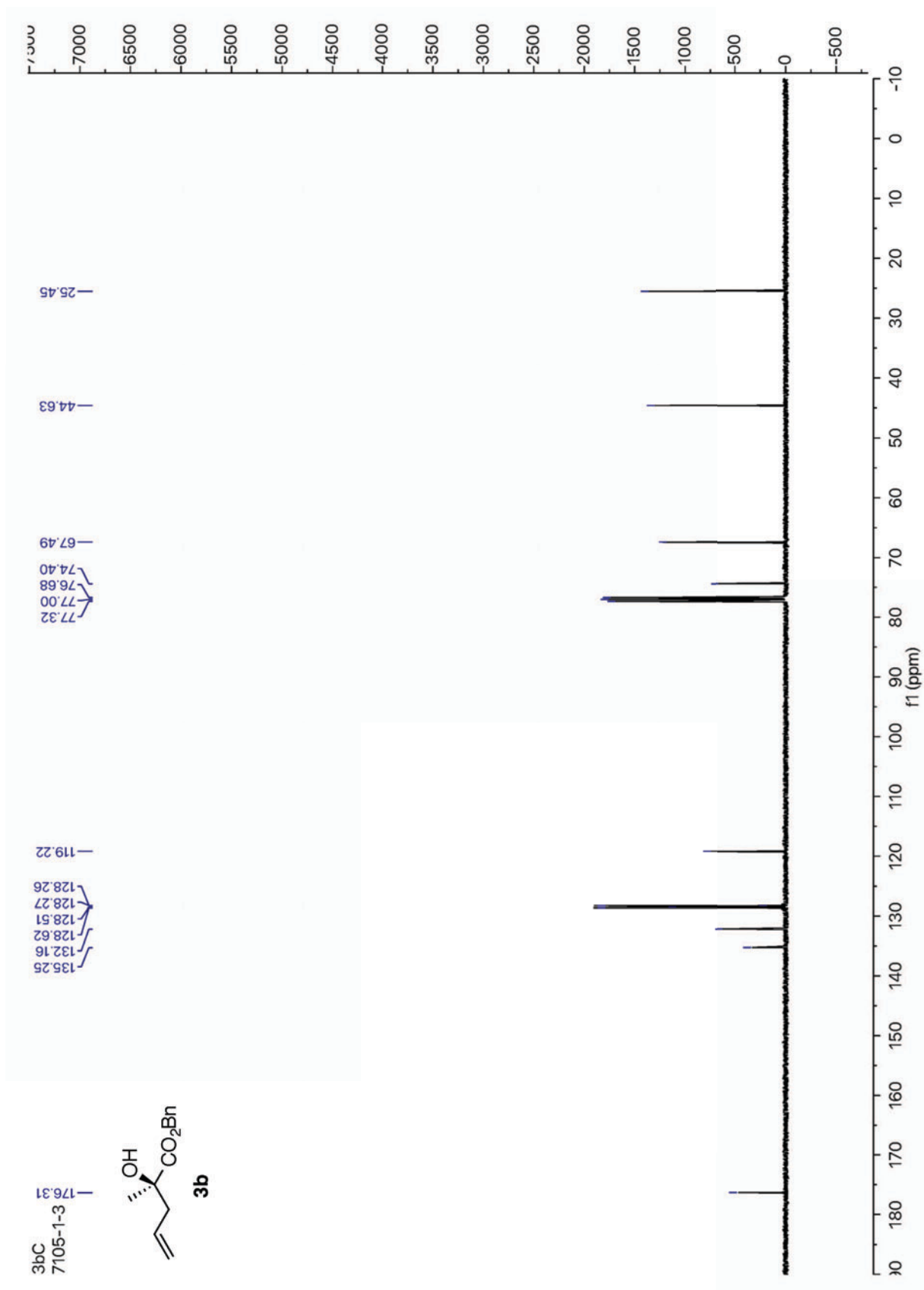
¹H NMR spectra of compound **3a** (400 MHz, CDCl₃)



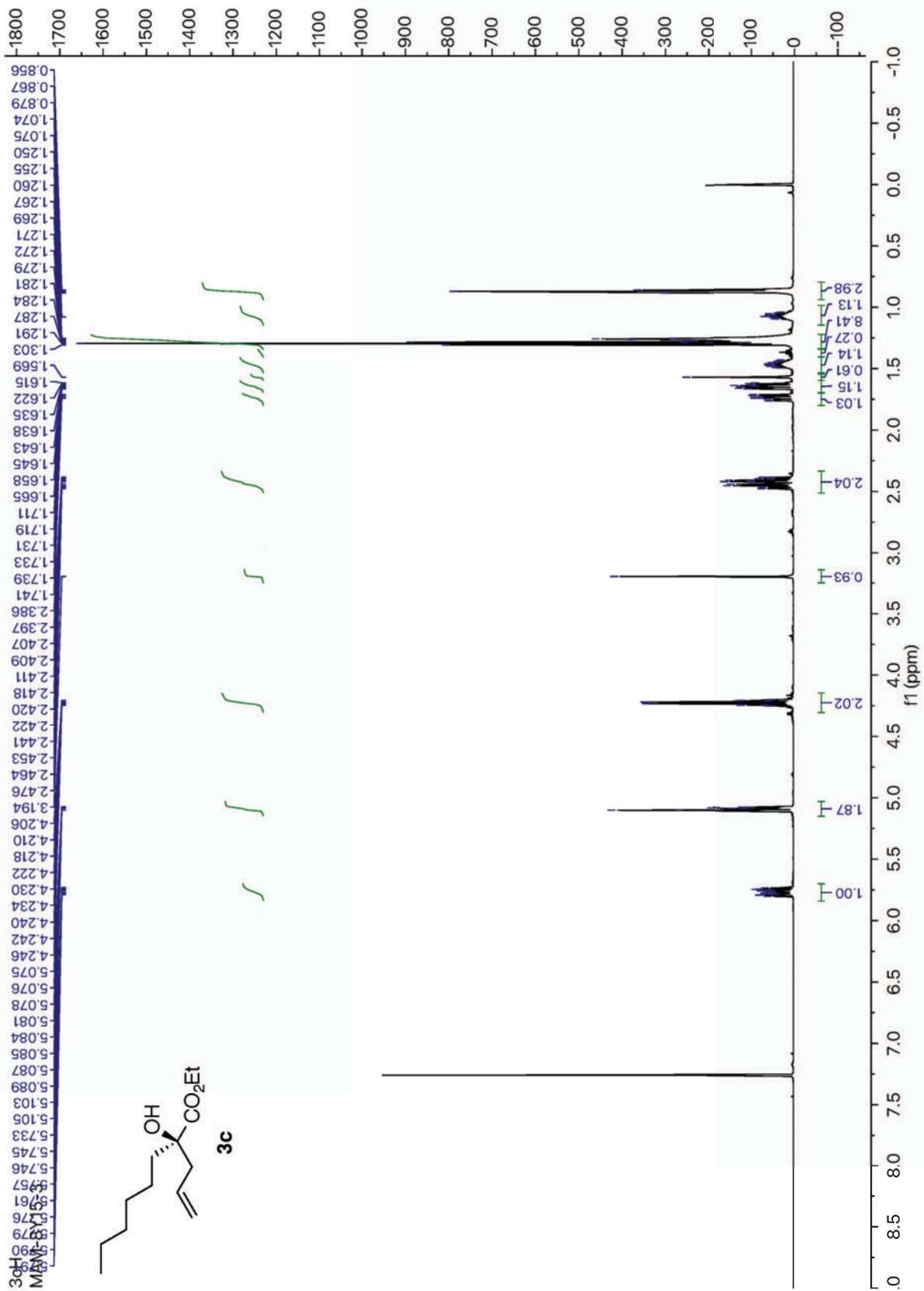
¹³C NMR spectra of compound **3a** (100 MHz, CDCl₃)



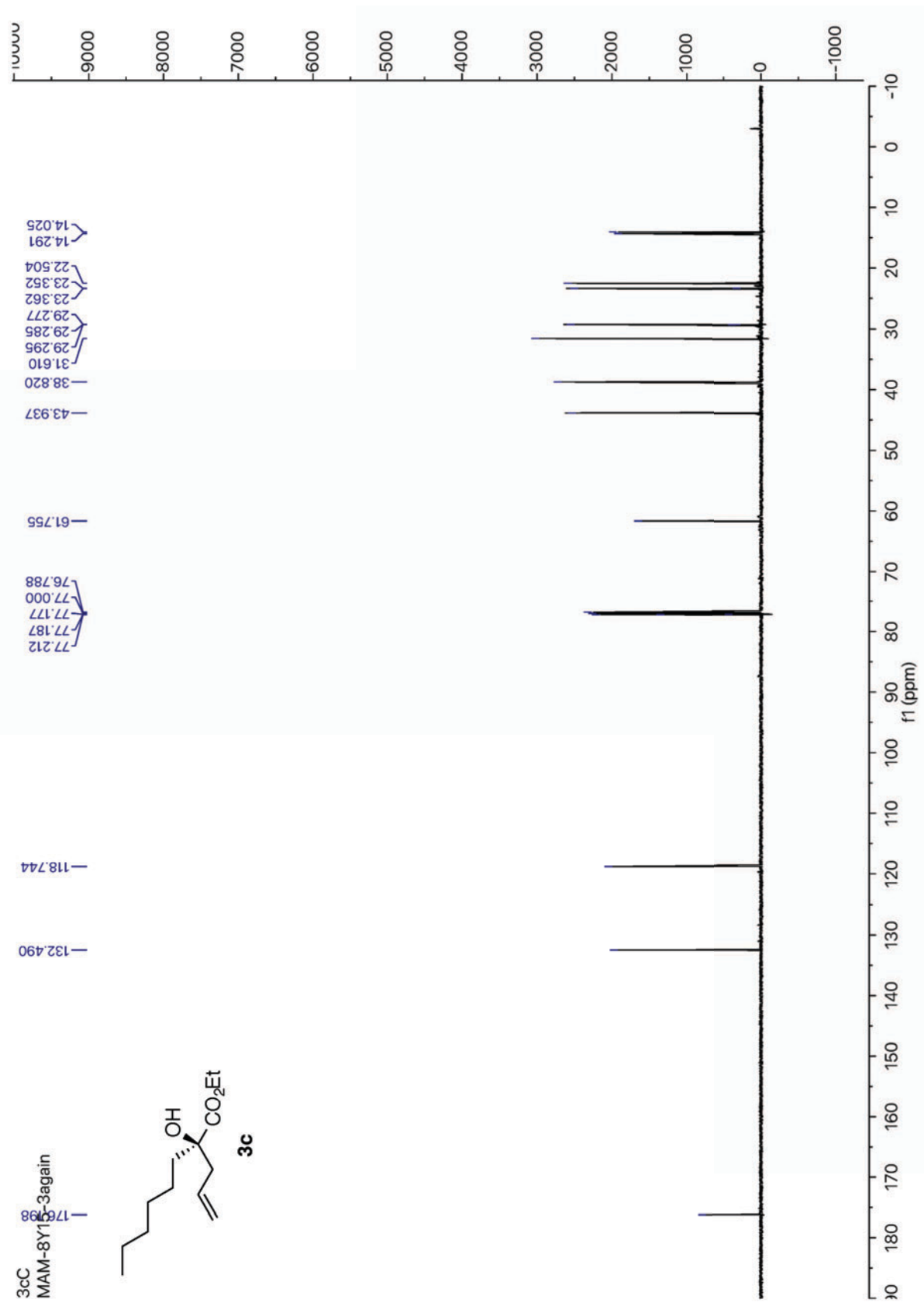
¹H NMR spectra of compound **3b** (400 MHz, CDCl₃)



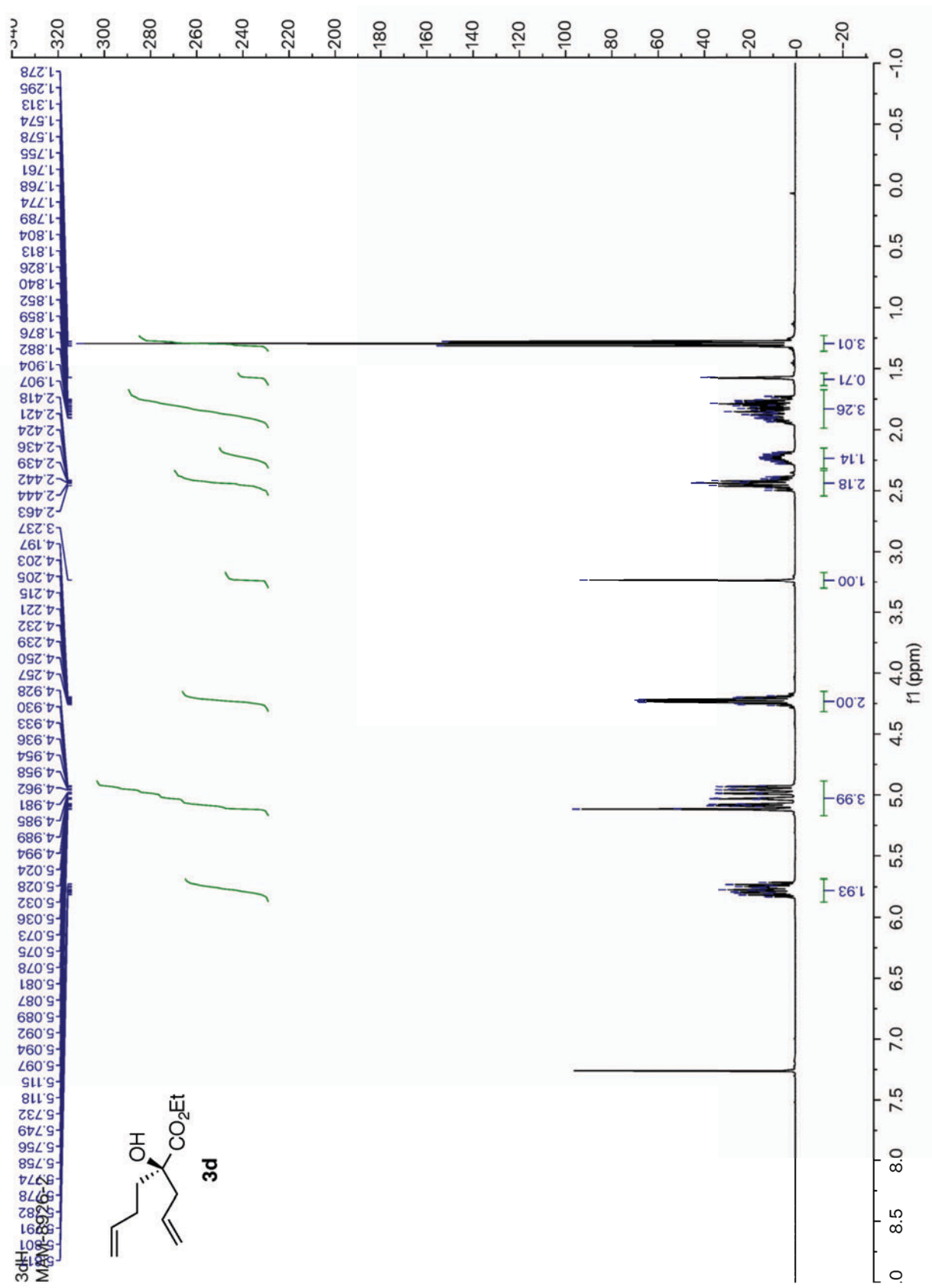
¹³C NMR spectra of compound **3b** (100 MHz, CDCl₃)



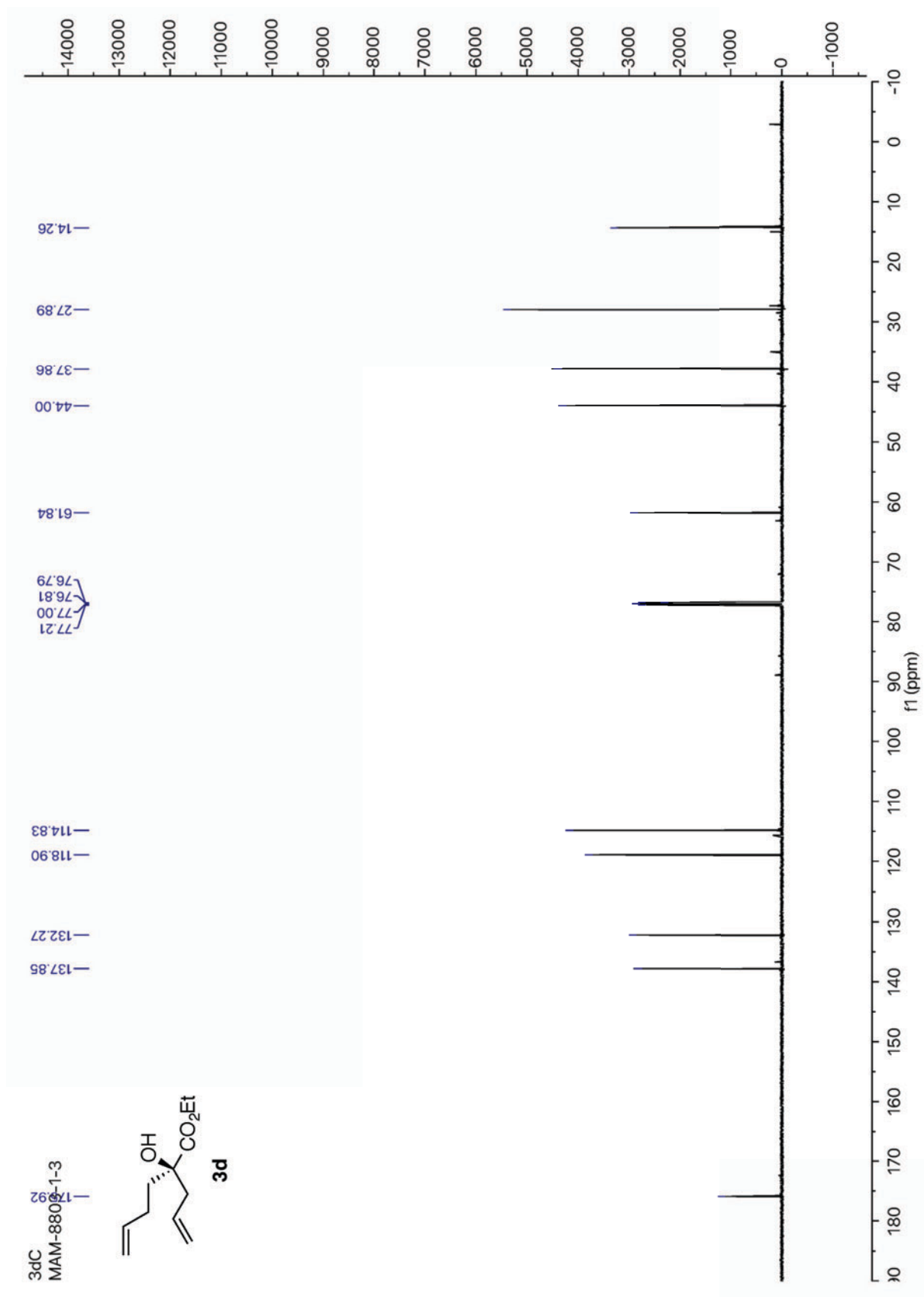
¹H NMR spectra of compound **3c** (600 MHz, CDCl₃)



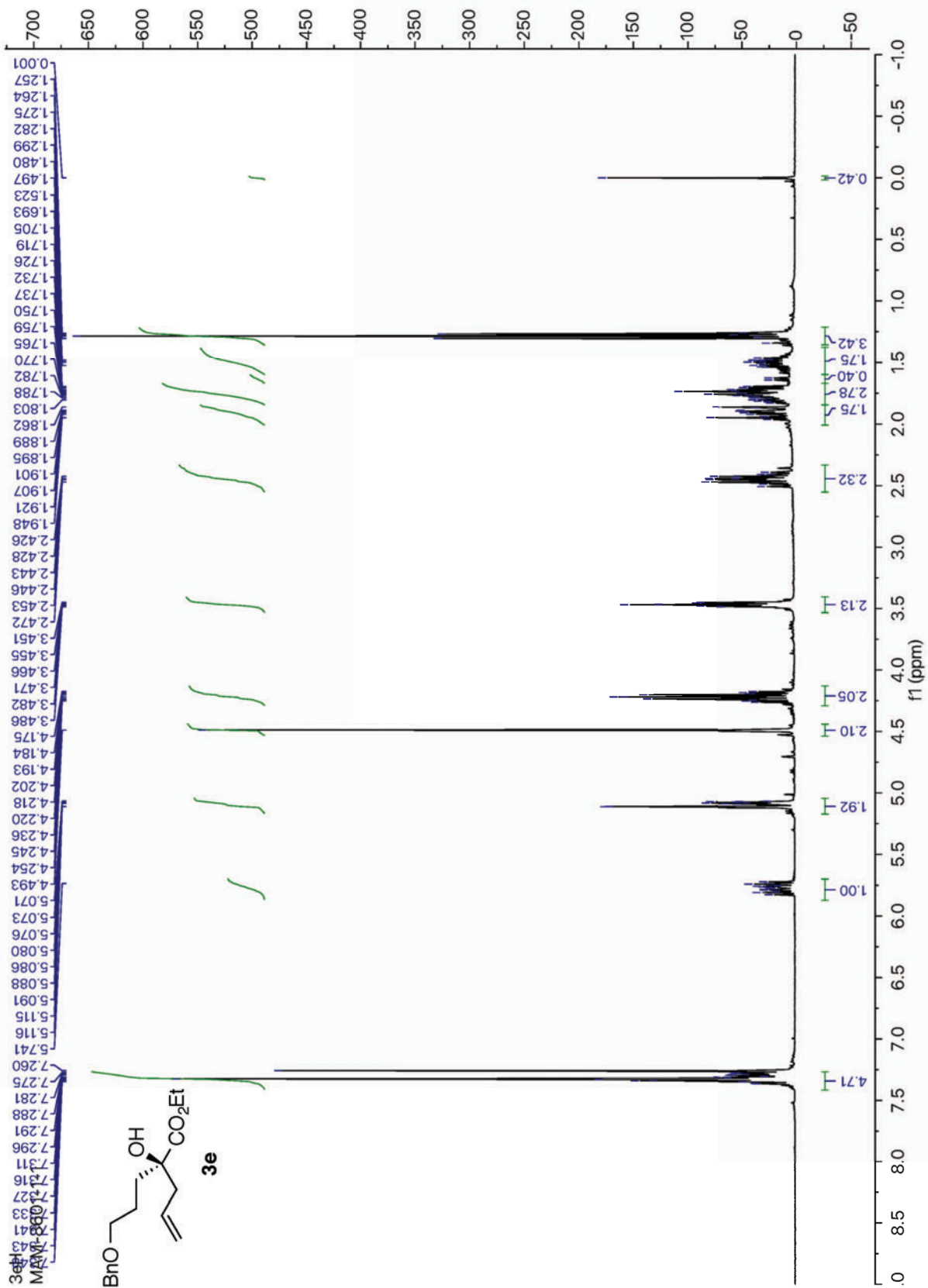
¹³C NMR spectra of compound **3c** (150 MHz, CDCl₃)



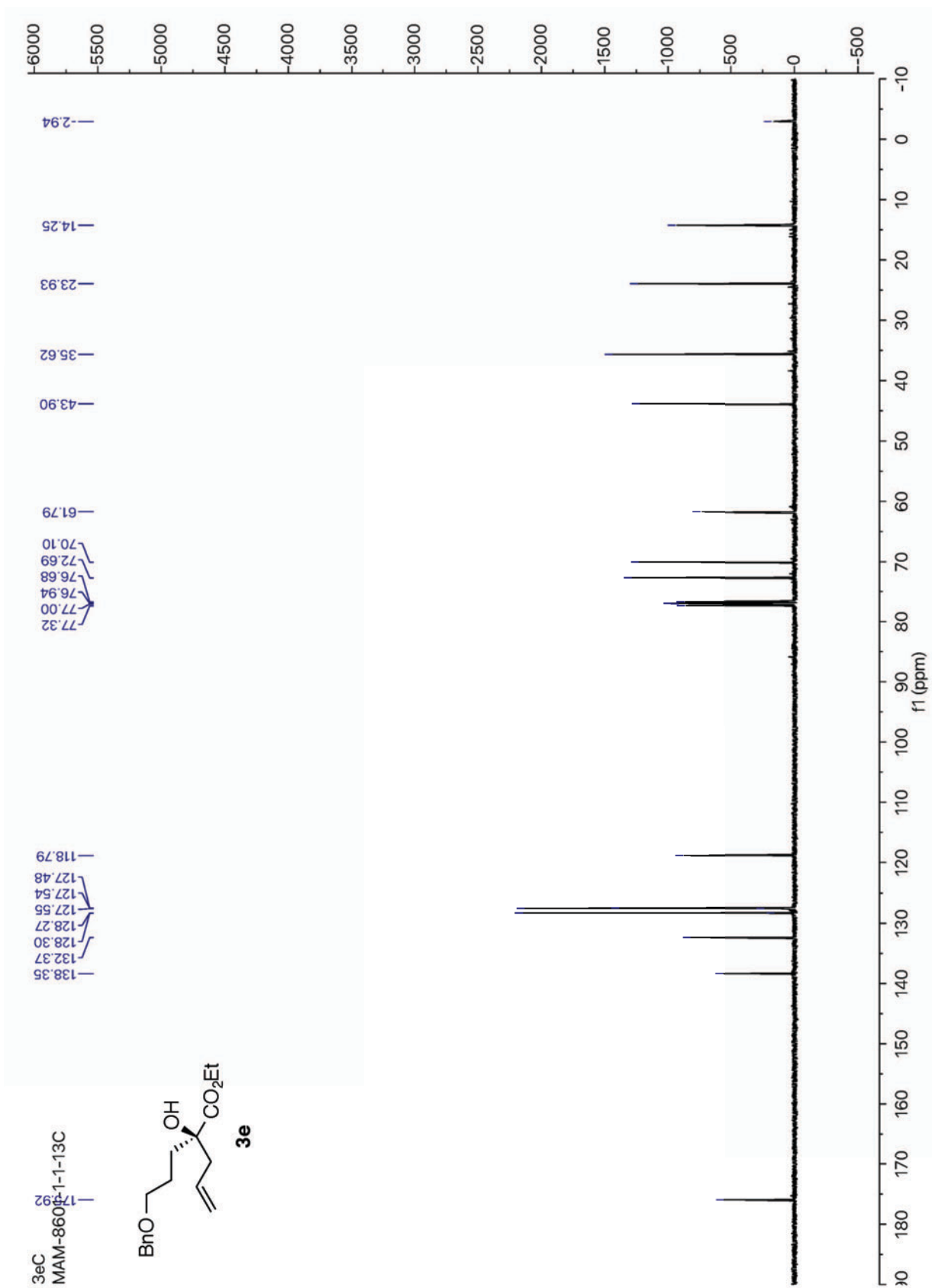
¹H NMR spectra of compound **3d** (400 MHz, CDCl₃)



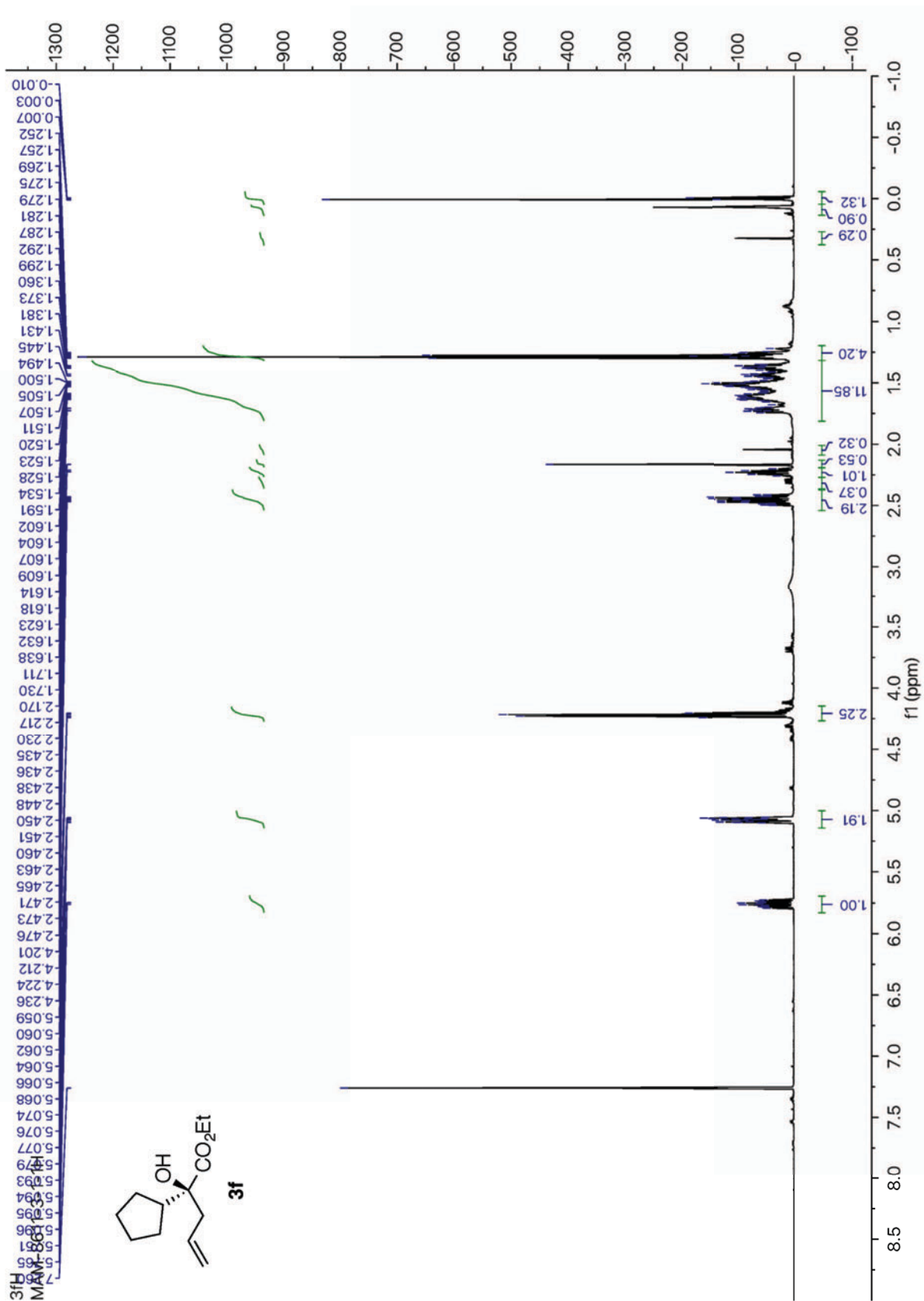
¹³C NMR spectra of compound **3d** (150 MHz, CDCl₃)



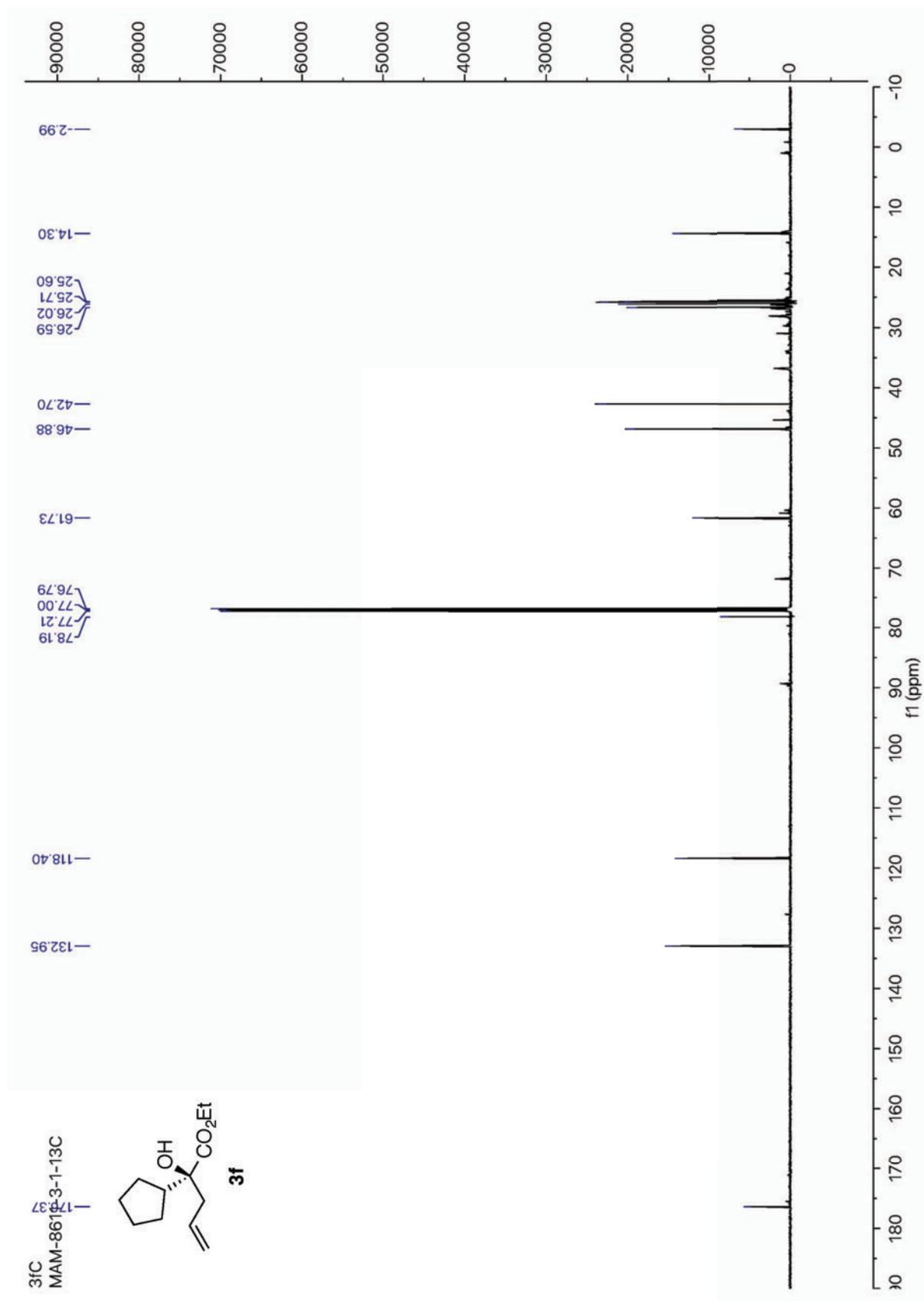
¹H NMR spectra of compound **3e** (400 MHz, CDCl₃)



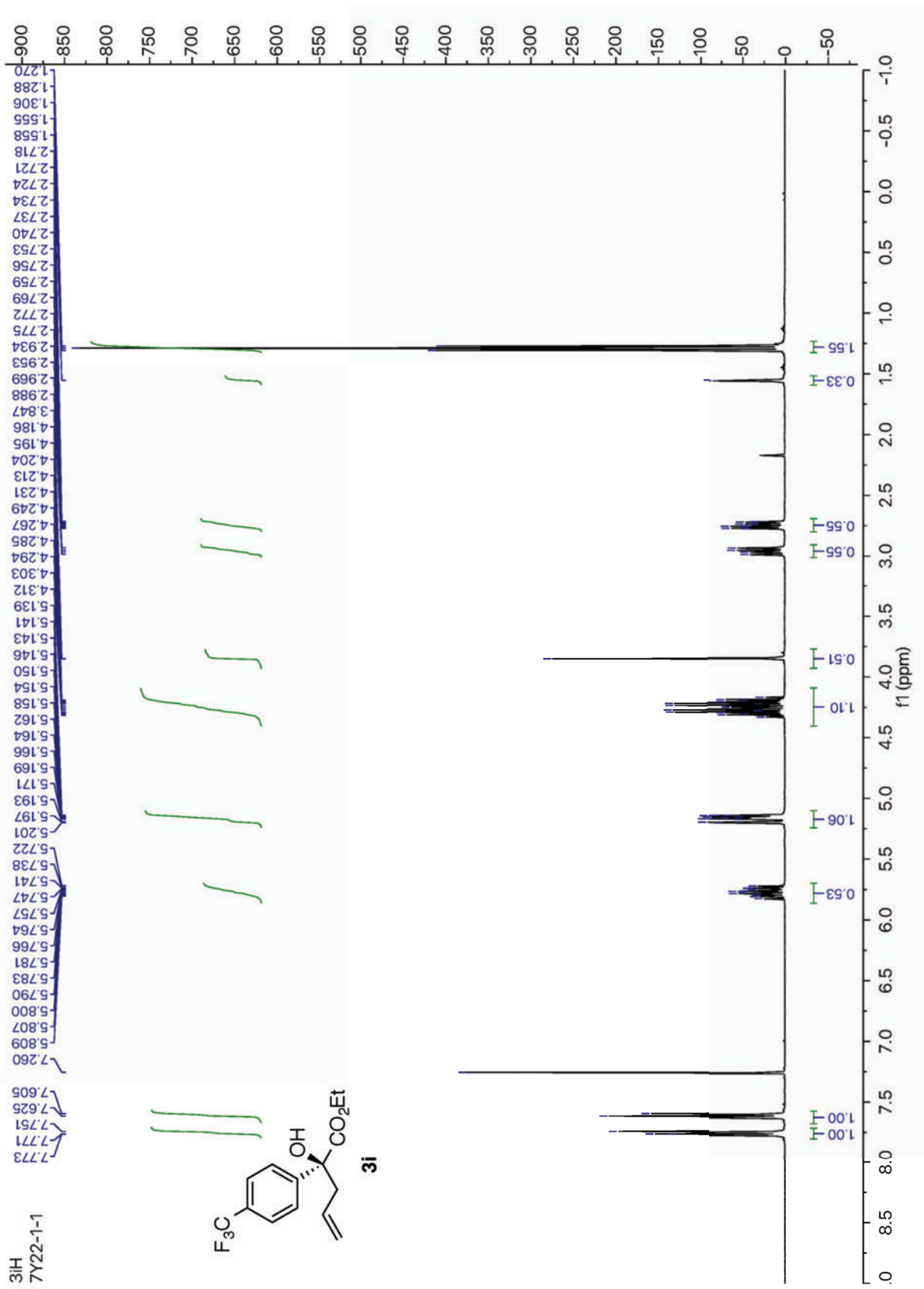
¹³C NMR spectra of compound **3e** (100 MHz, CDCl₃)



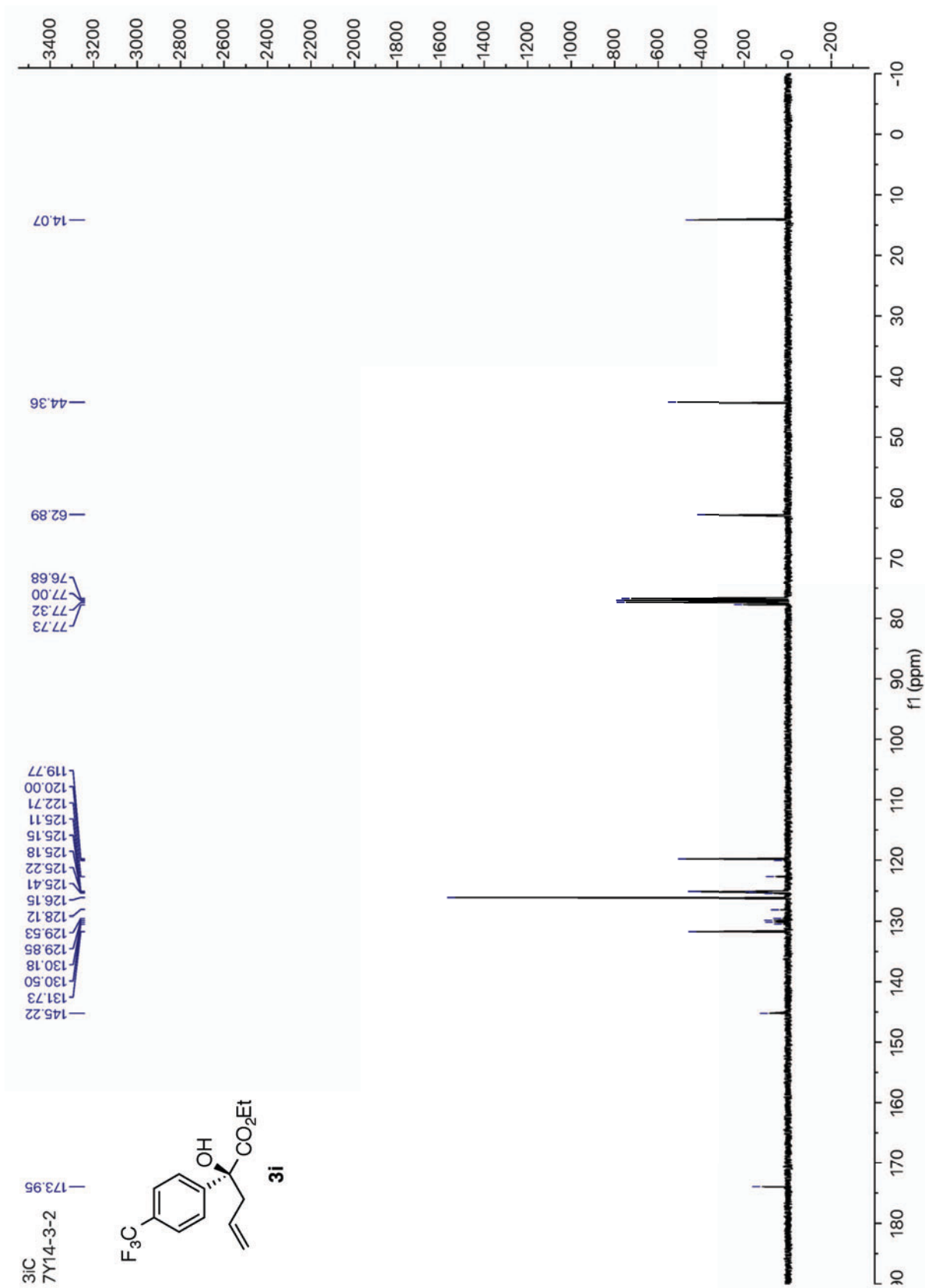
¹H NMR spectra of compound **3f** (600 MHz, CDCl₃)



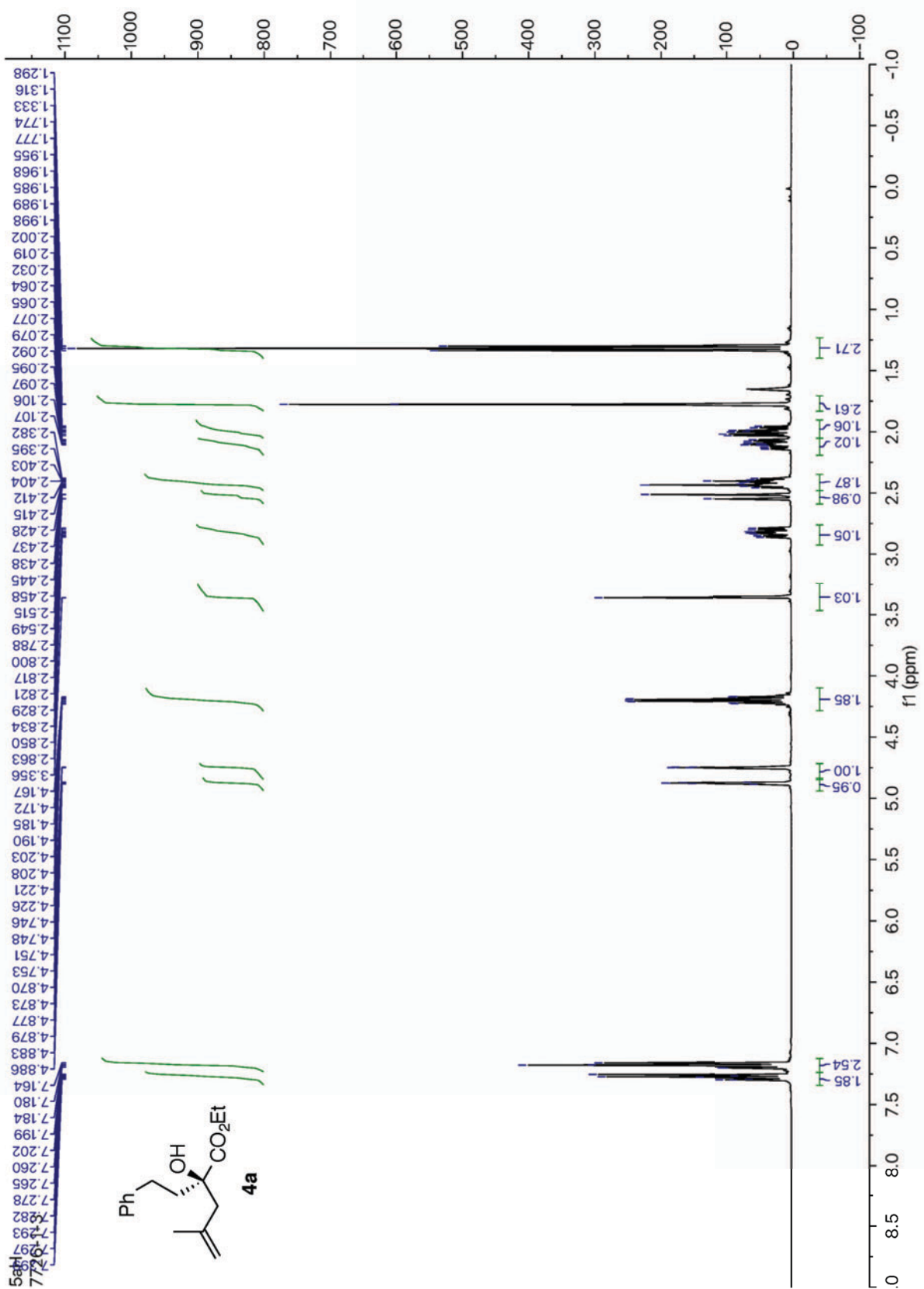
¹³C NMR spectra of compound **3f** (150 MHz, CDCl₃)



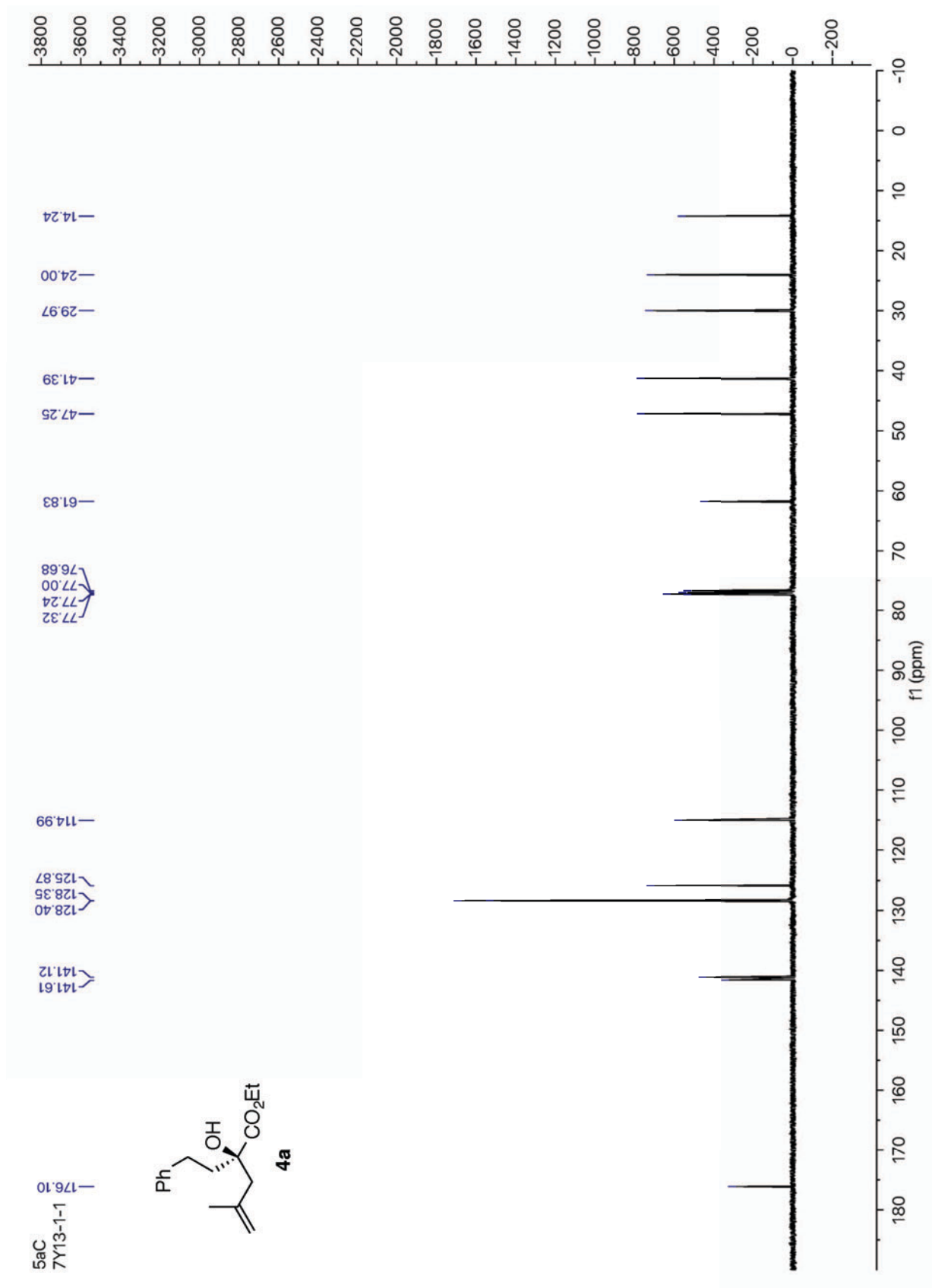
¹H NMR spectra of compound **3i** (400 MHz, CDCl₃)



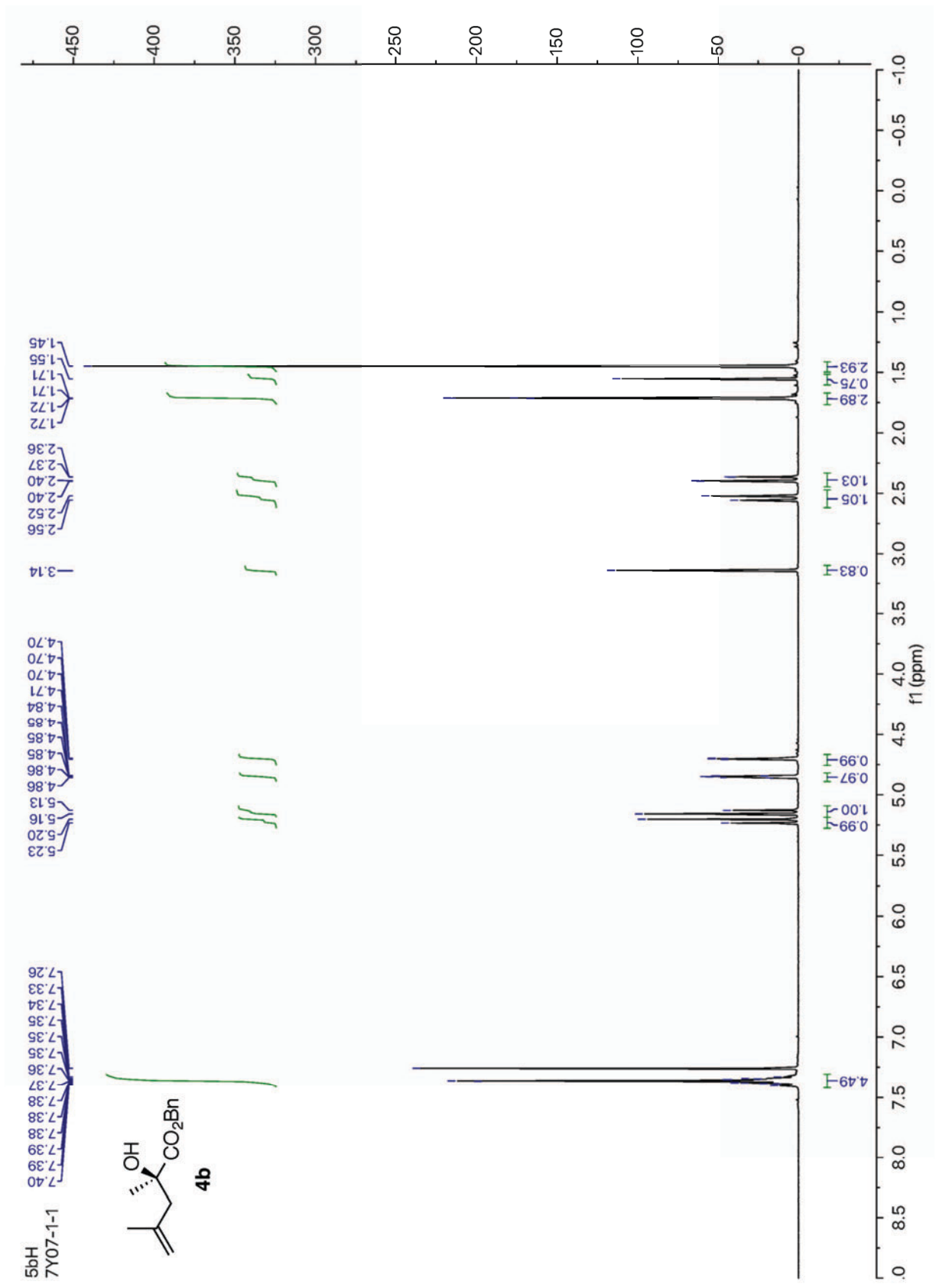
^{13}C NMR spectra of compound **3i** (100 MHz, CDCl_3)



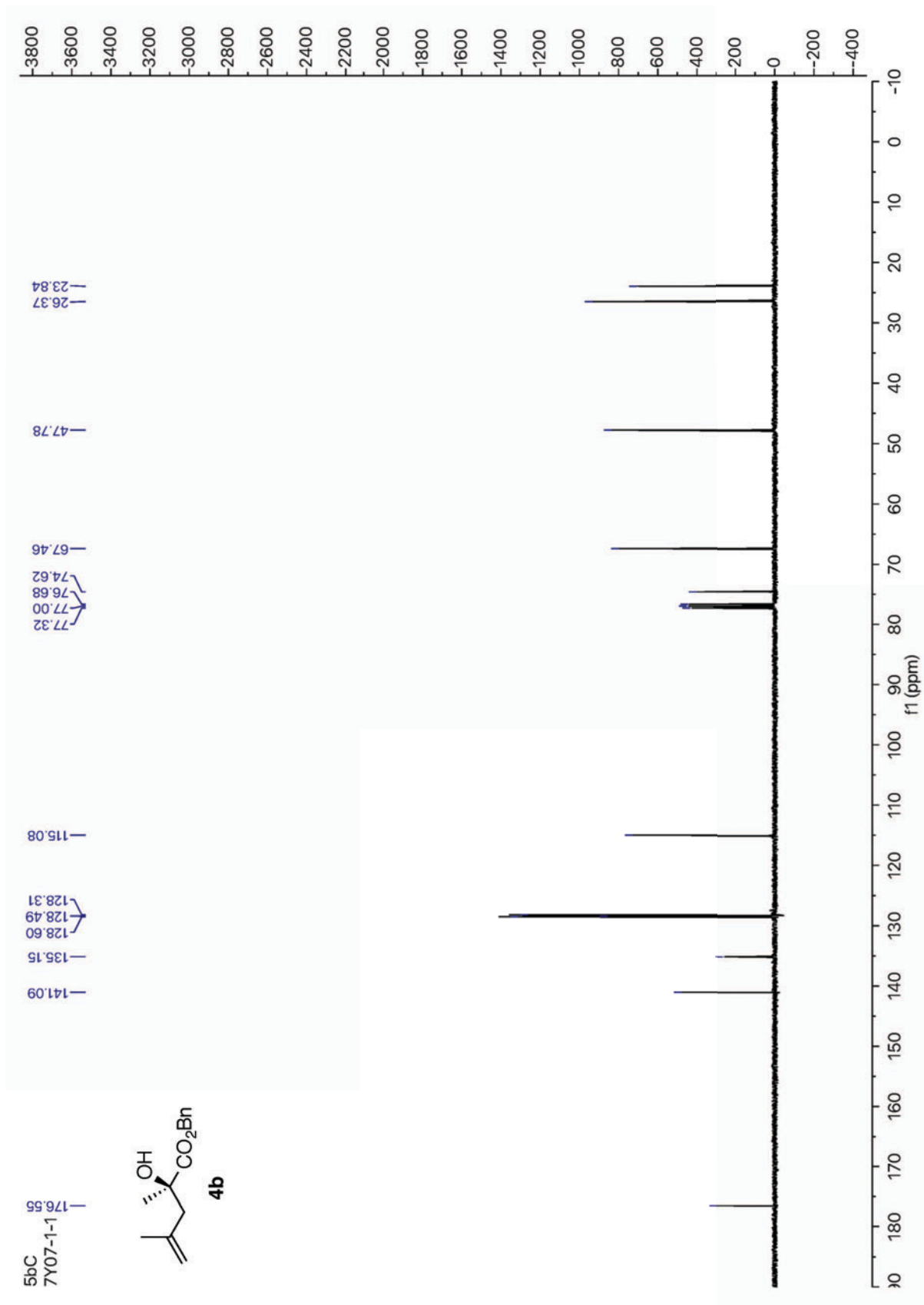
¹H NMR spectra of compound **4a** (400 MHz, CDCl₃)



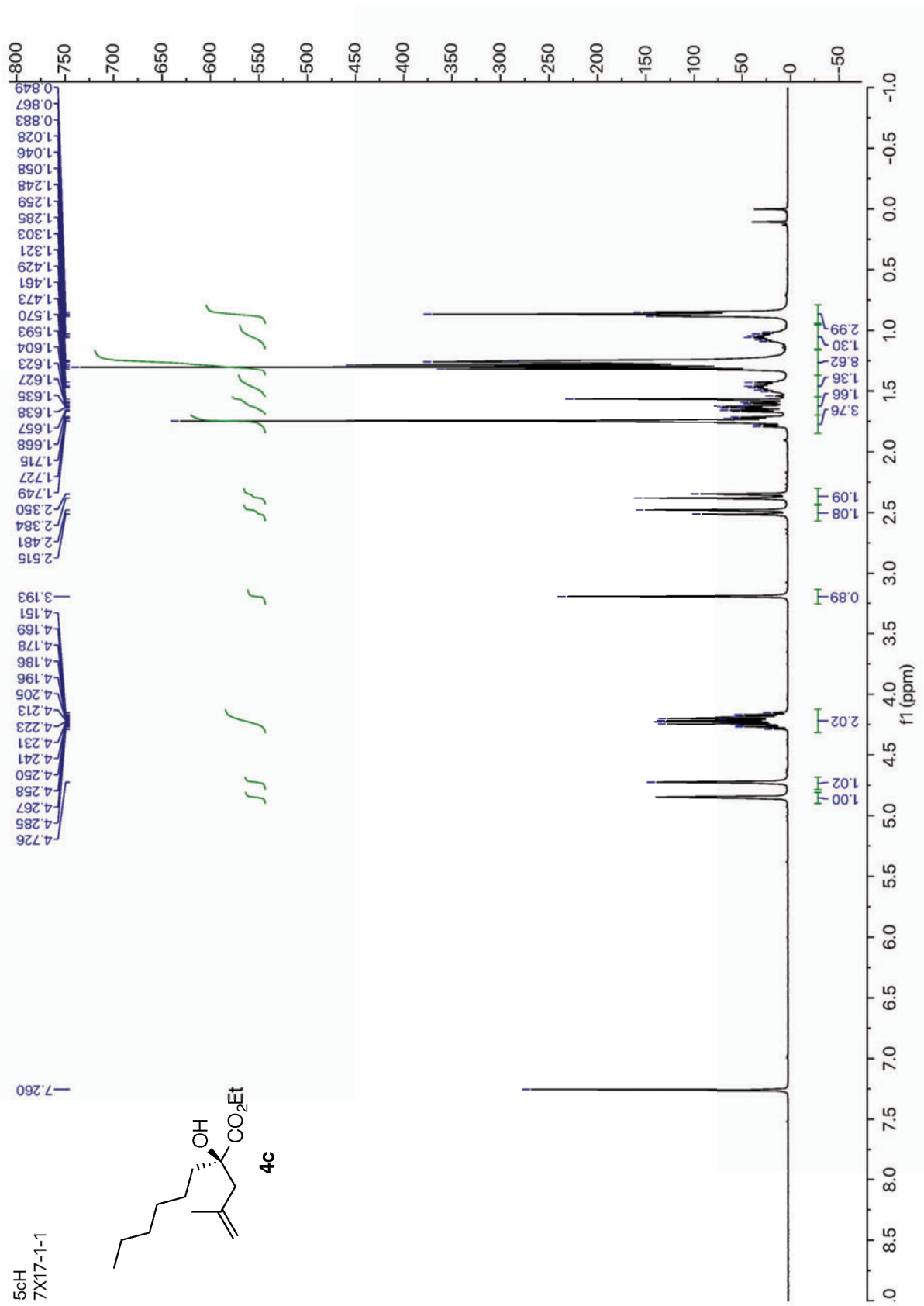
¹³C NMR spectra of compound **4a** (100 MHz, CDCl₃)



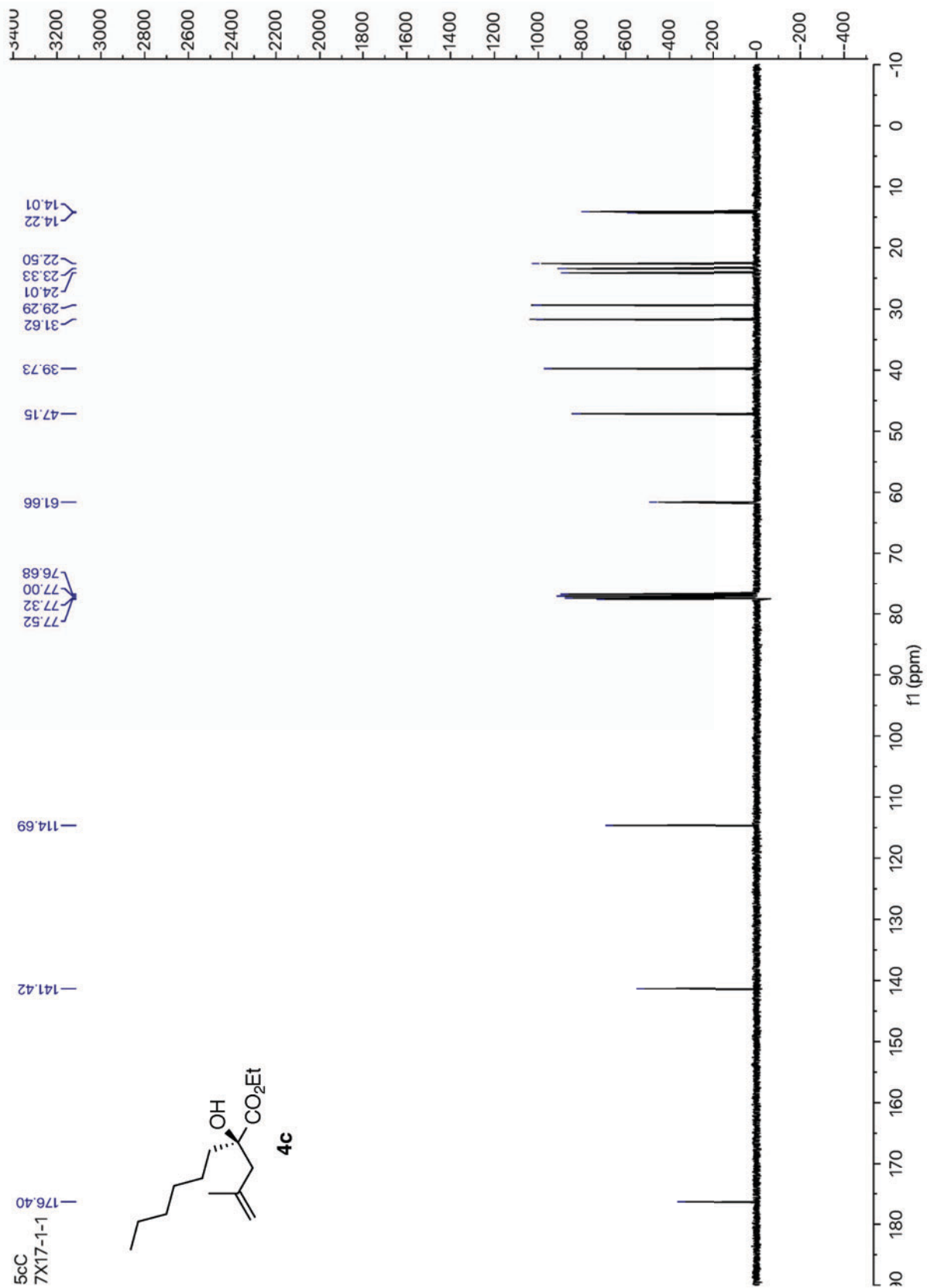
¹H NMR spectra of compound **4b** (400 MHz, CDCl₃)



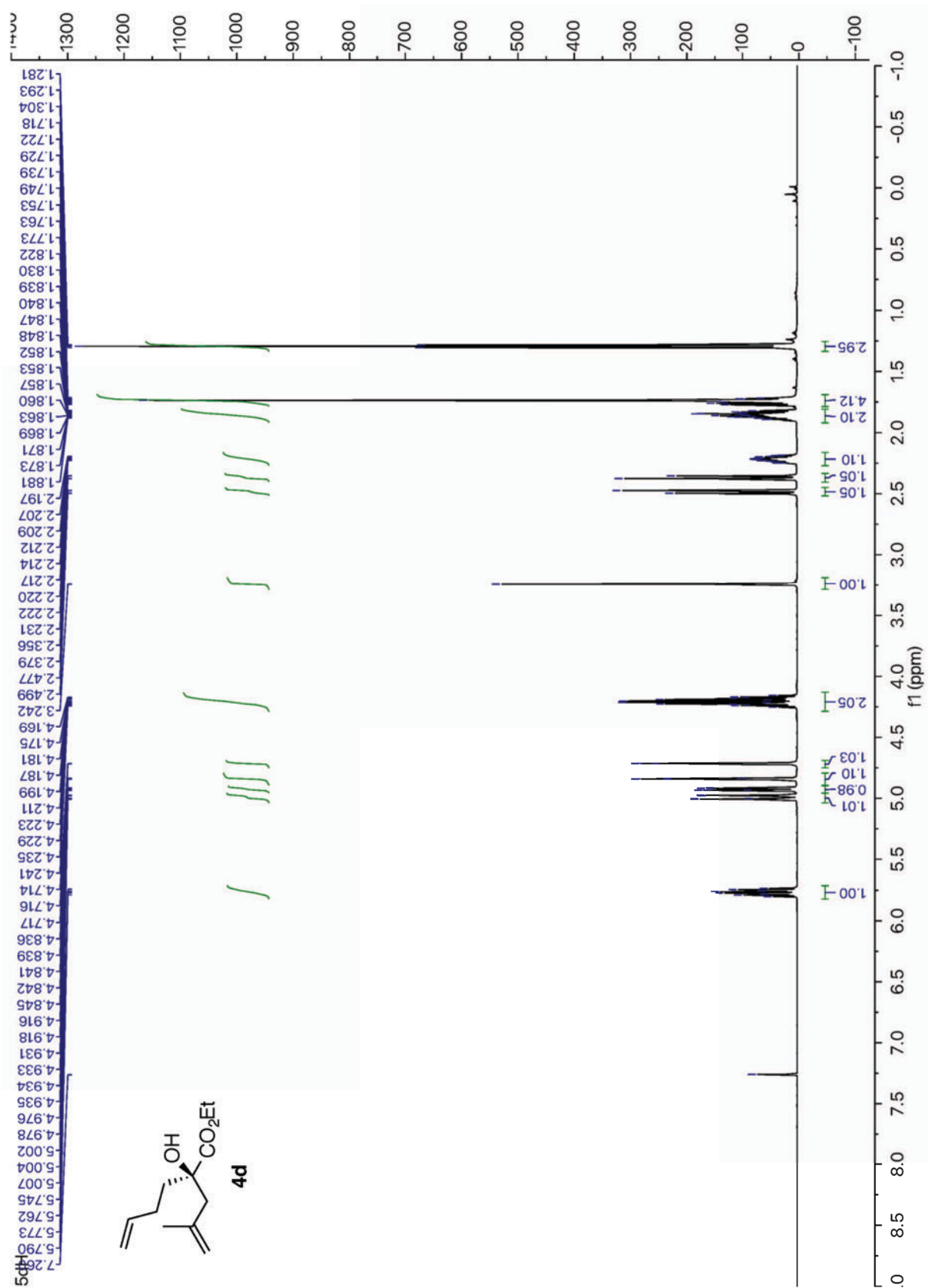
¹³C NMR spectra of compound **4b** (100 MHz, CDCl₃)



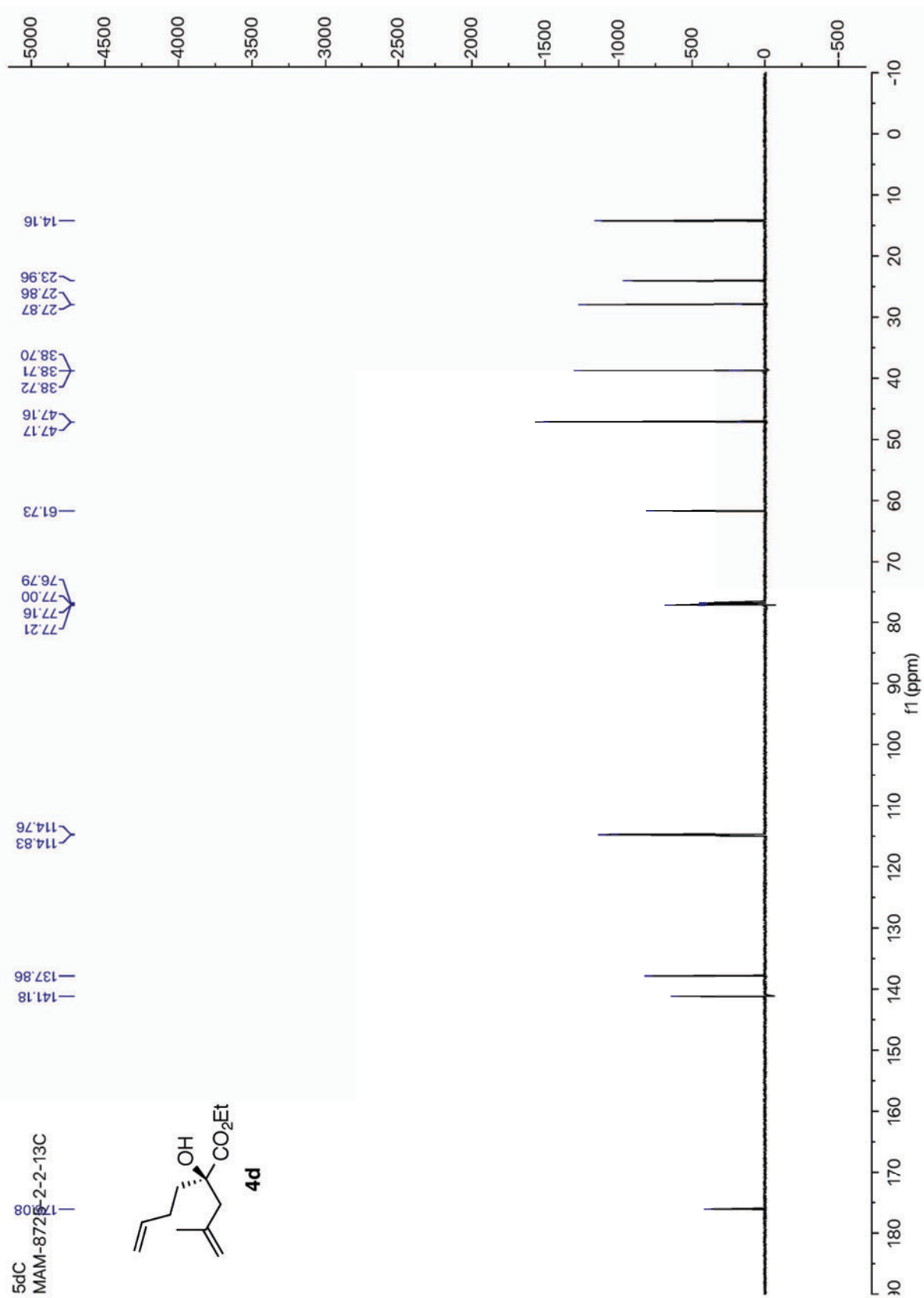
¹H NMR spectra of compound **4c** (400 MHz, CDCl₃)



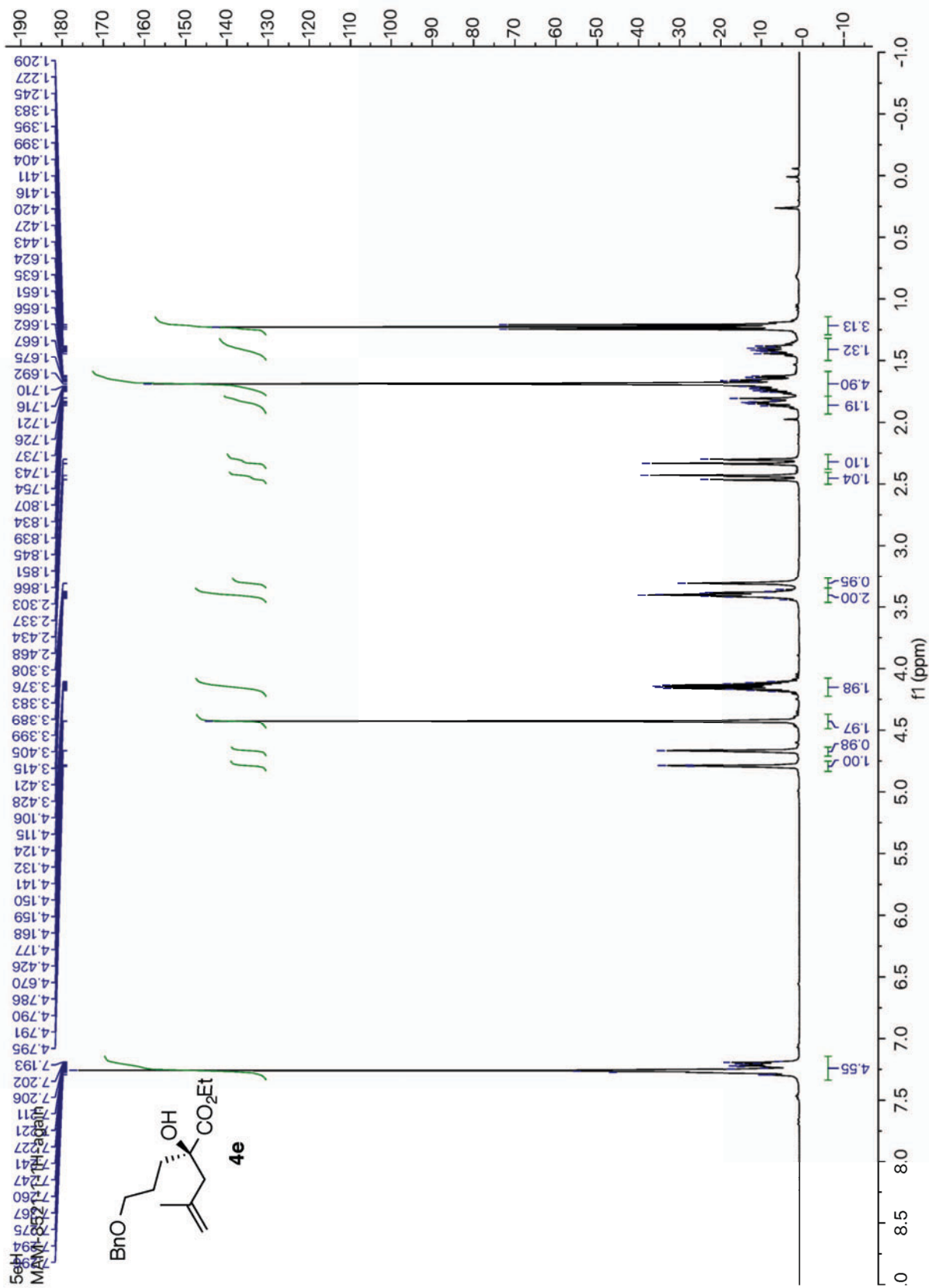
¹³C NMR spectra of compound **4c** (100 MHz, CDCl₃)



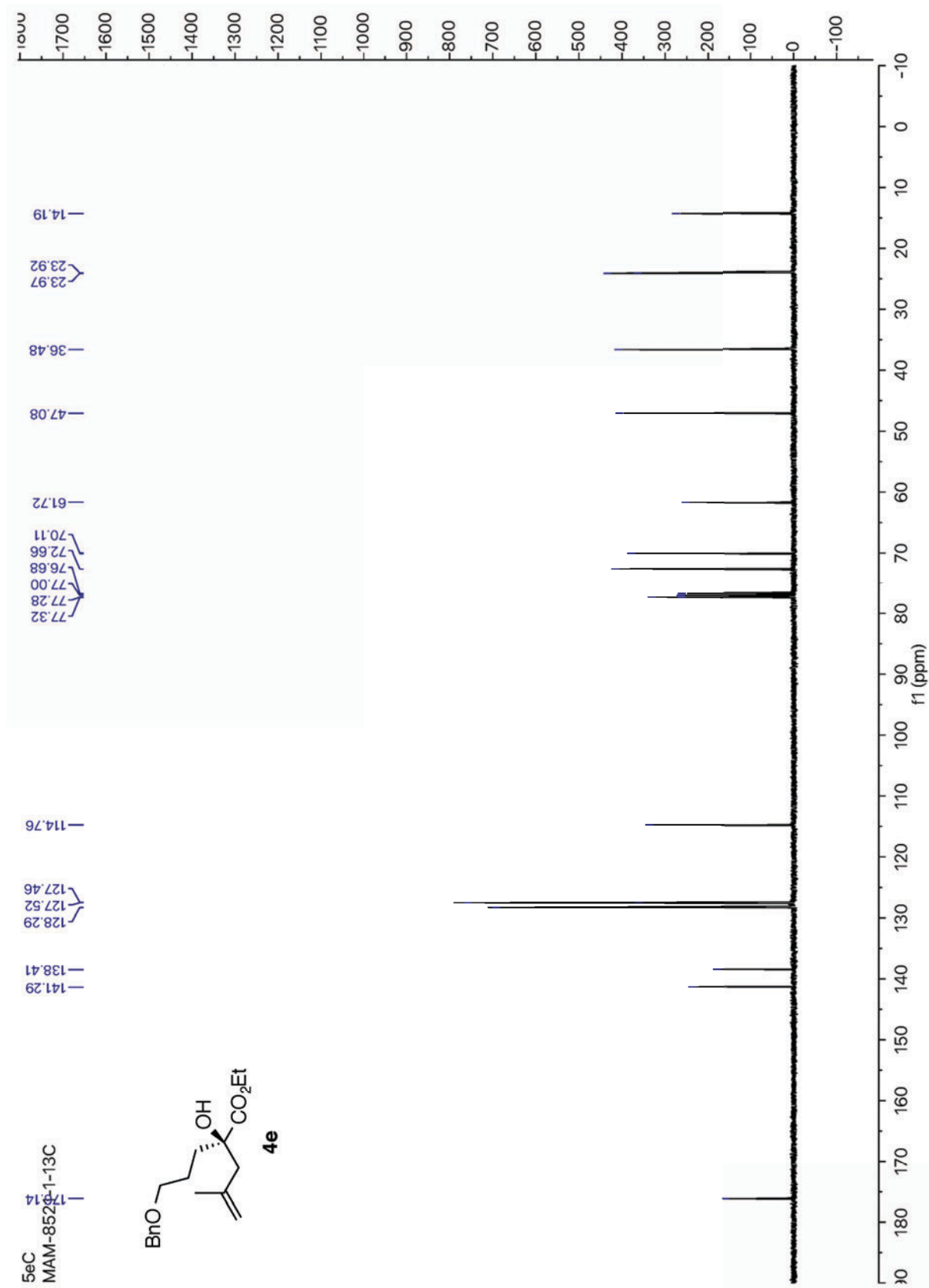
¹H NMR spectra of compound **4d** (600 MHz, CDCl₃)



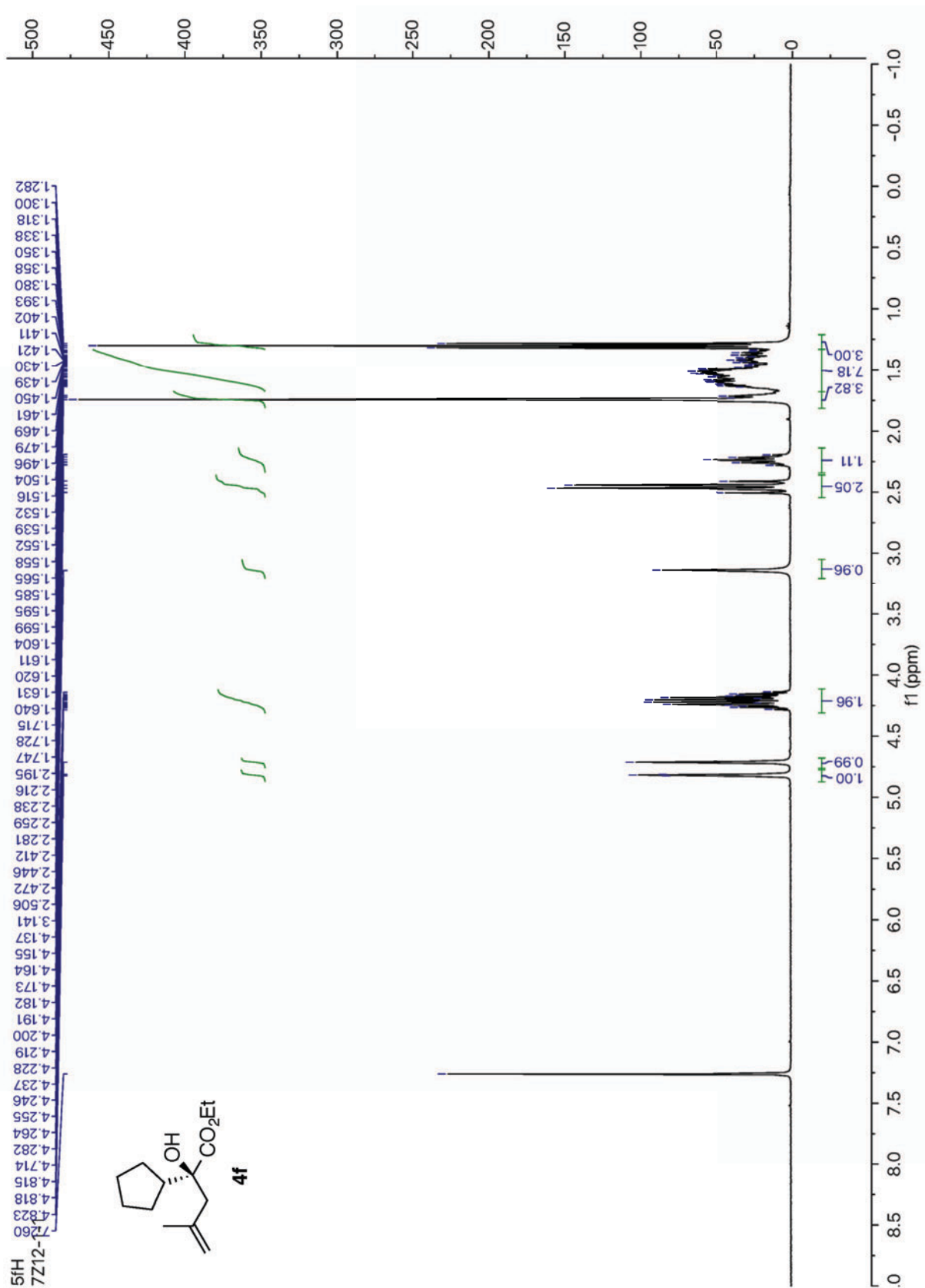
¹³C NMR spectra of compound **4d** (150 MHz, CDCl₃)



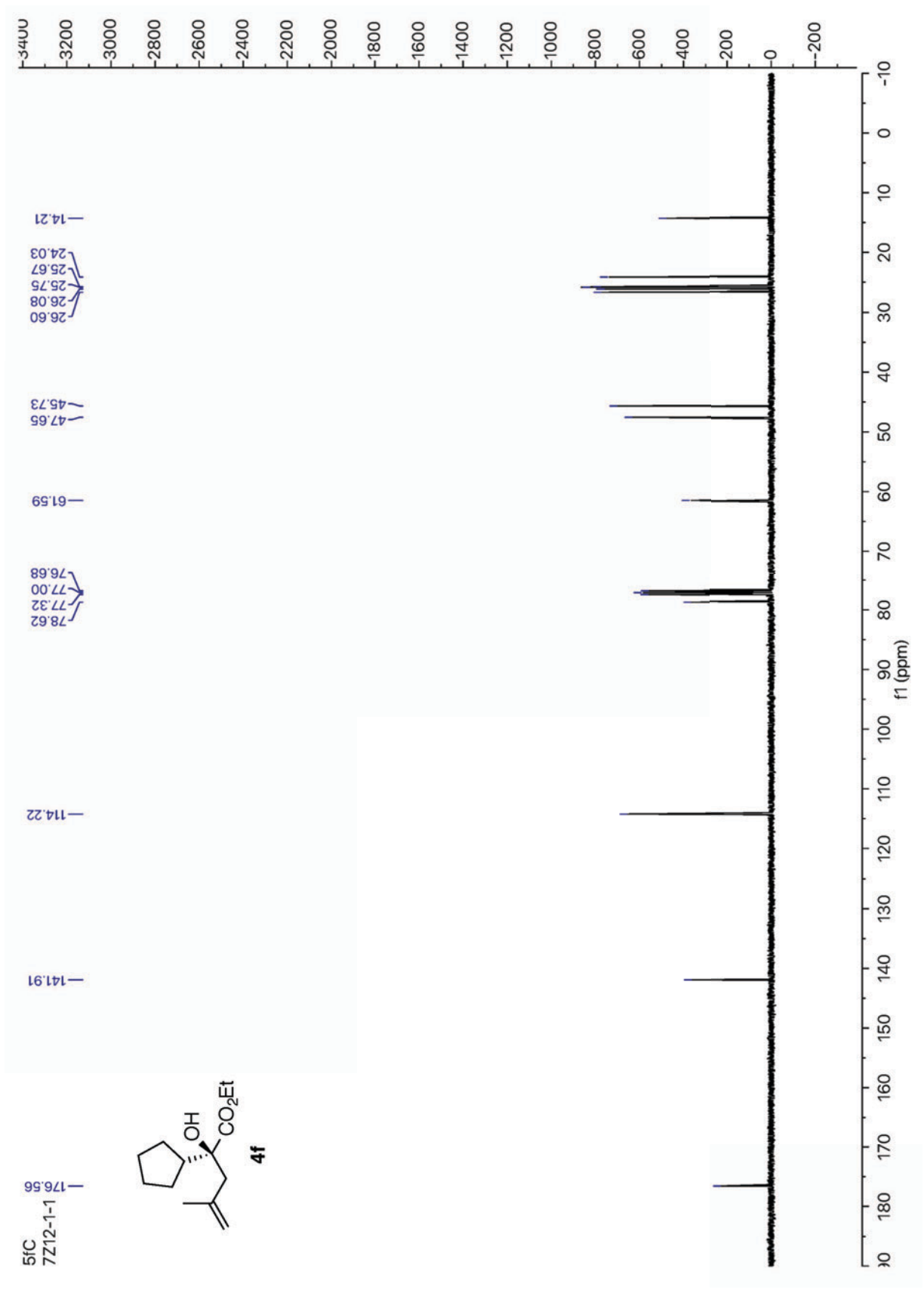
¹H NMR spectra of compound 4e (400 MHz, CDCl₃)



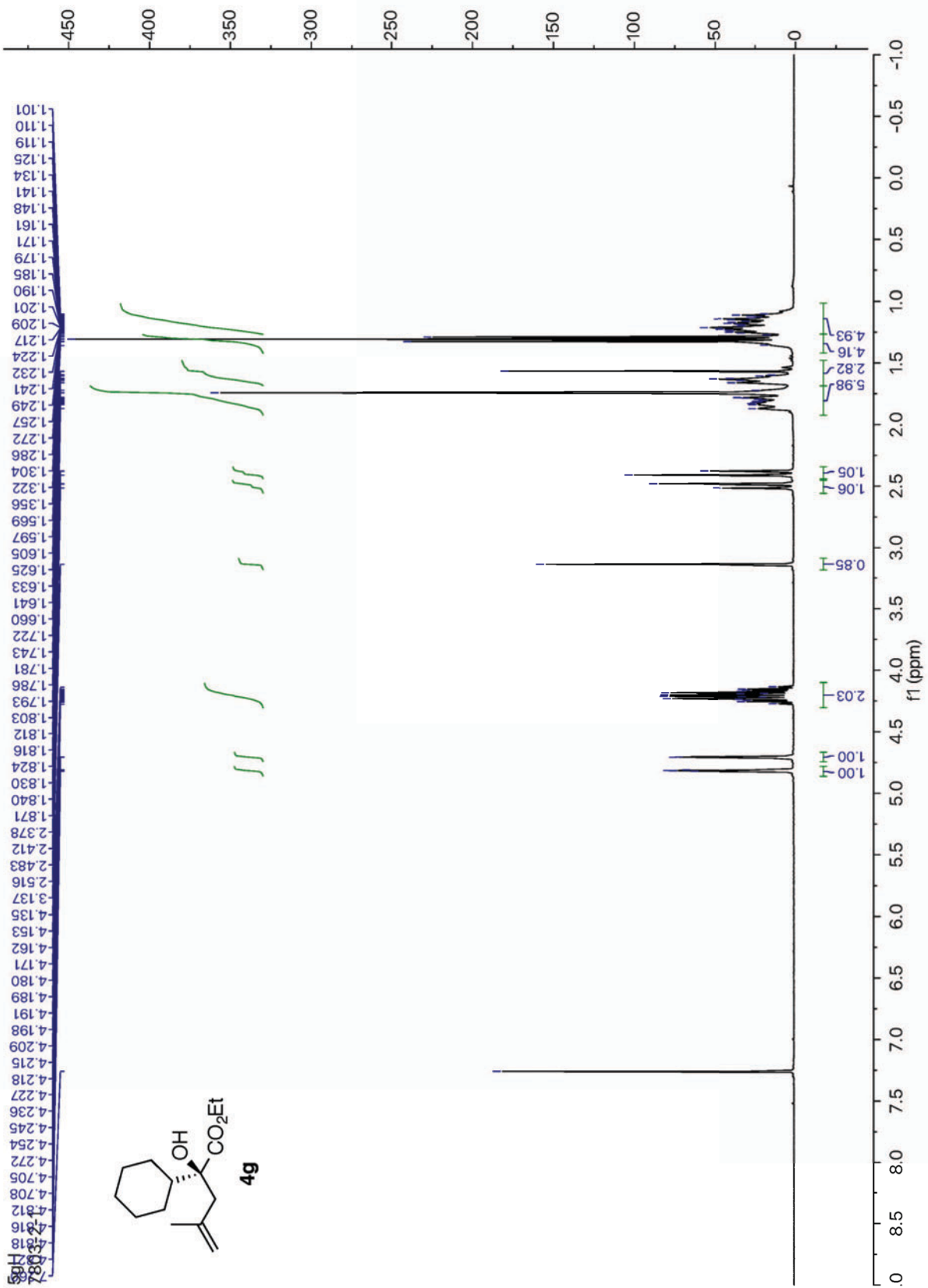
¹³C NMR spectra of compound **4e** (100 MHz, CDCl₃)



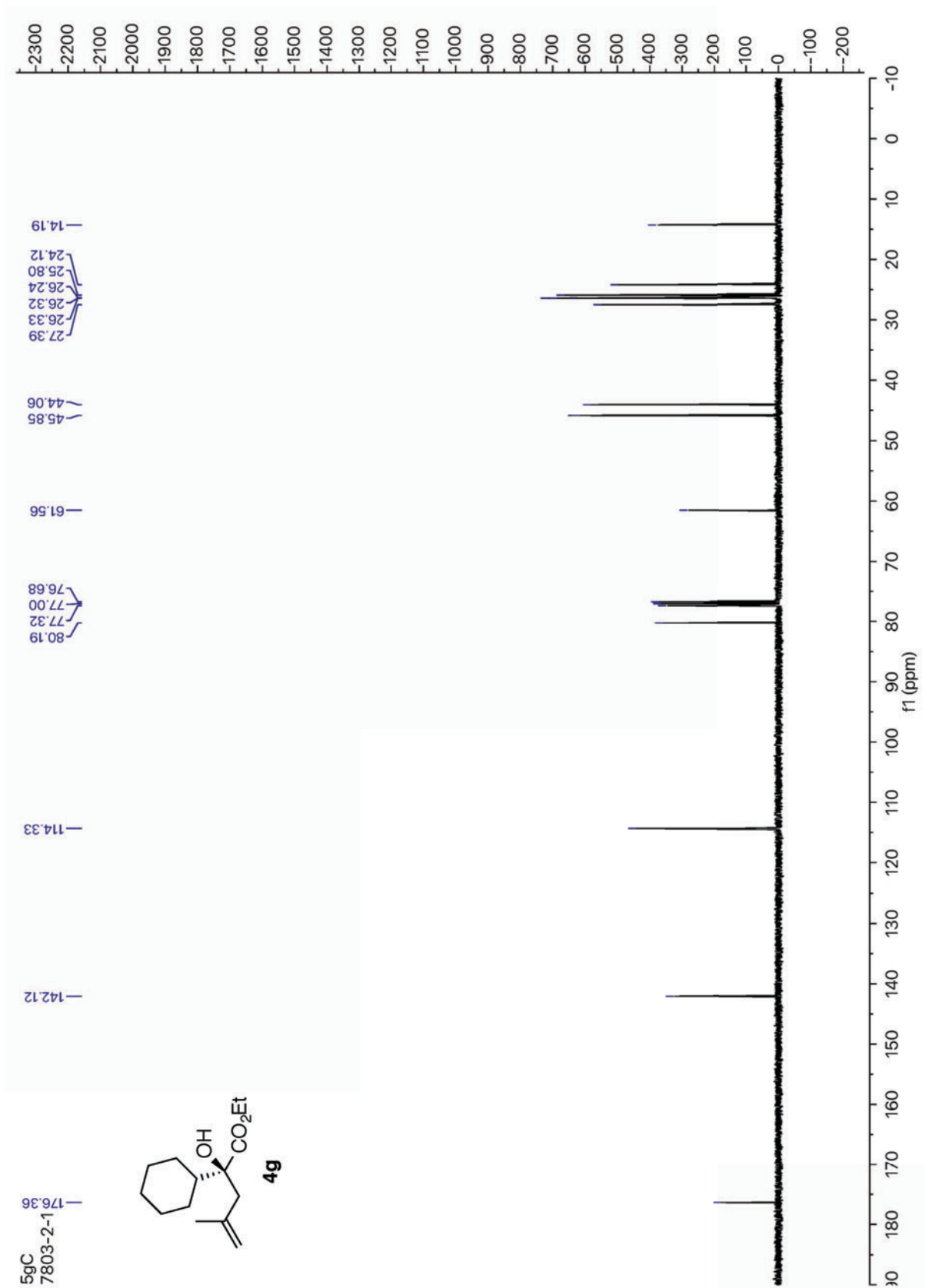
¹H NMR spectra of compound **4f** (400 MHz, CDCl₃)



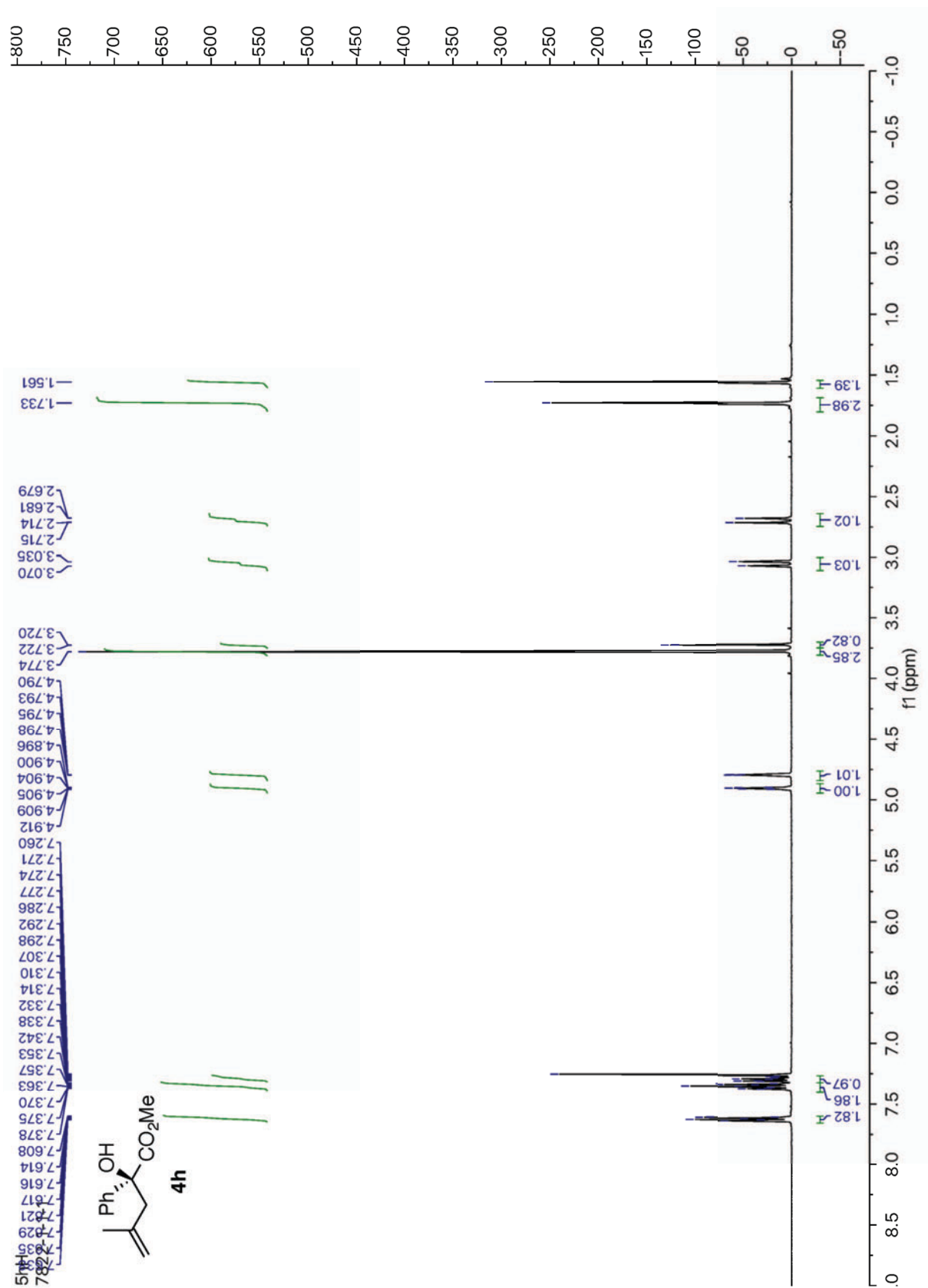
¹³C NMR spectra of compound **4f** (100 MHz, CDCl₃)



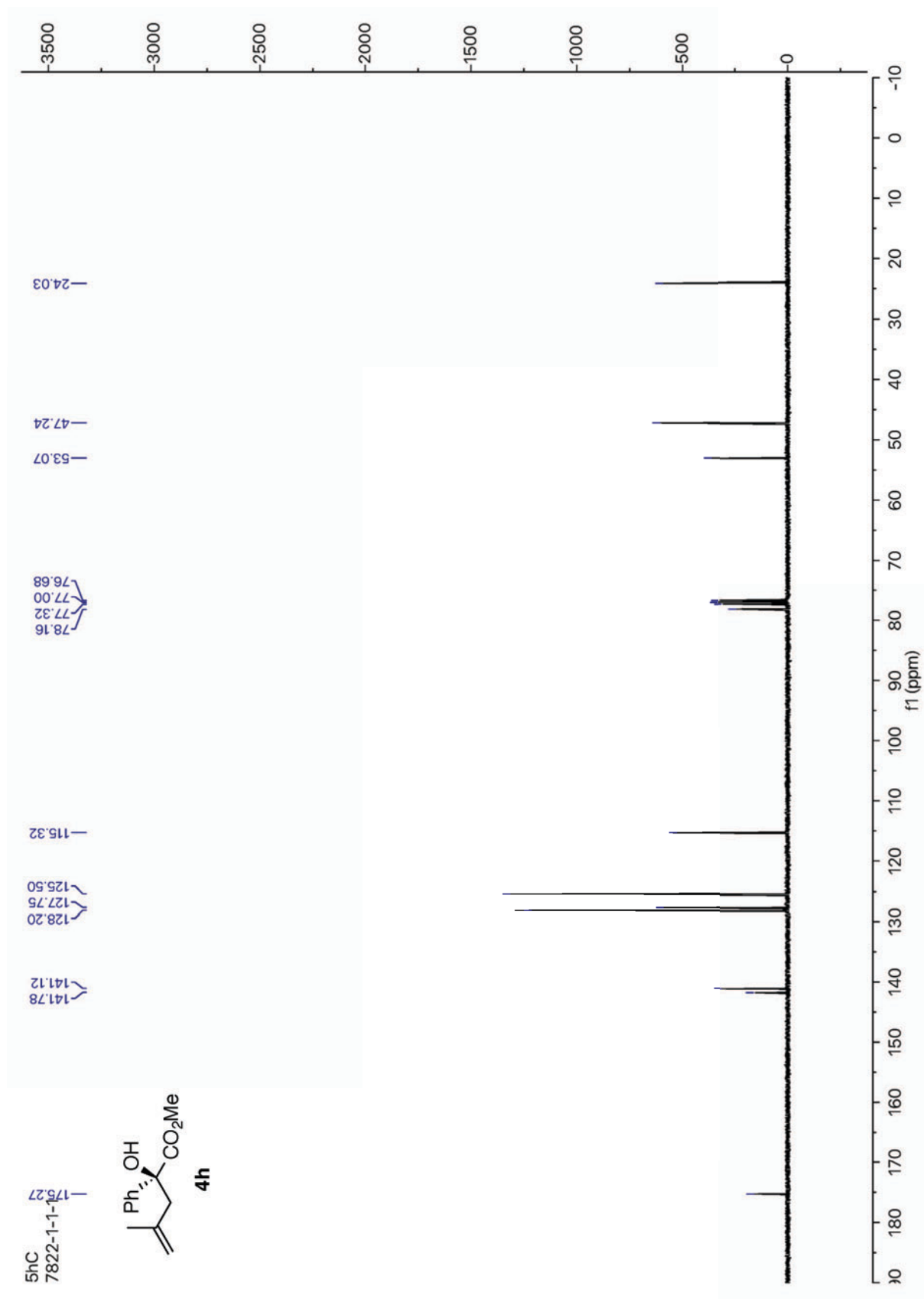
¹H NMR spectra of compound 4g (400 MHz, CDCl₃)



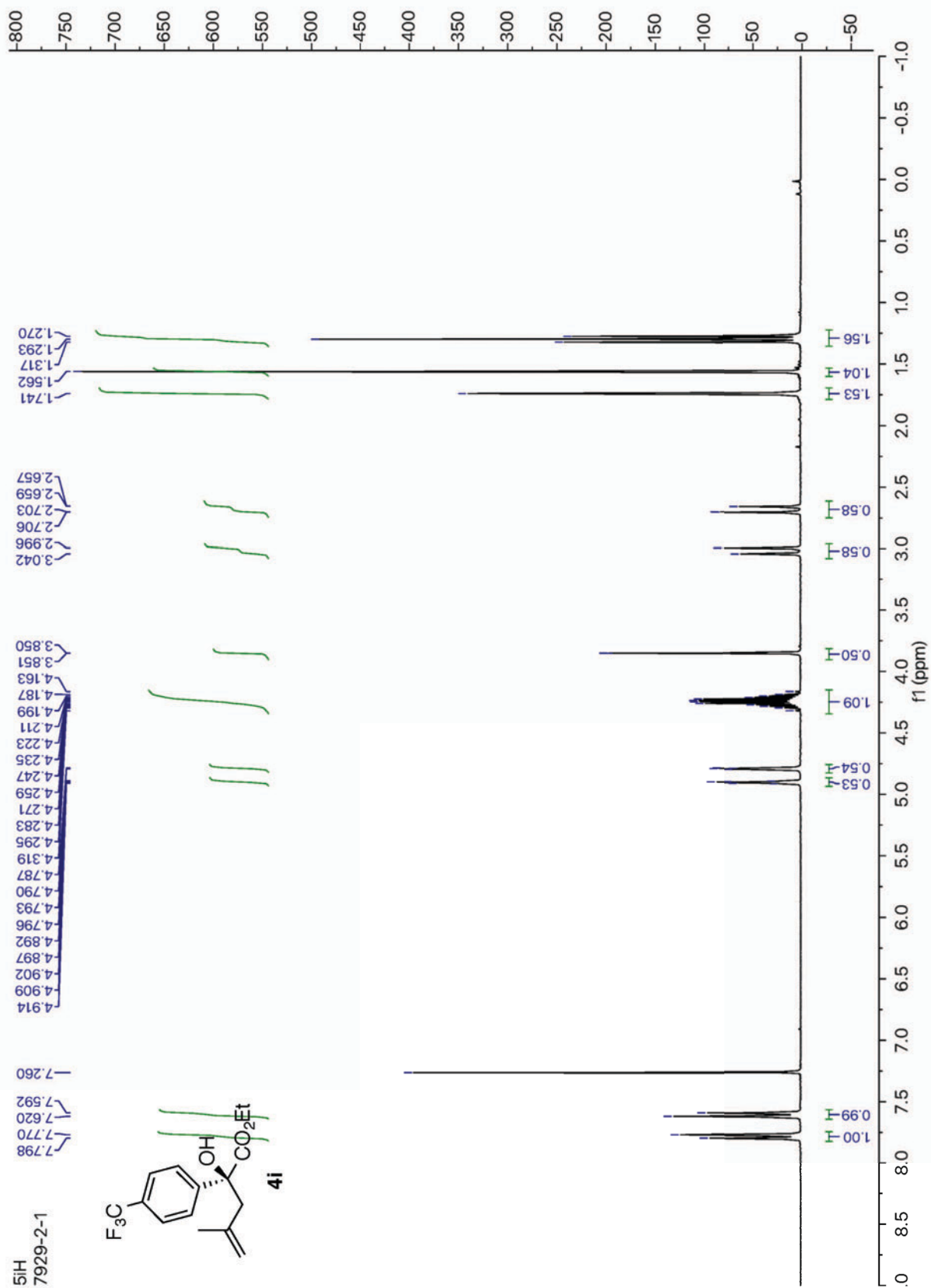
¹³C NMR spectra of compound **4g** (100 MHz, CDCl₃)



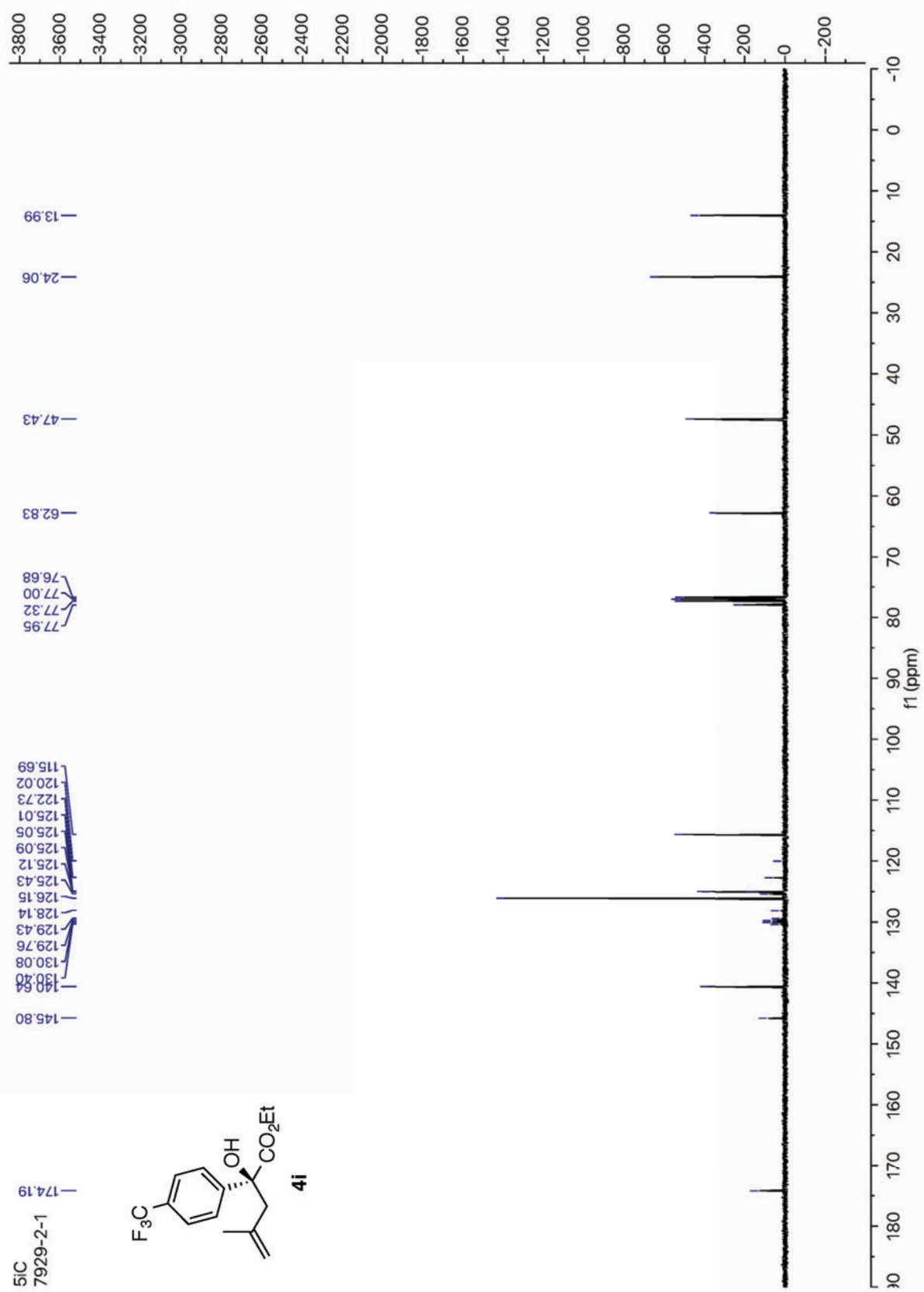
¹H NMR spectra of compound **4h** (400 MHz, CDCl₃)



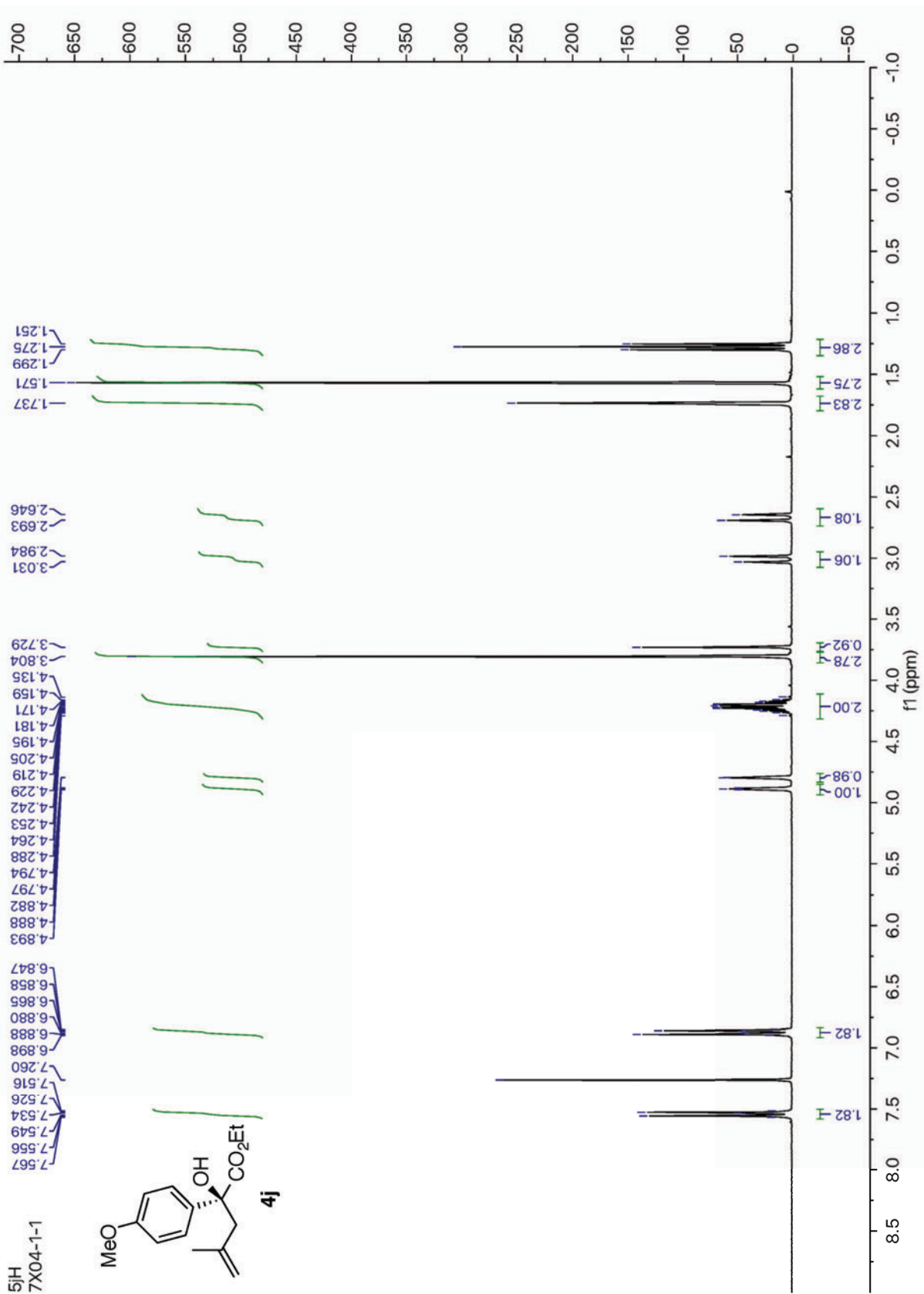
¹³C NMR spectra of compound **4h** (100 MHz, CDCl₃)



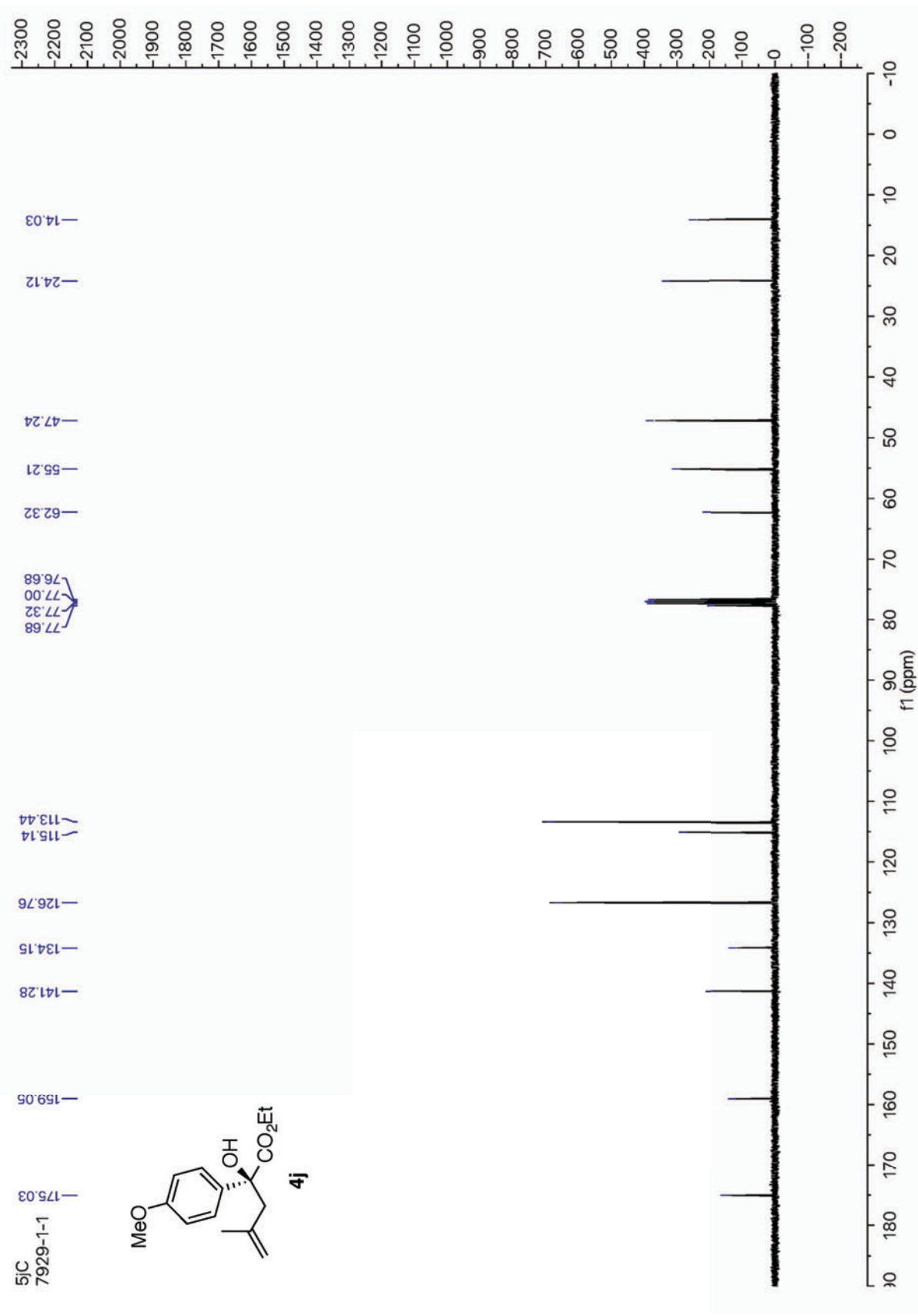
¹H NMR spectra of compound **4i** (300 MHz, CDCl₃)



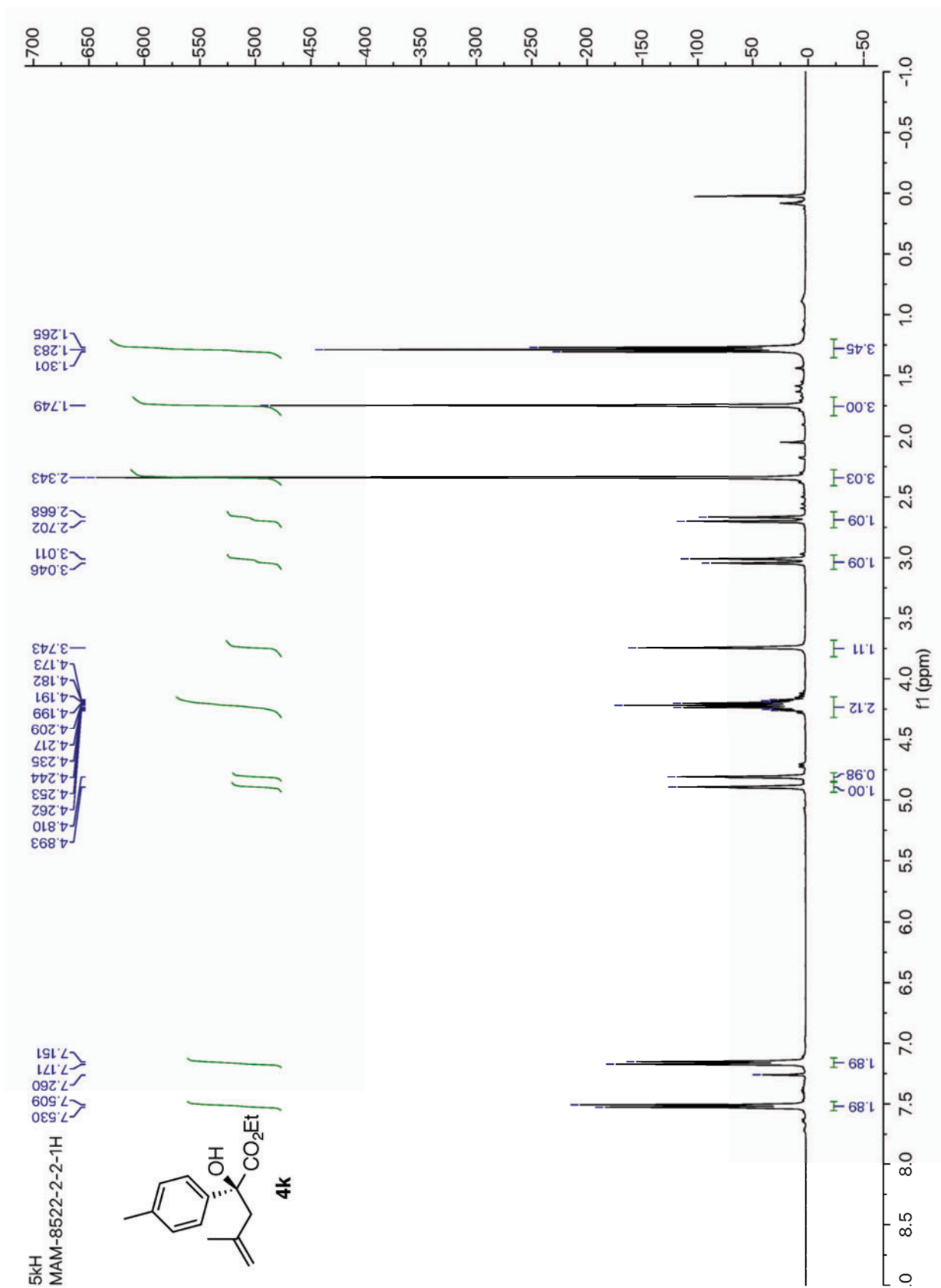
¹³C NMR spectra of compound **4i** (100 MHz, CDCl₃)



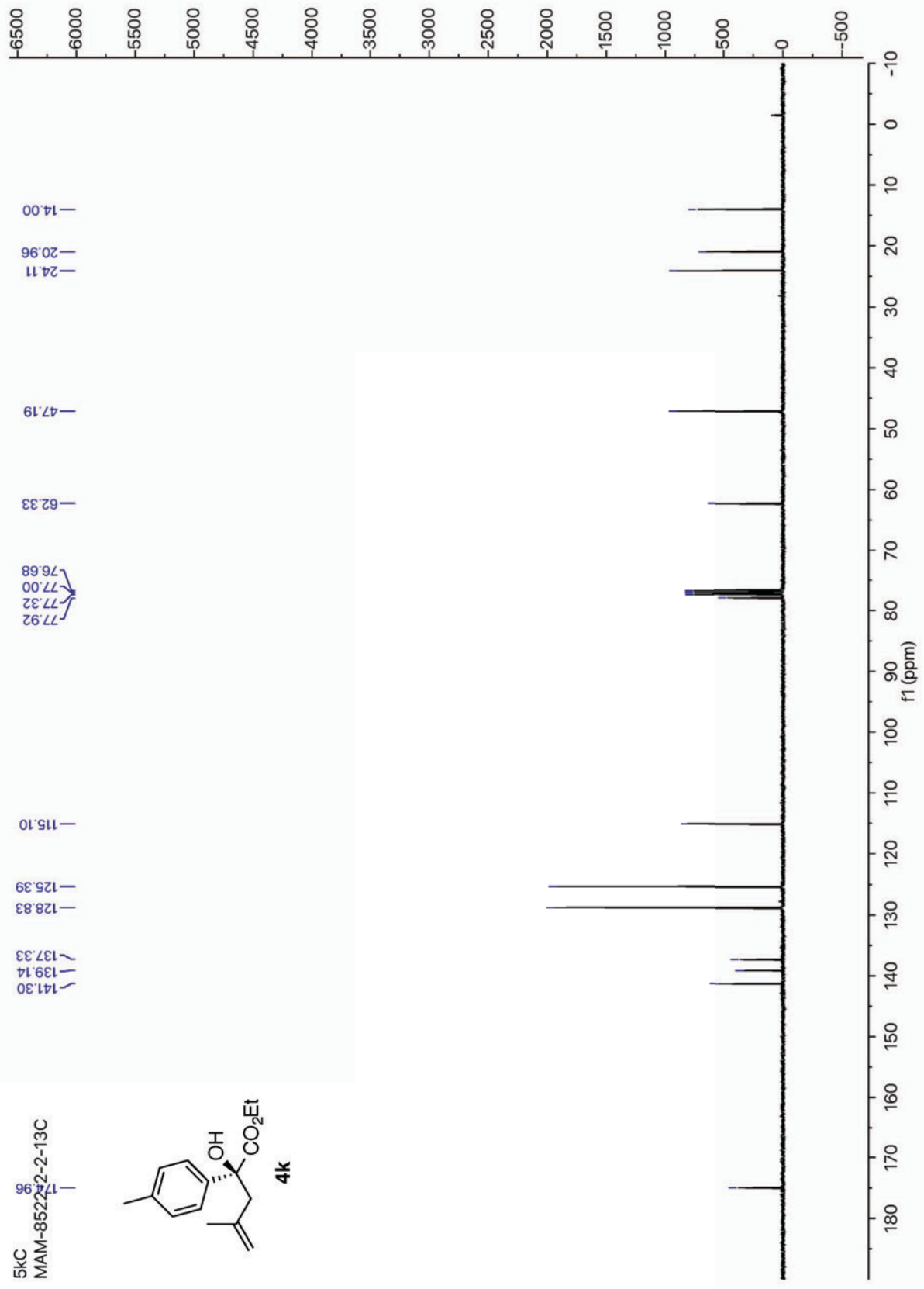
¹H NMR spectra of compound **4j** (300 MHz, CDCl₃)



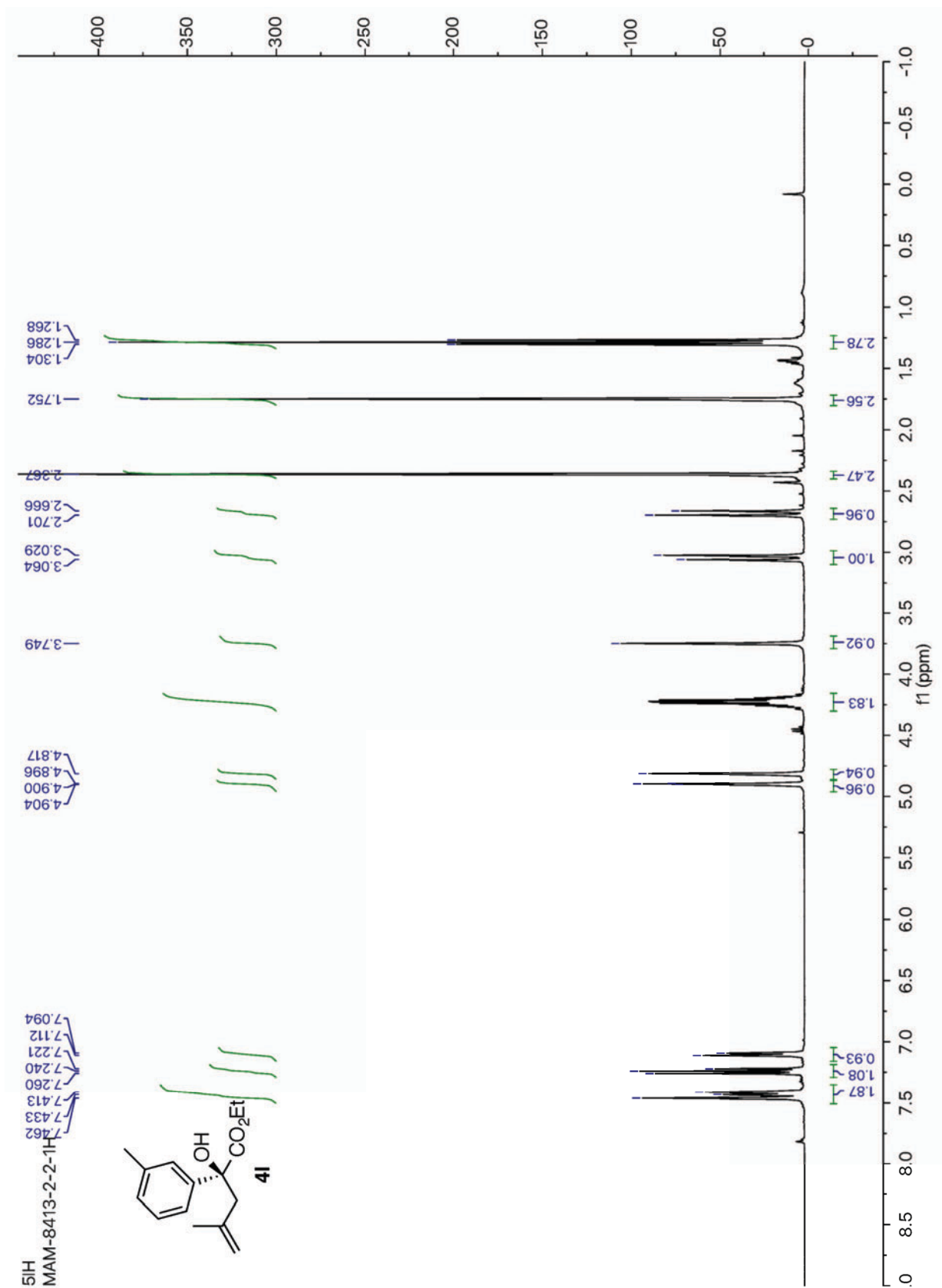
¹³C NMR spectra of compound **4j** (100 MHz, CDCl₃)



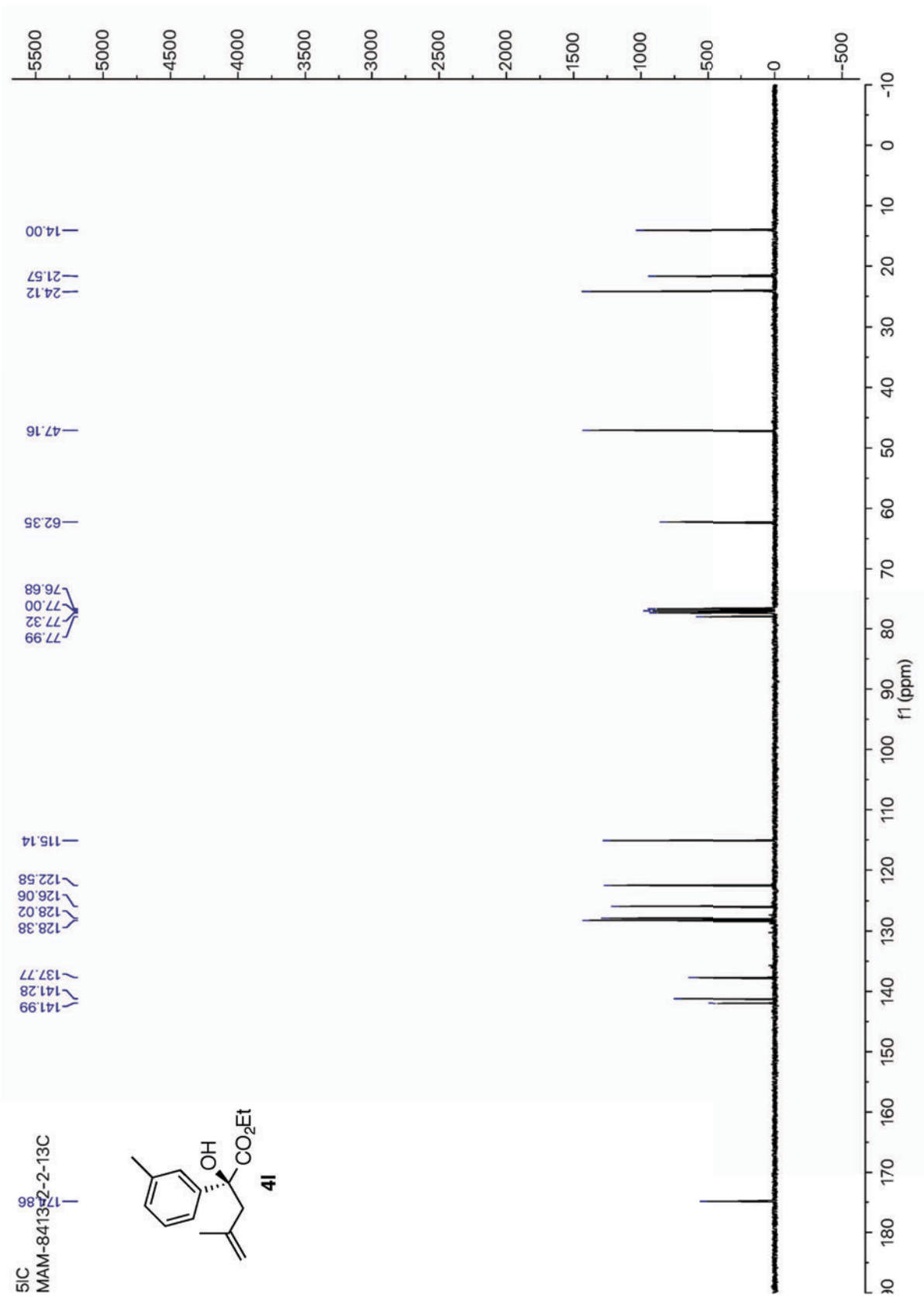
¹H NMR spectra of compound **4k** (400 MHz, CDCl₃)



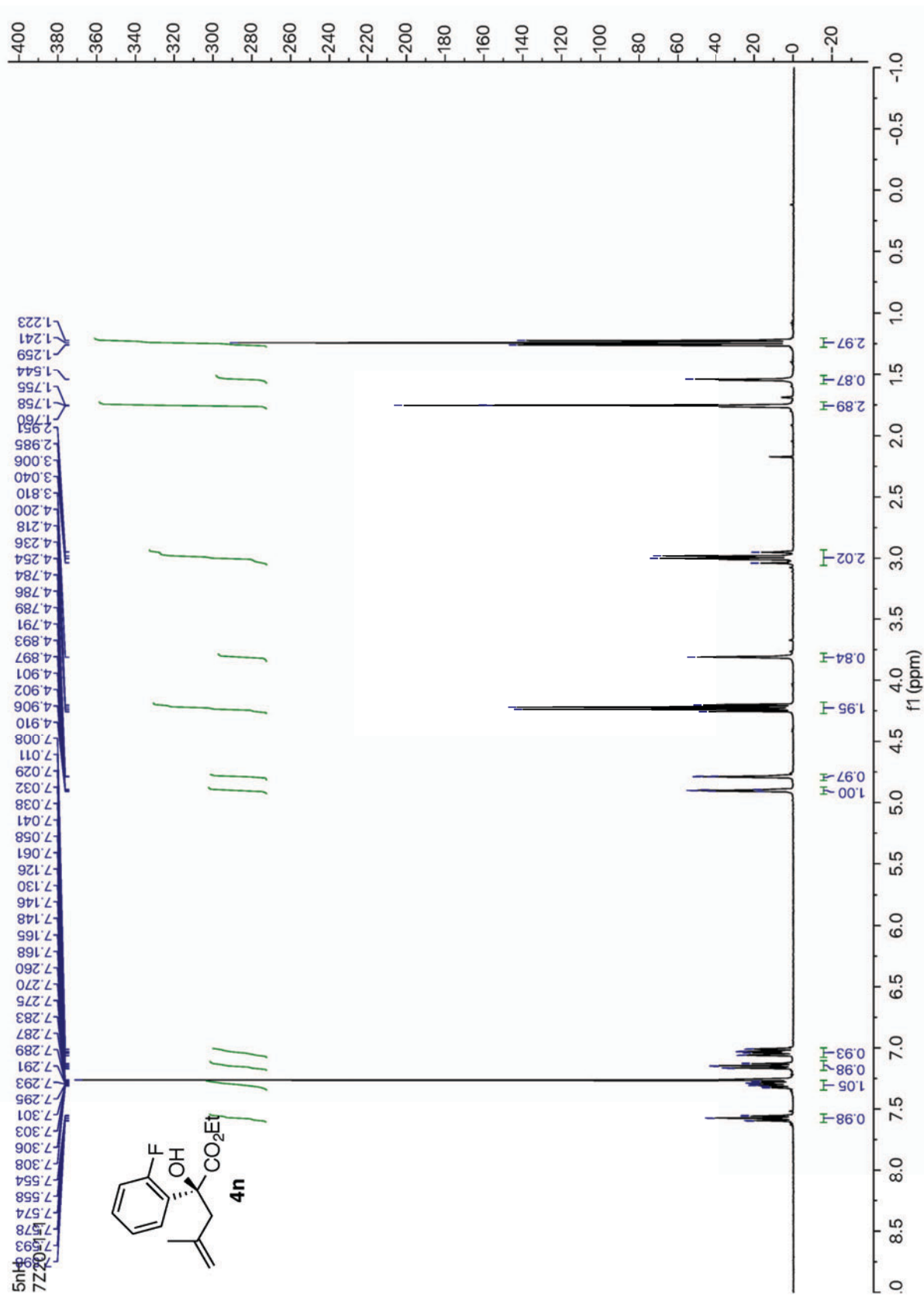
¹³C NMR spectra of compound **4k** (100 MHz, CDCl₃)



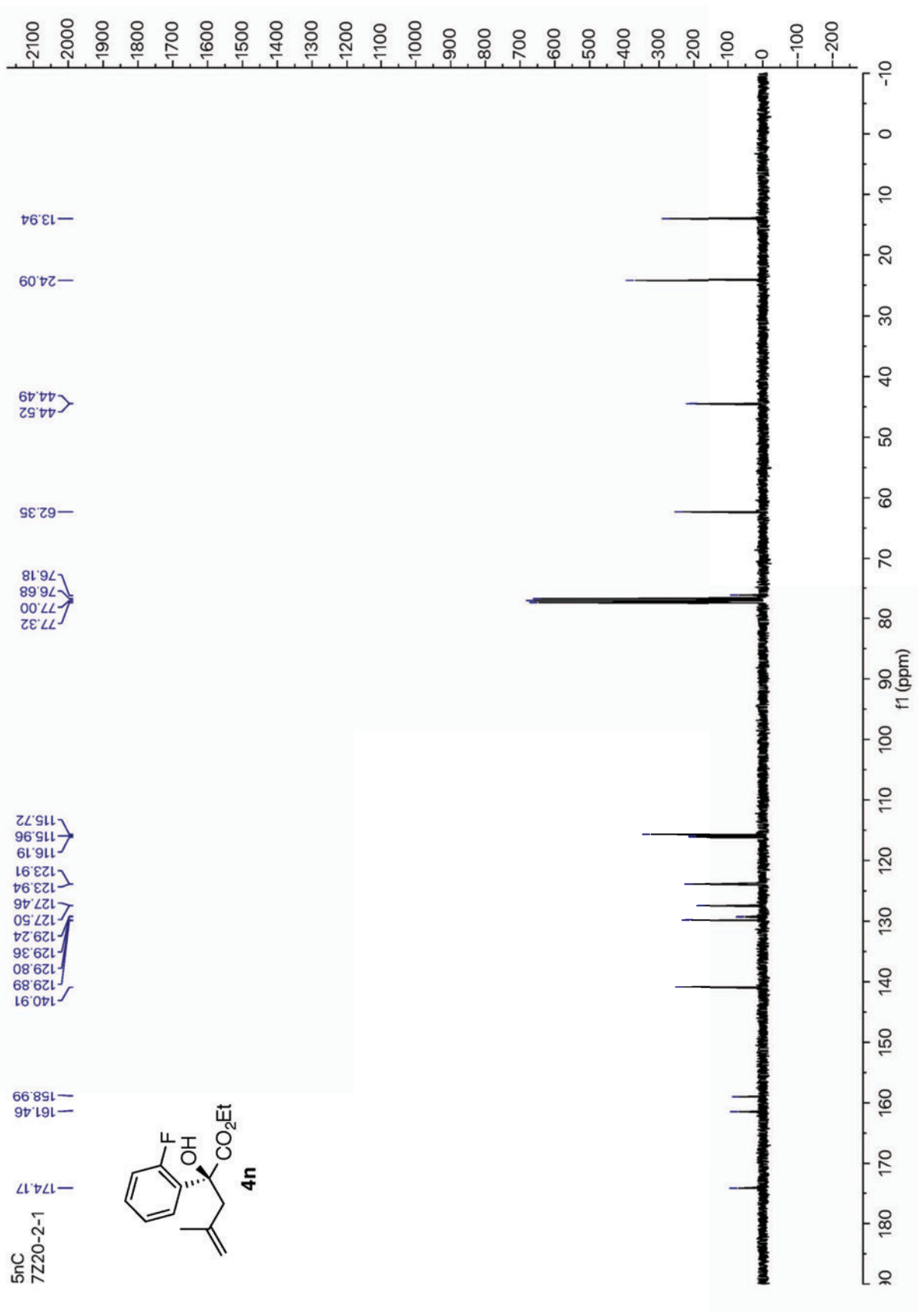
¹H NMR spectra of compound **4I** (400 MHz, CDCl₃)



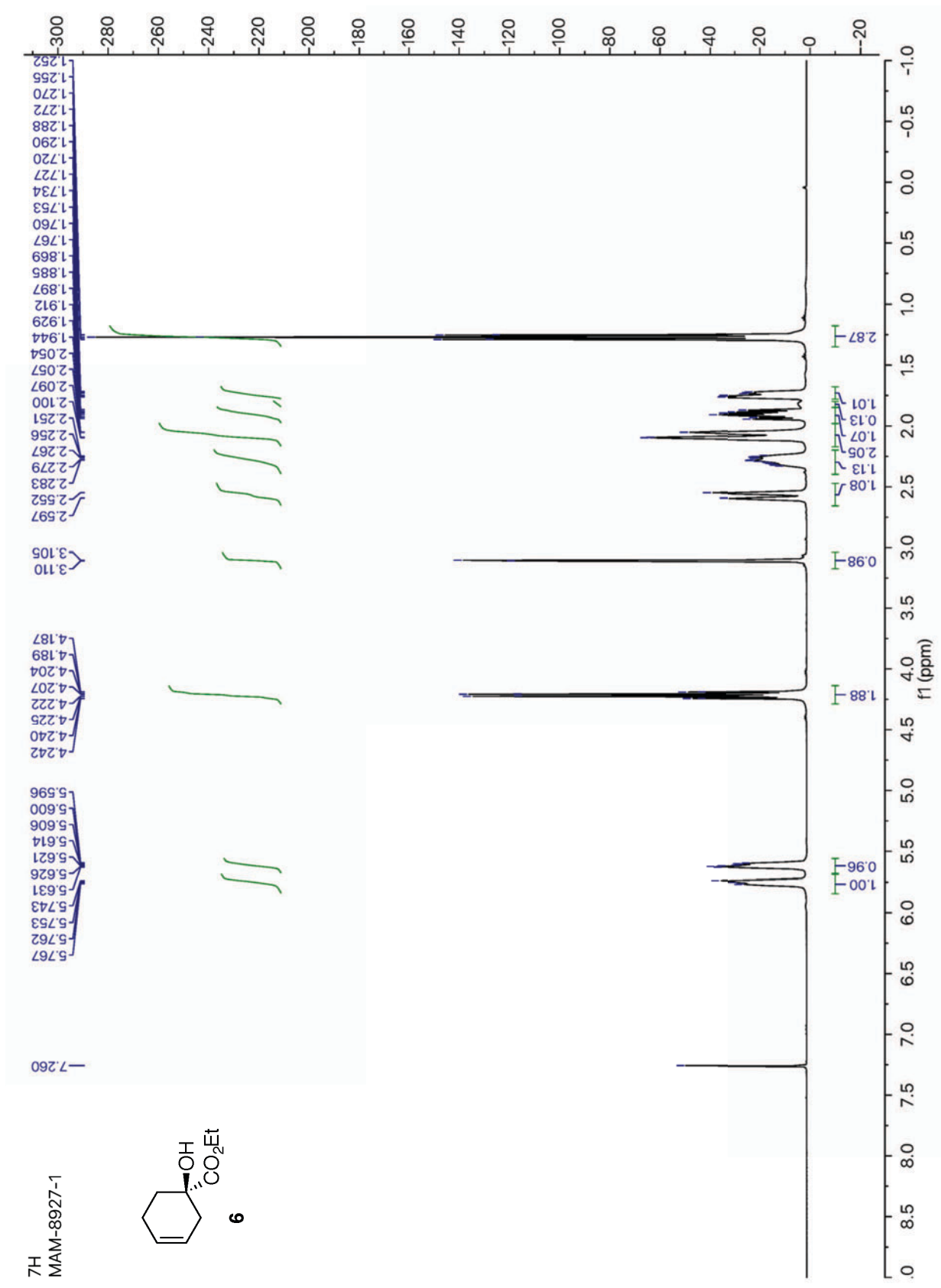
^{13}C NMR spectra of compound **4I** (100 MHz, CDCl_3)



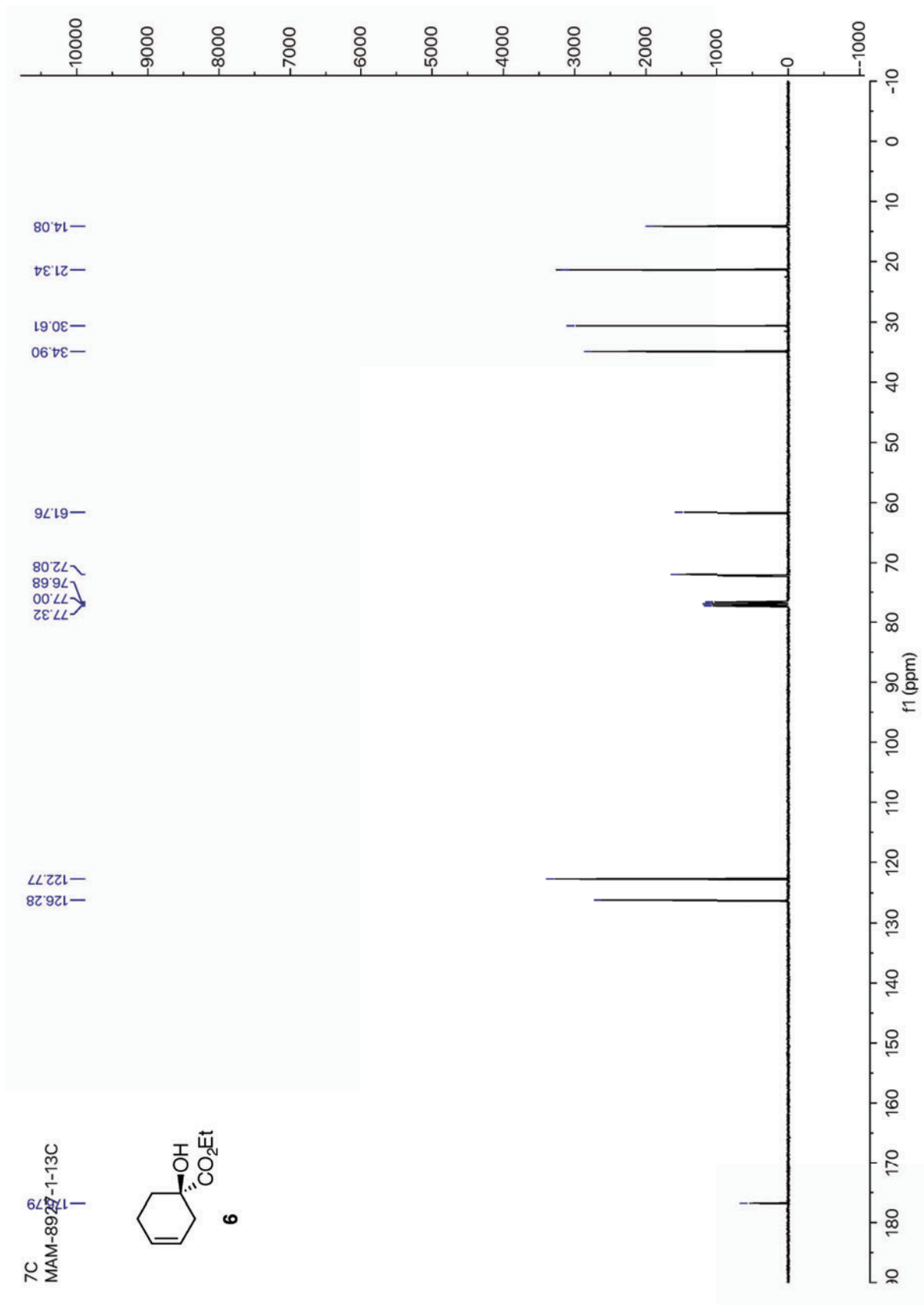
¹H NMR spectra of compound **4n** (400 MHz, CDCl₃)



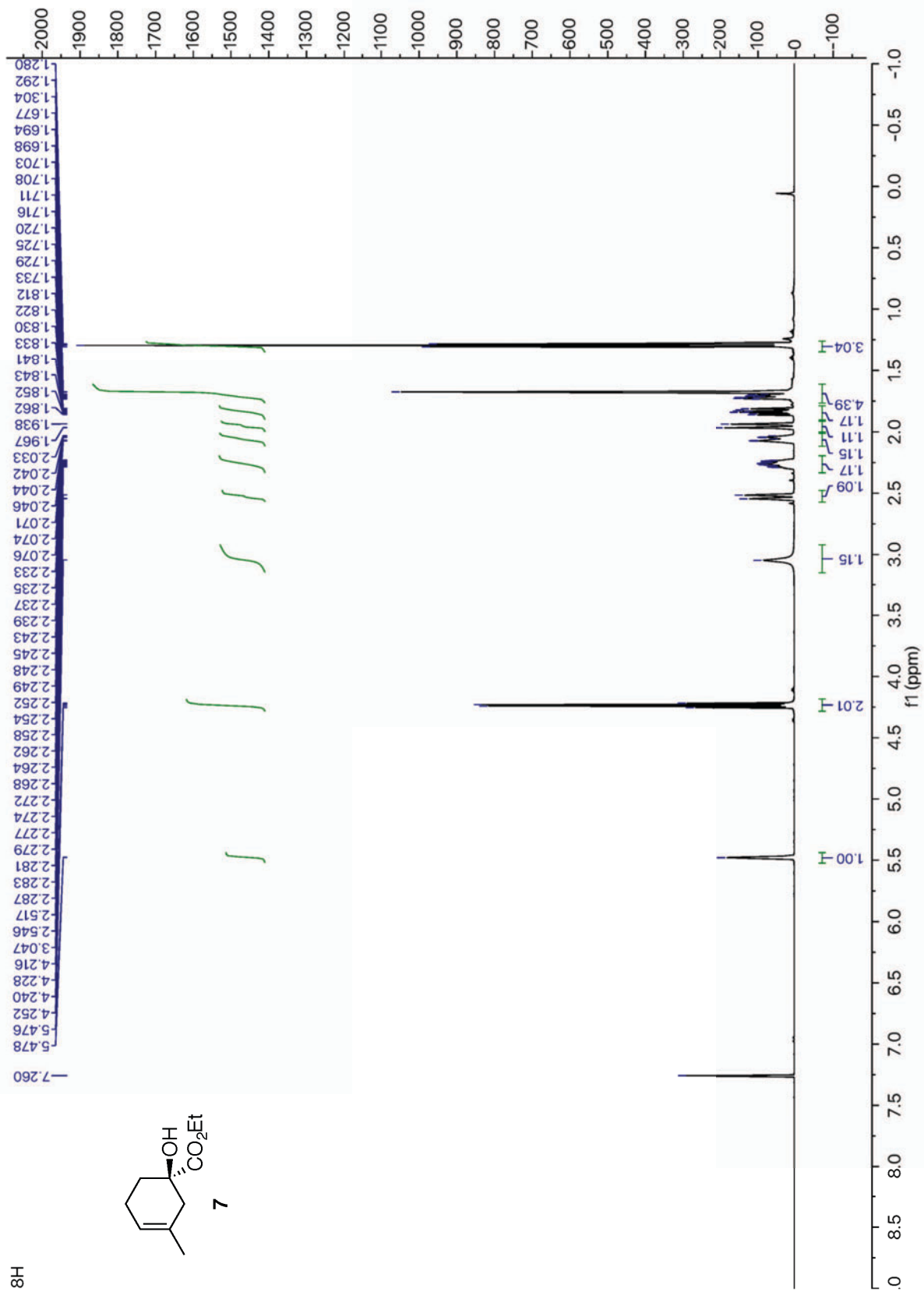
¹³C NMR spectra of compound **4n** (100 MHz, CDCl₃)



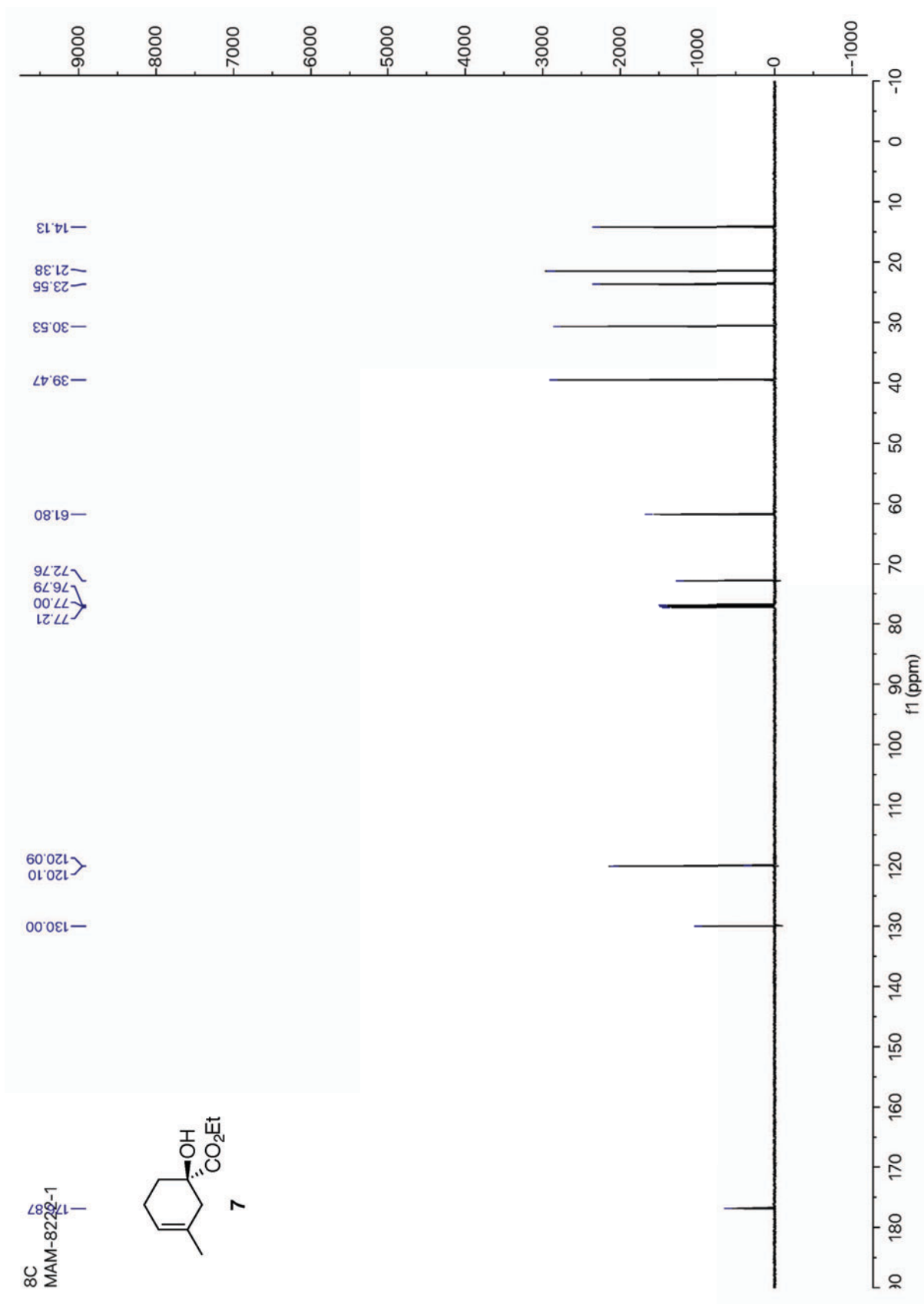
¹H NMR spectra of compound **6** (400 MHz, CDCl₃)



^{13}C NMR spectra of compound **6** (100 MHz, CDCl_3)

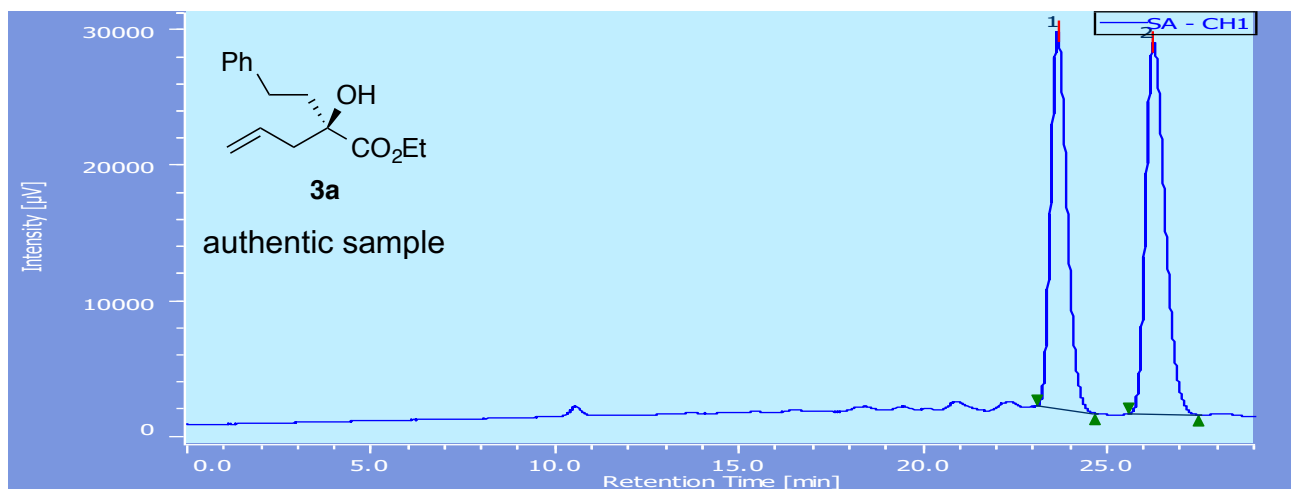


¹H NMR spectra of compound 7 (600 MHz, CDCl₃)

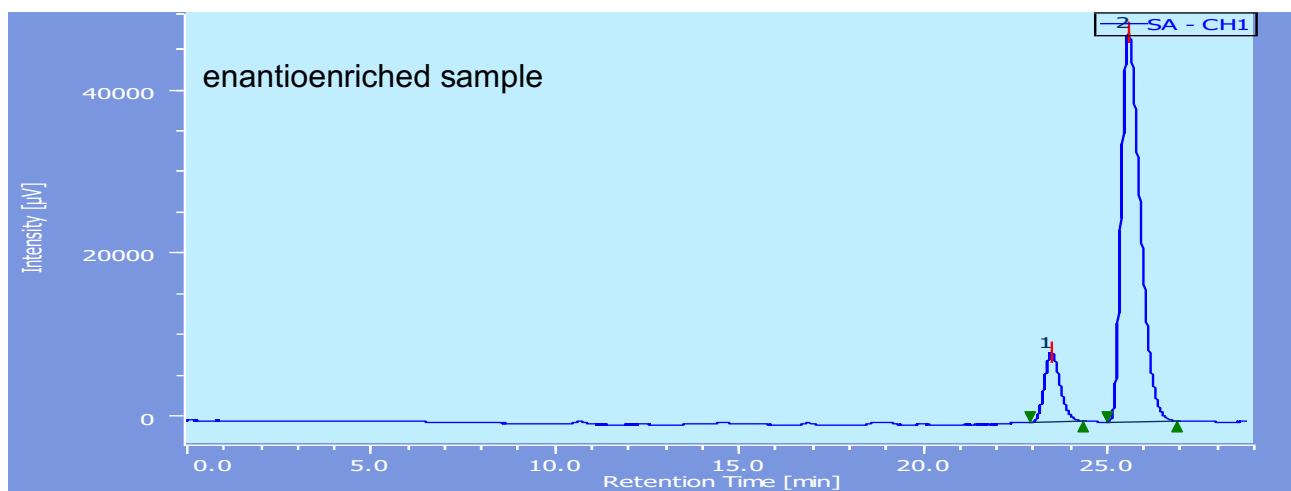


^{13}C NMR spectra of compound 7 (150 MHz, CDCl_3)

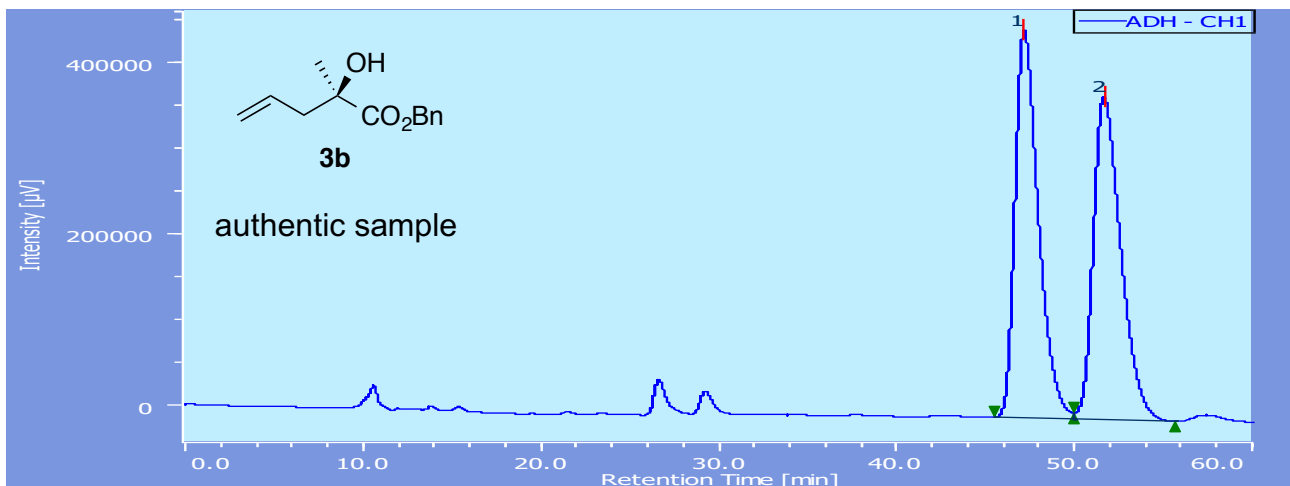
Chiral HPLC Charts of New Compounds



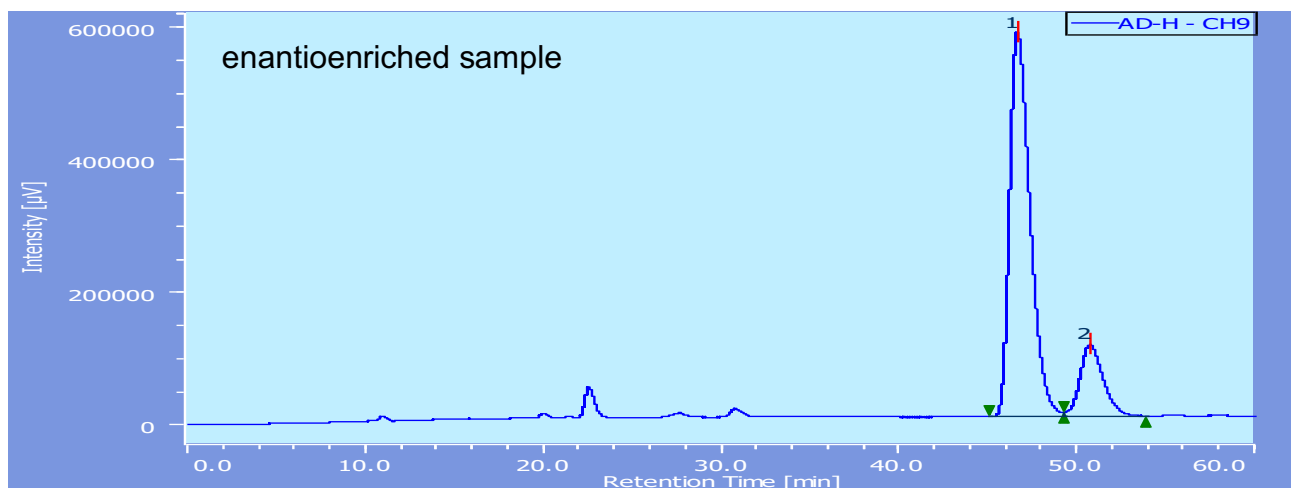
peak	retention time	area	hight	area, %	hight, %
1	23.617	854805	27765	46.311	50.434
2	26.217	991006	27287	53.689	49.566



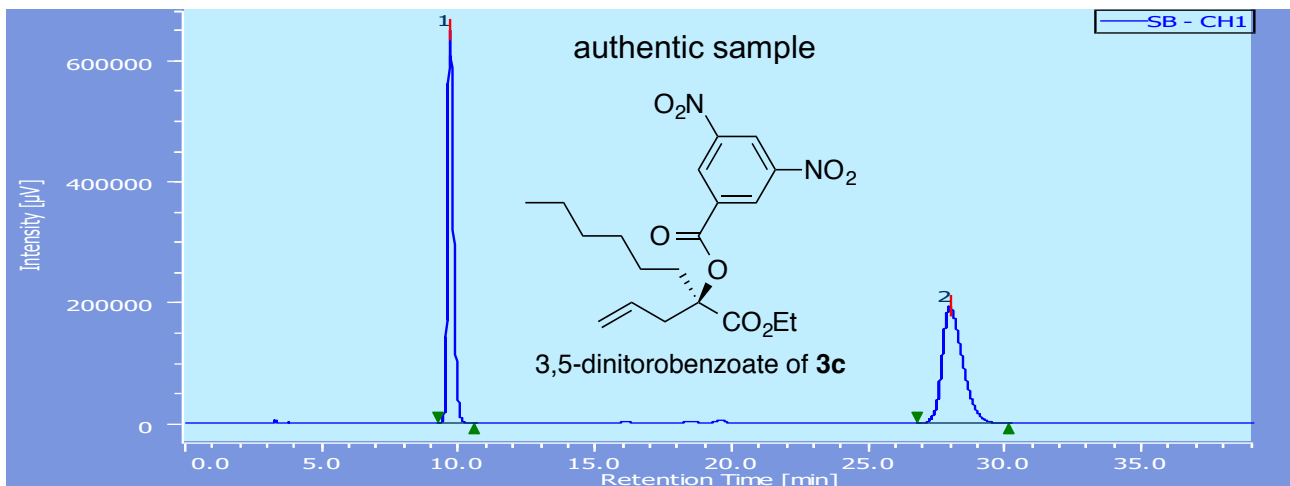
peak	retention time	area	hight	area, %	hight, %
1	23.442	254249	8548	12.988	15.230
2	25.533	1703385	47579	87.012	84.770



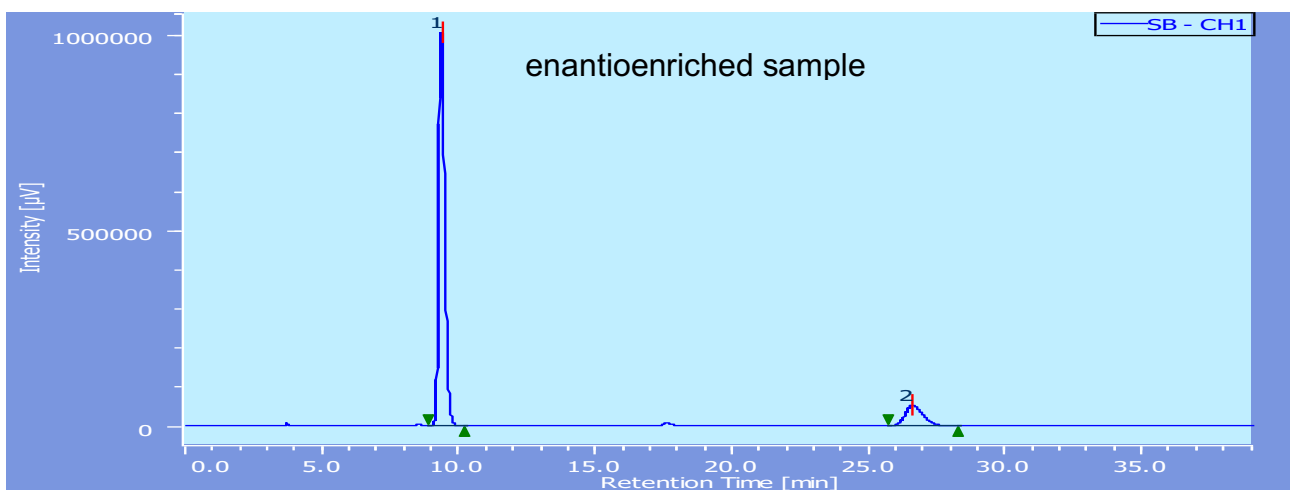
peak	retention time	area	hight	area, %	hight, %
1	47.075	41272906	451280	50.621	54.570
2	51.558	40259831	375694	49.379	45.430



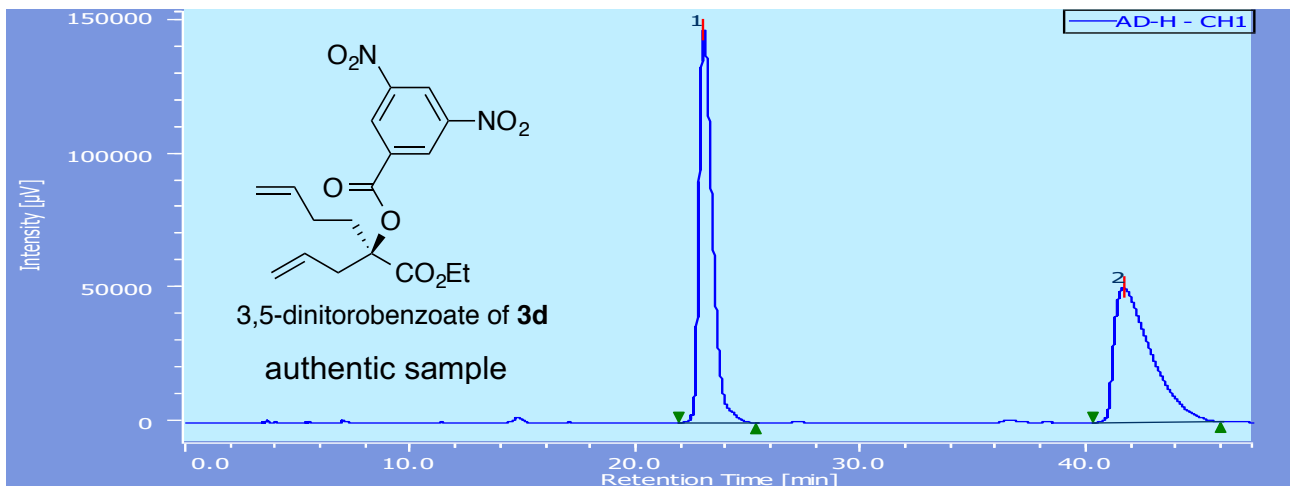
peak	retention time	area	hight	area, %	hight, %
1	46.590	46298311	579348	82.526	84.333
2	50.657	9803346	107631	17.474	15.667



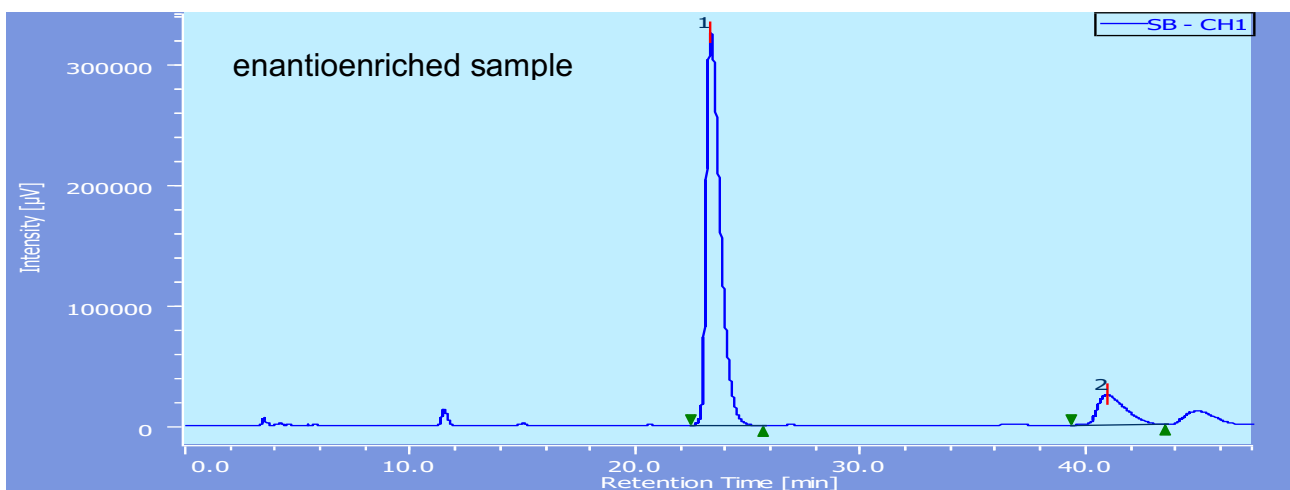
peak	retention time	area	hight	area, %	hight, %
1	9.675	9529135	647711	48.672	77.134
2	27.925	10049024	192009	51.328	22.866



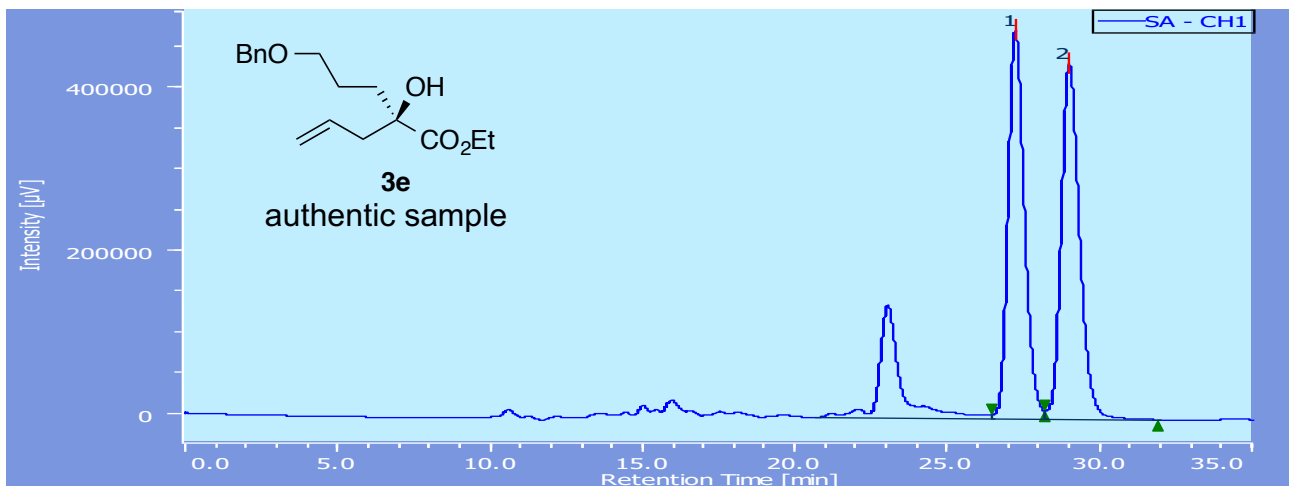
peak	retention time	area	hight	area, %	hight, %
1	9.383	15956972	1002517	86.871	94.993
2	26.575	2411598	52842	13.129	5.007



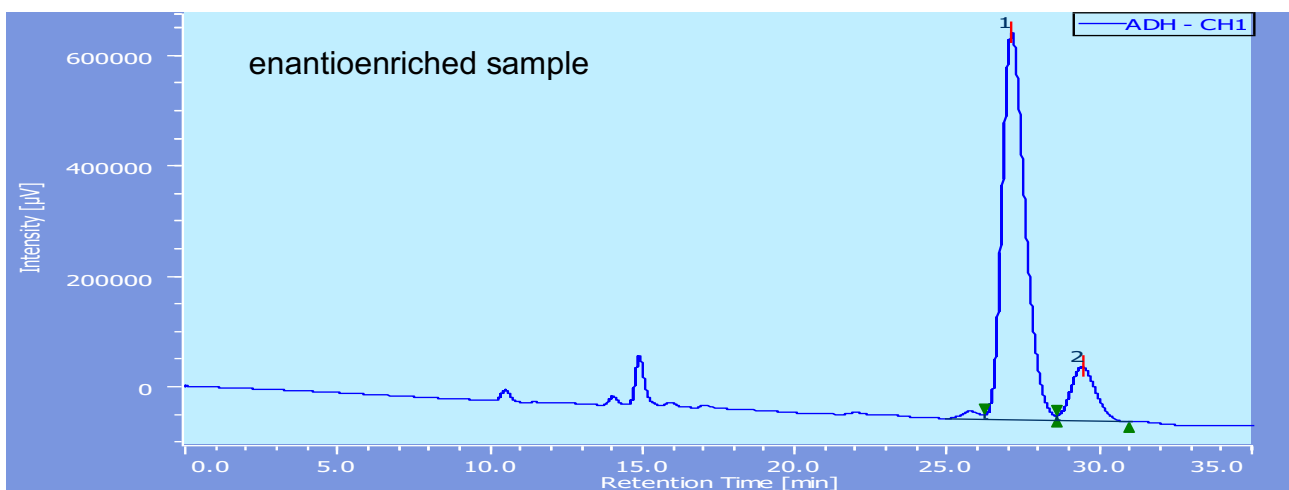
peak	retention time	area	hight	area, %	hight, %
1	23.000	6075661	146360	51.453	74.446
2	41.608	5732500	50239	48.547	25.554



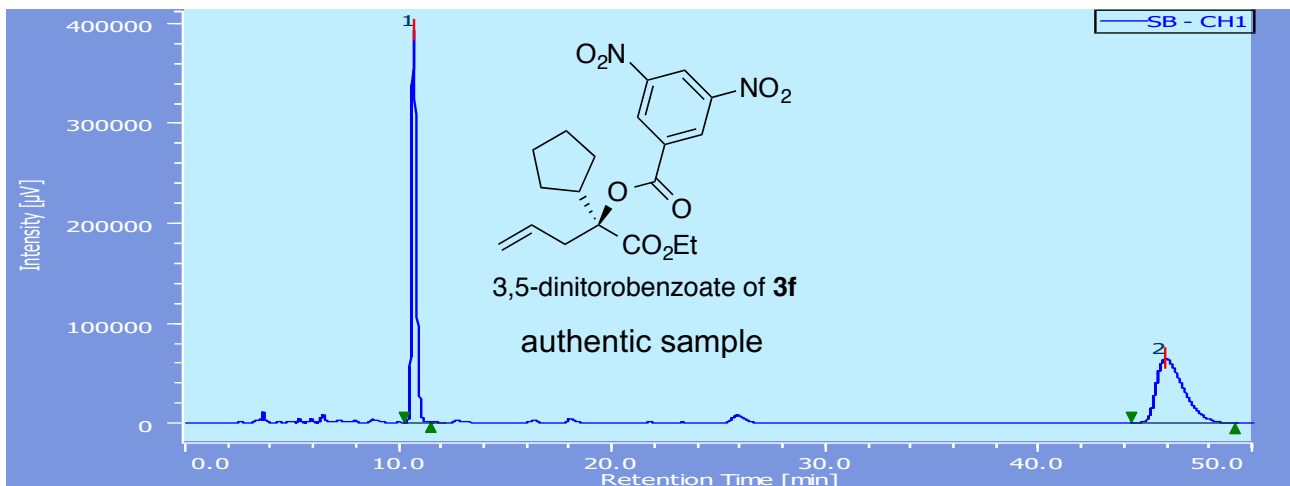
peak	retention time	area	hight	area, %	hight, %
1	23.308	14164853	324815	86.814	92.904
2	40.842	2151433	24809	13.186	7.096



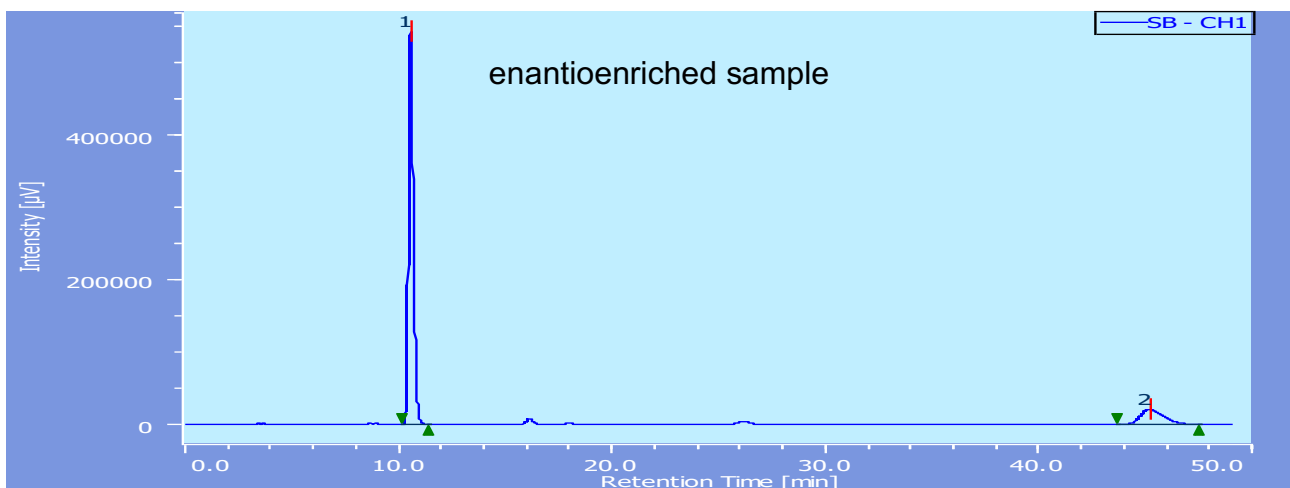
peak	retention time	area	hight	area, %	hight, %
1	27.175	17801104	475186	49.521	52.259
2	28.942	18145229	434107	50.479	47.741



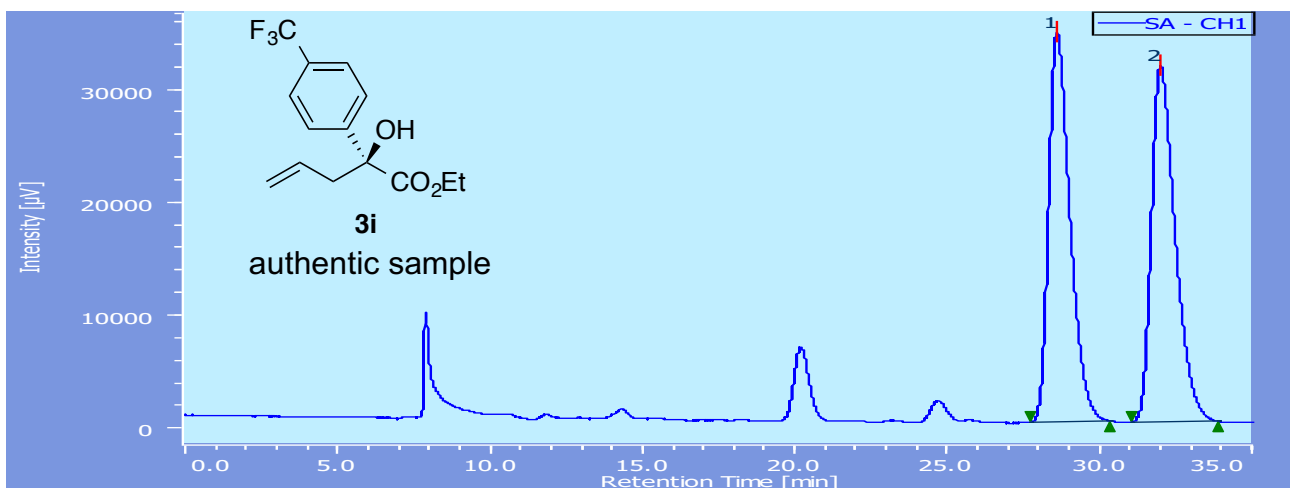
peak	retention time	area	hight	area, %	hight, %
1	27.058	36854353	699211	86.698	87.640
2	29.367	5654384	98613	13.302	12.360



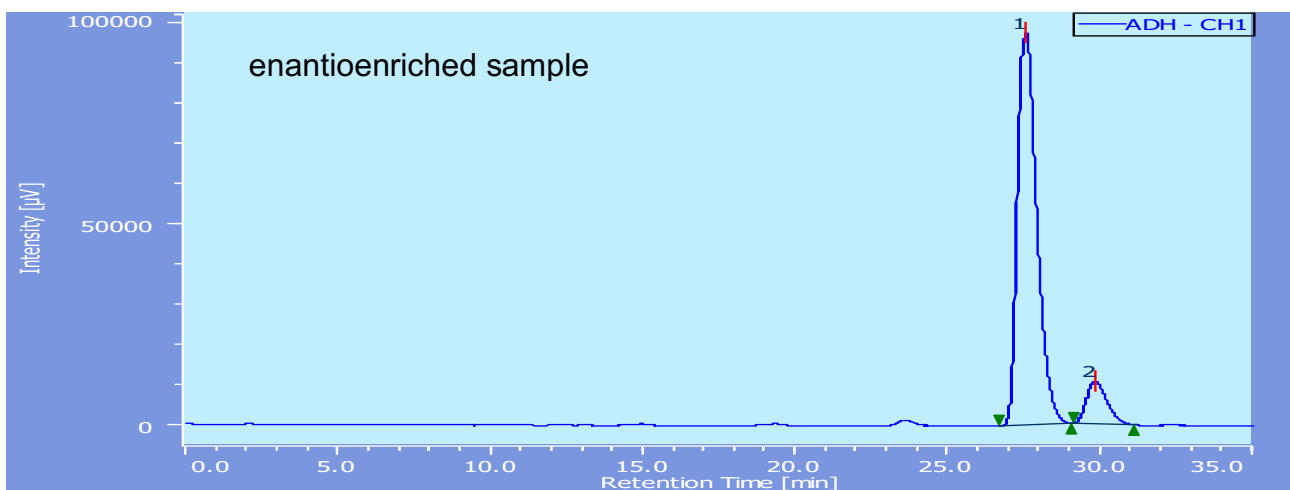
peak	retention time	area	hight	area, %	hight, %
1	10.692	5760819	391486	50.232	85.895
2	45.858	5707596	64286	49.768	14.105



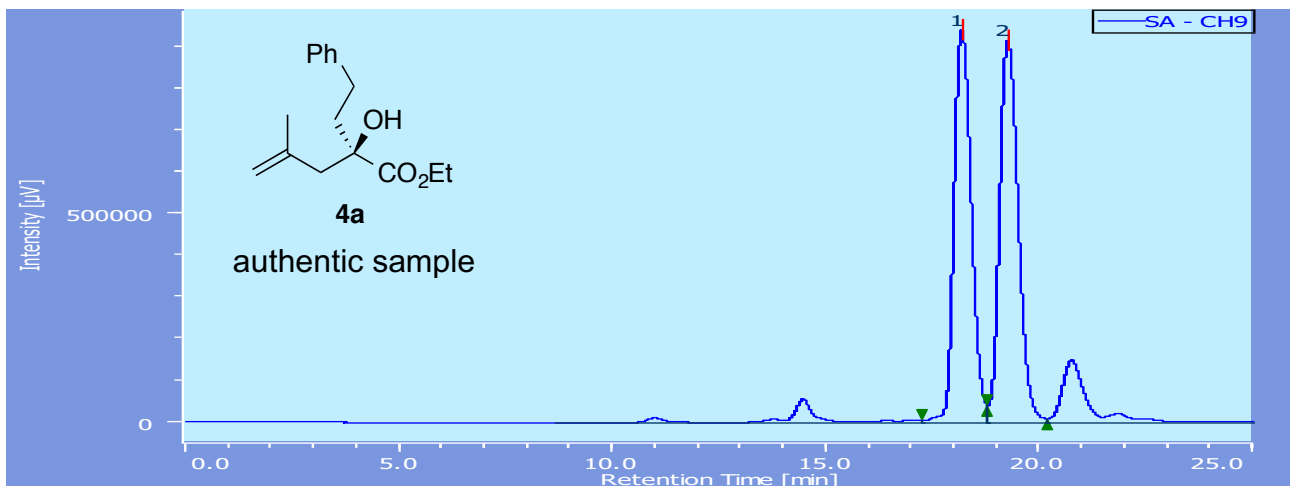
peak	retention time	area	hight	area, %	hight, %
1	10.542	8760510	541283	84.274	96.265
2	45.108	1634816	21000	15.726	3.735



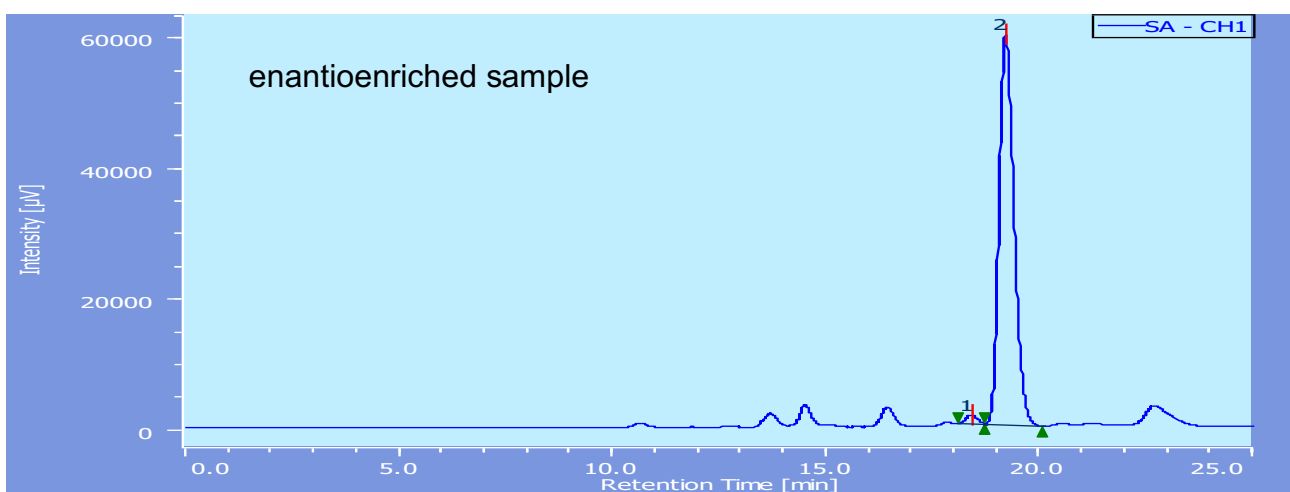
peak	retention time	area	hight	area, %	hight, %
1	28.542	1668497	34431	49.496	52.262
2	31.933	1702475	31450	50.504	47.738



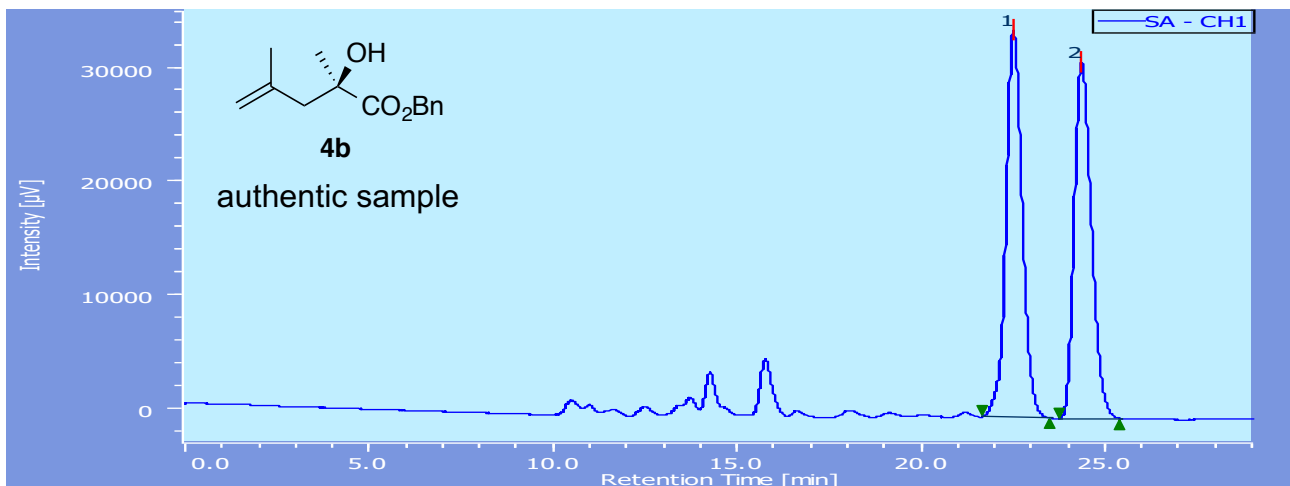
peak	retention time	area	hight	area, %	hight, %
1	27.542	4330337	97280	89.667	90.144
2	29.783	499007	10636	10.333	9.856



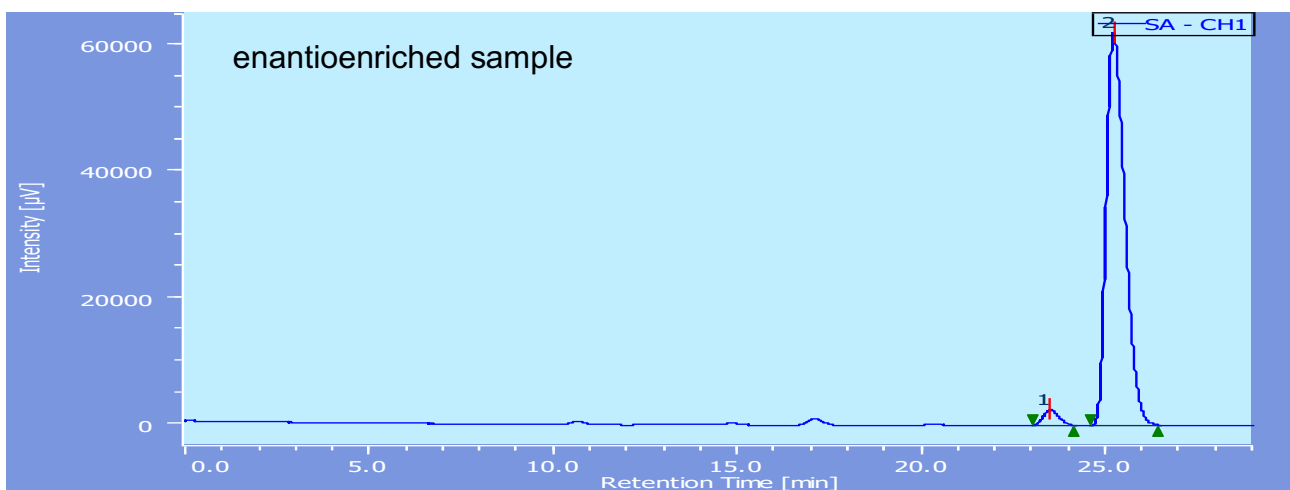
peak	retention time	area	hight	area, %	hight, %
1	18.162	26759913	940147	48.977	50.691
2	19.237	27877805	914507	51.023	49.309



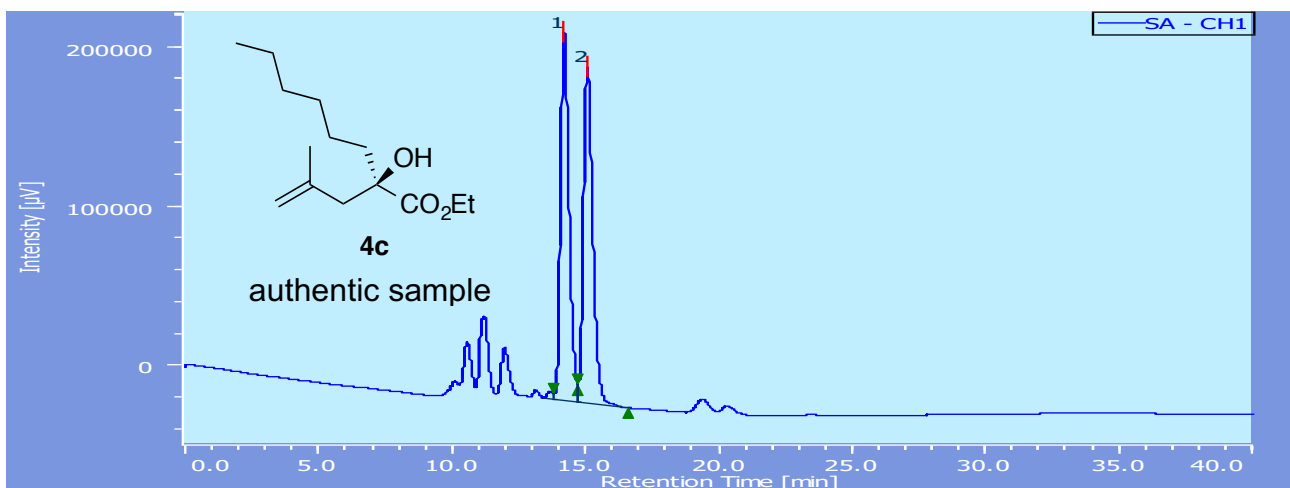
peak	retention time	area	hight	area, %	hight, %
1	18.392	27900	1391	1.891	2.281
2	19.183	1447885	59564	98.109	97.719



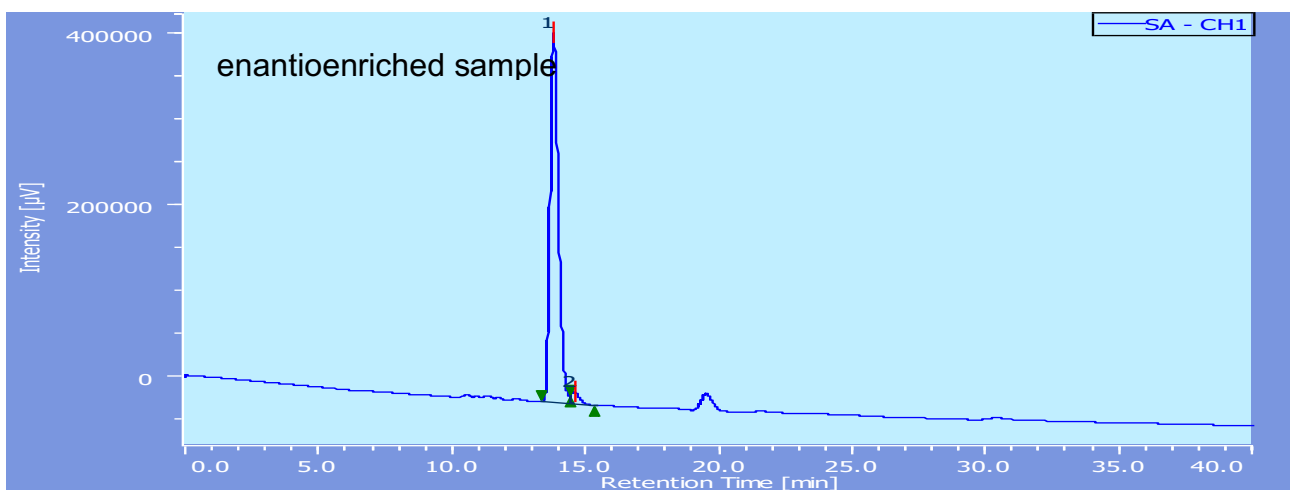
peak	retention time	area	hight	area, %	hight, %
1	22.467	1044691	33958	50.741	52.131
2	24.317	1014164	31182	49.259	47.869



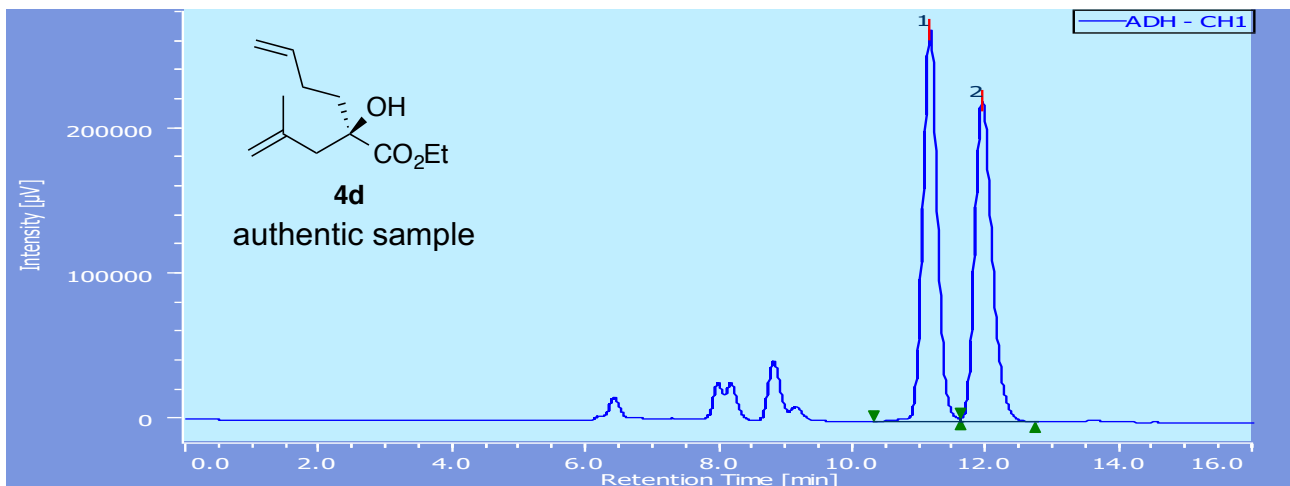
peak	retention time	area	hight	area, %	hight, %
1	23.467	71809	2418	3.188	3.759
2	25.183	2180921	61927	96.812	96.241



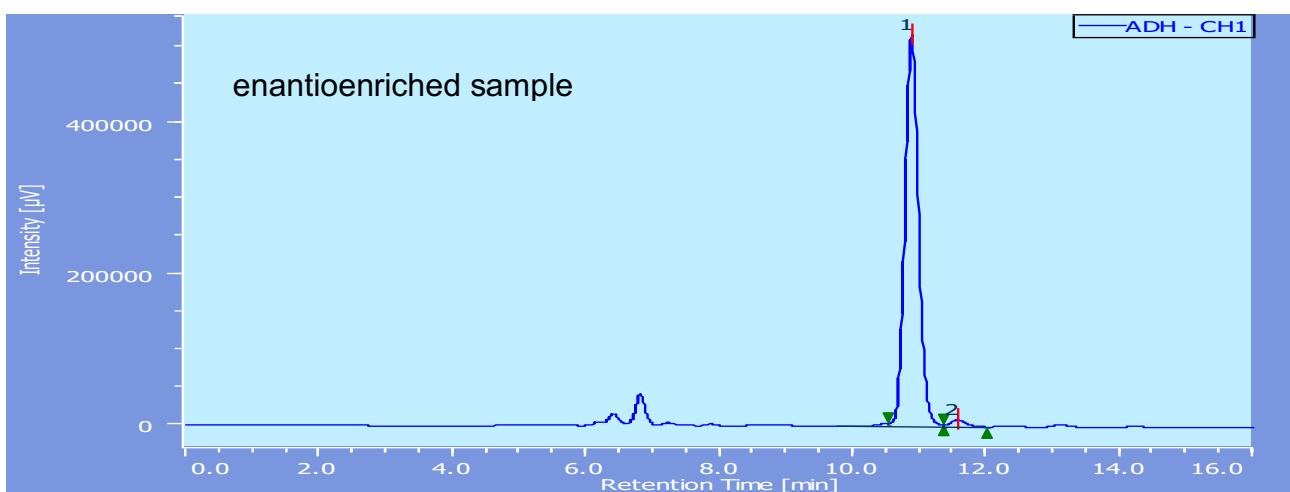
peak	retention time	area	hight	area, %	hight, %
1	14.183	5111456	230627	49.733	52.322
2	15.042	5166264	210157	50.267	47.678



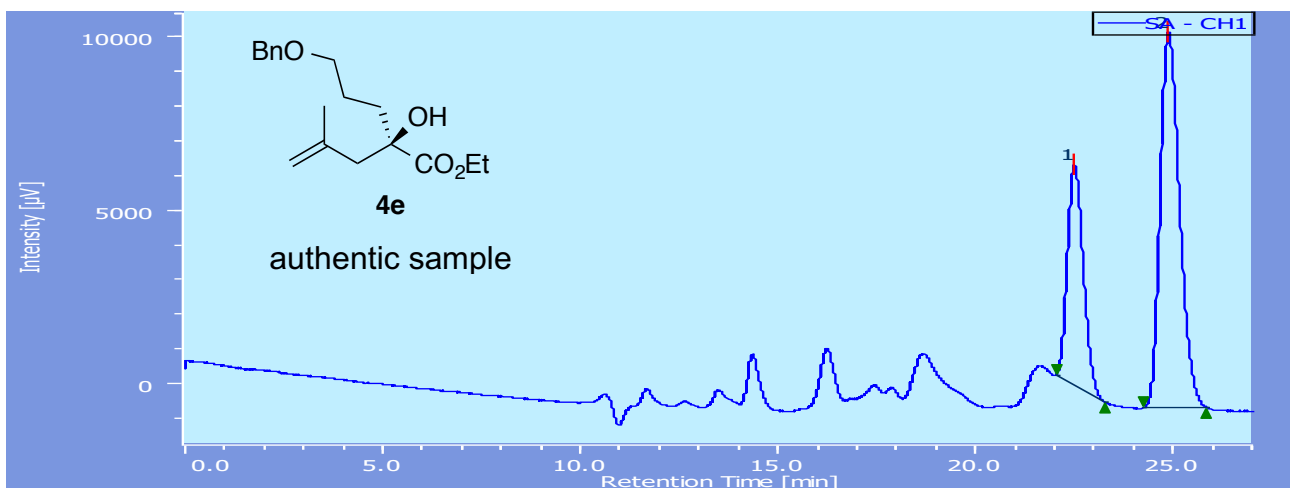
peak	retention time	area	hight	area, %	hight, %
1	13.783	9456551	430158	96.844	96.857
2	14.550	308221	13959	3.156	3.143



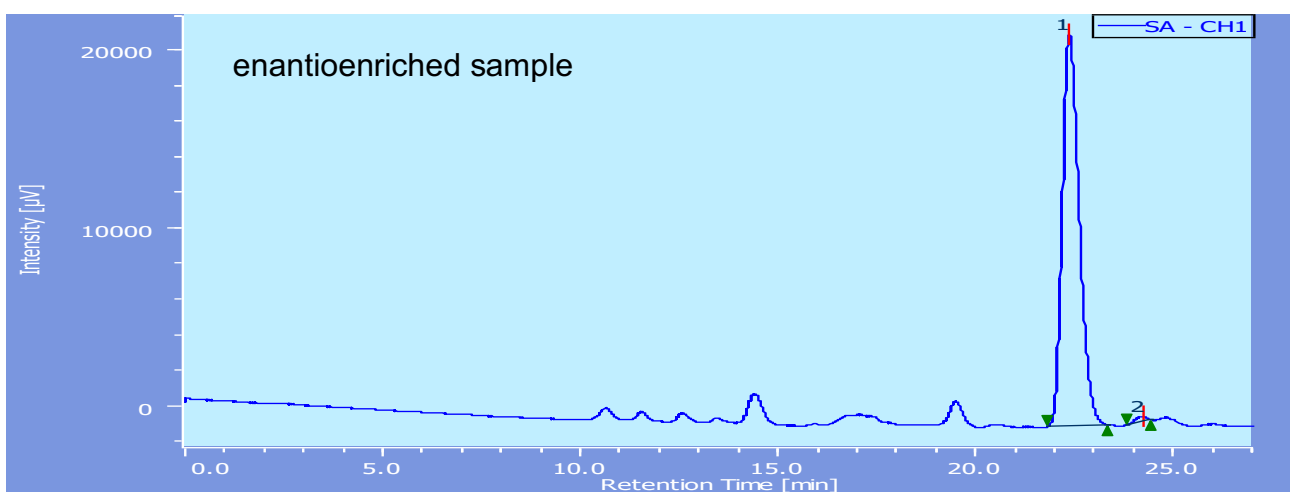
peak	retention time	area	hight	area, %	hight, %
1	11.150	4082391	268789	50.397	55.027
2	11.933	4018120	219678	49.603	44.973



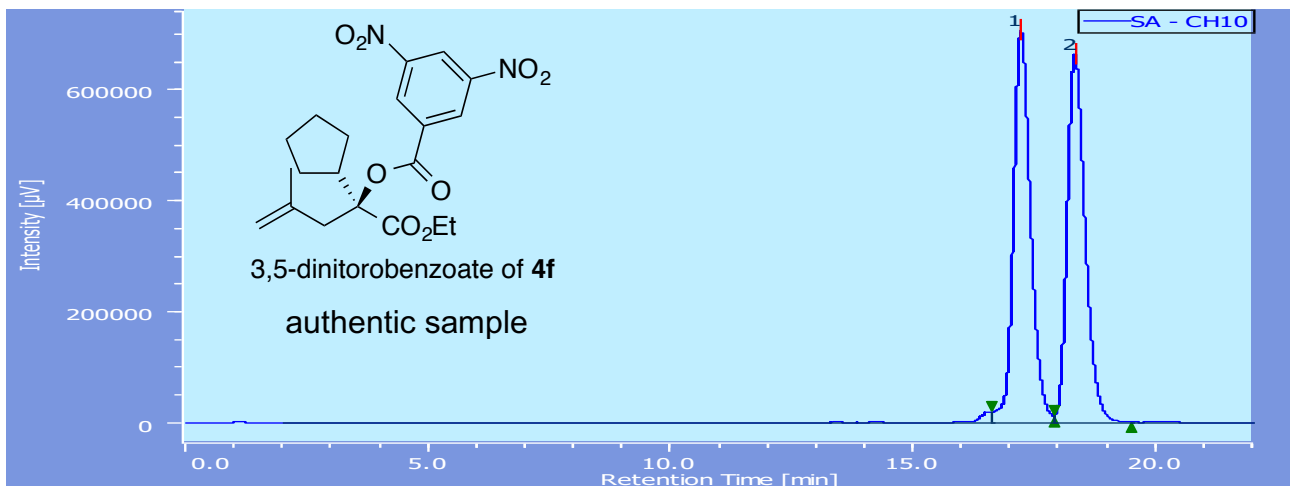
peak	retention time	area	hight	area, %	hight, %
1	10.875	7434726	516941	97.996	98.199
2	11.550	152057	9481	2.004	1.801



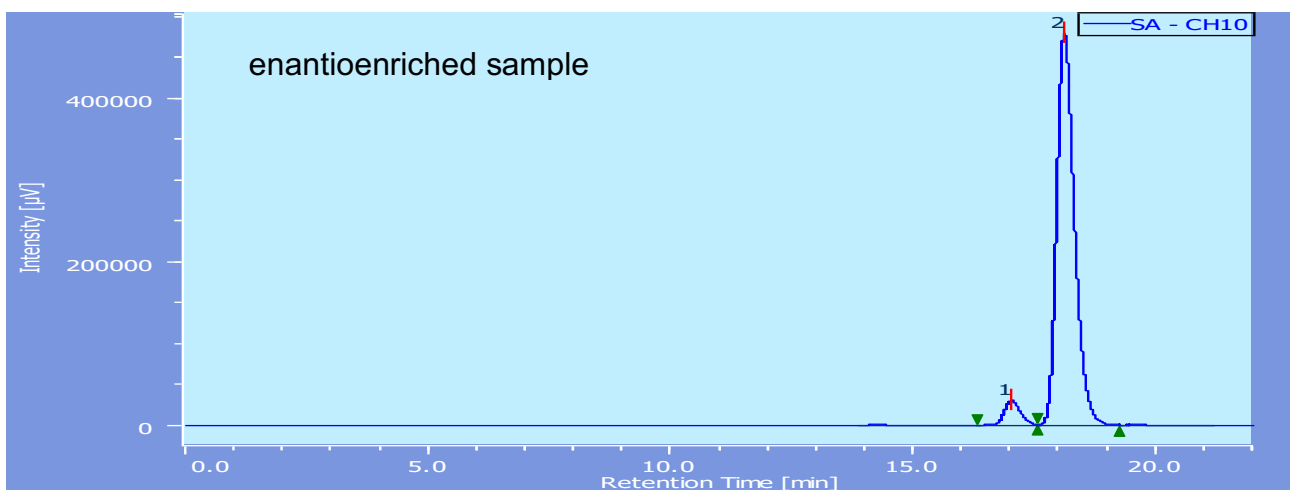
peak	retention time	area	hight	area, %	hight, %
1	22.458	178414	6319	32.711	36.949
2	24.833	367016	10783	67.289	63.051



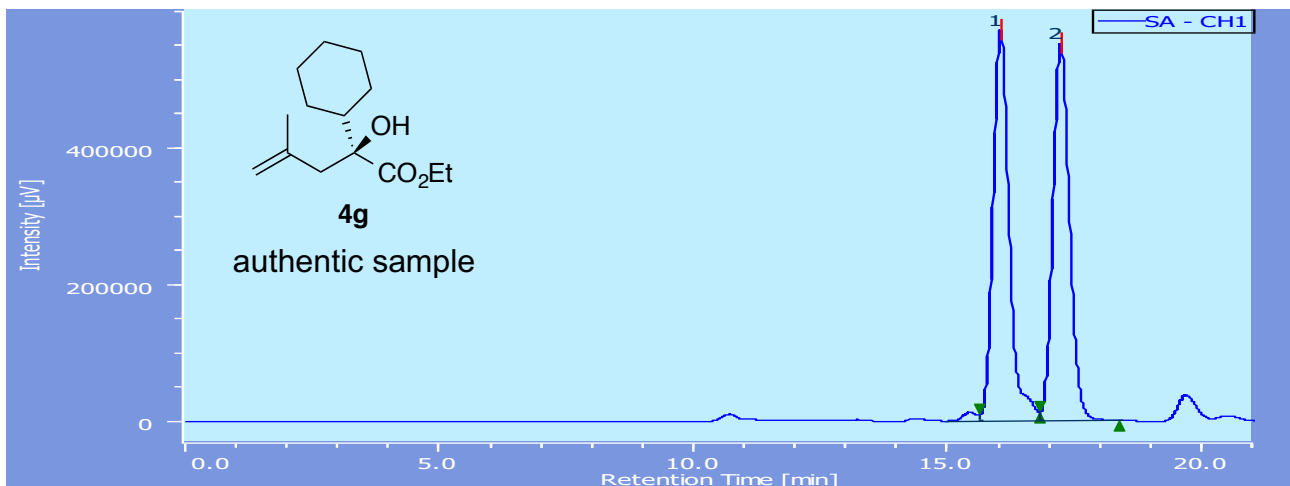
peak	retention time	area	hight	area, %	hight, %
1	22.333	655198	21975	99.086	98.773
2	24.175	6045	273	0.914	1.227



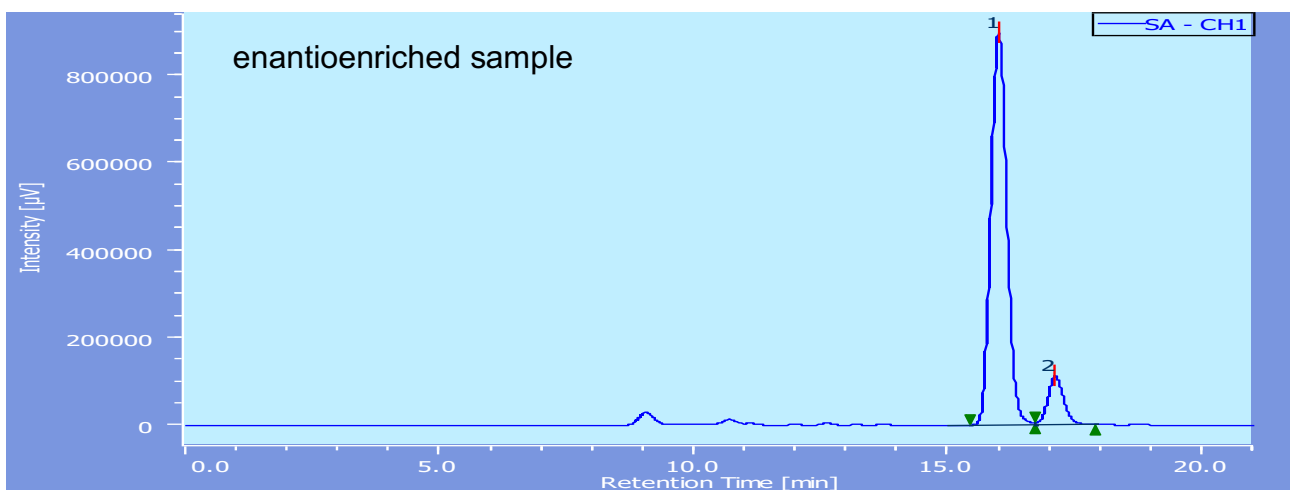
peak	retention time	area	hight	area, %	hight, %
1	17.202	17519894	705798	50.532	51.592
2	18.310	17151168	662241	49.468	48.408



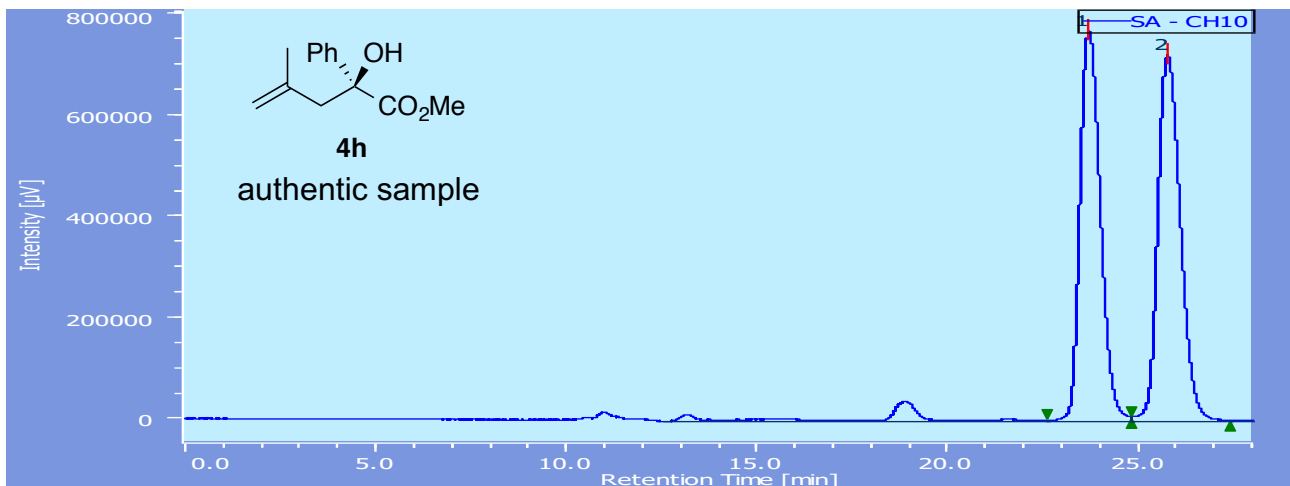
peak	retention time	area	hight	area, %	hight, %
1	17.007	765478	30868	5.901	6.053
2	18.092	12205609	479073	94.099	93.947



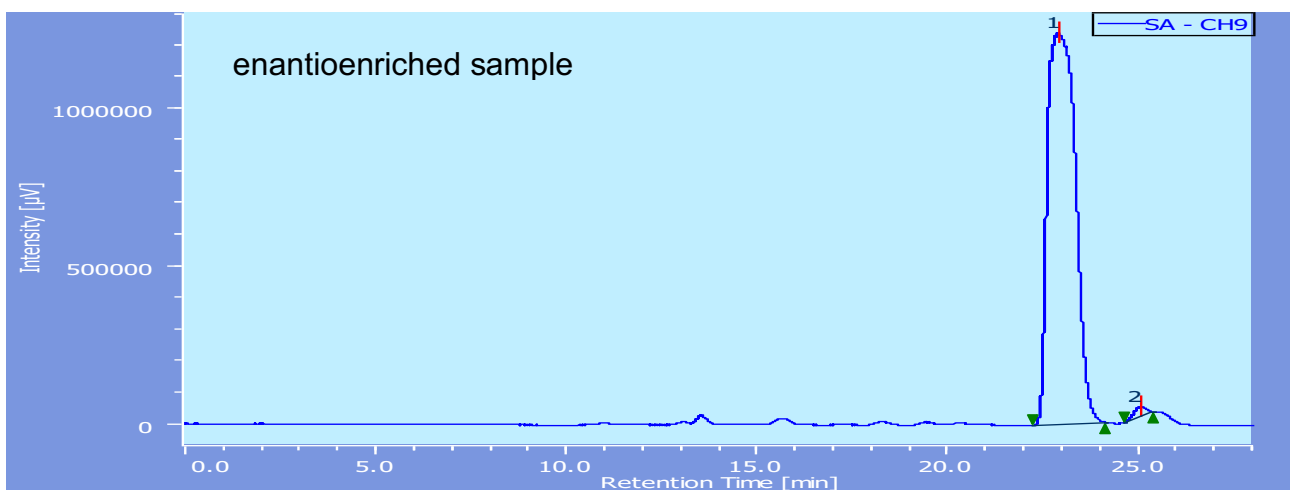
peak	retention time	area	hight	area, %	hight, %
1	16.017	12693677	570745	50.319	50.923
2	17.200	12532662	550046	49.681	49.077



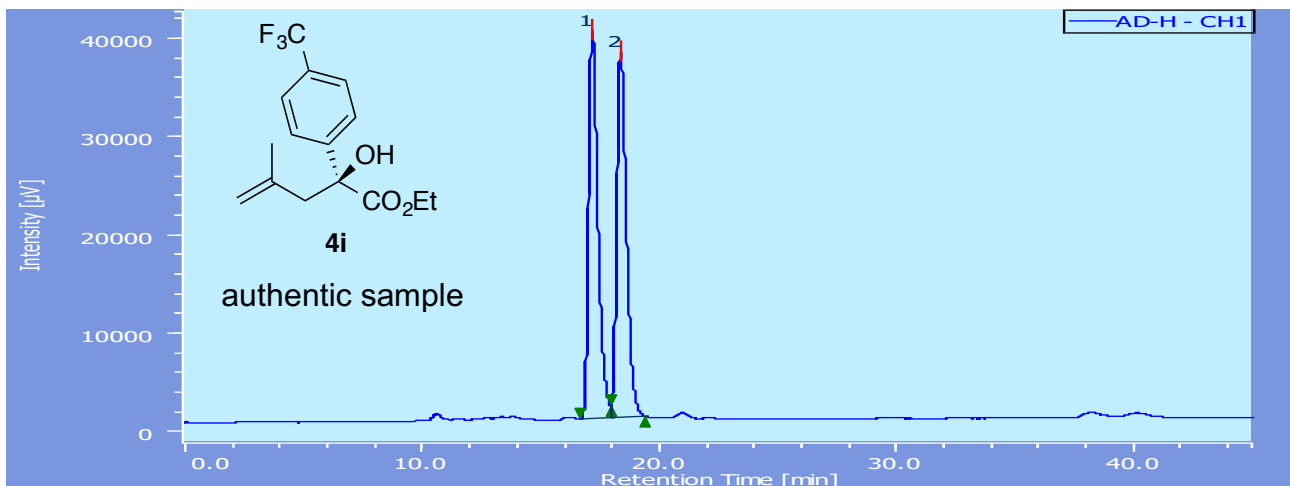
peak	retention time	area	hight	area, %	hight, %
1	15.983	19548334	894697	89.072	89.012
2	17.092	2398409	110440	10.928	10.988



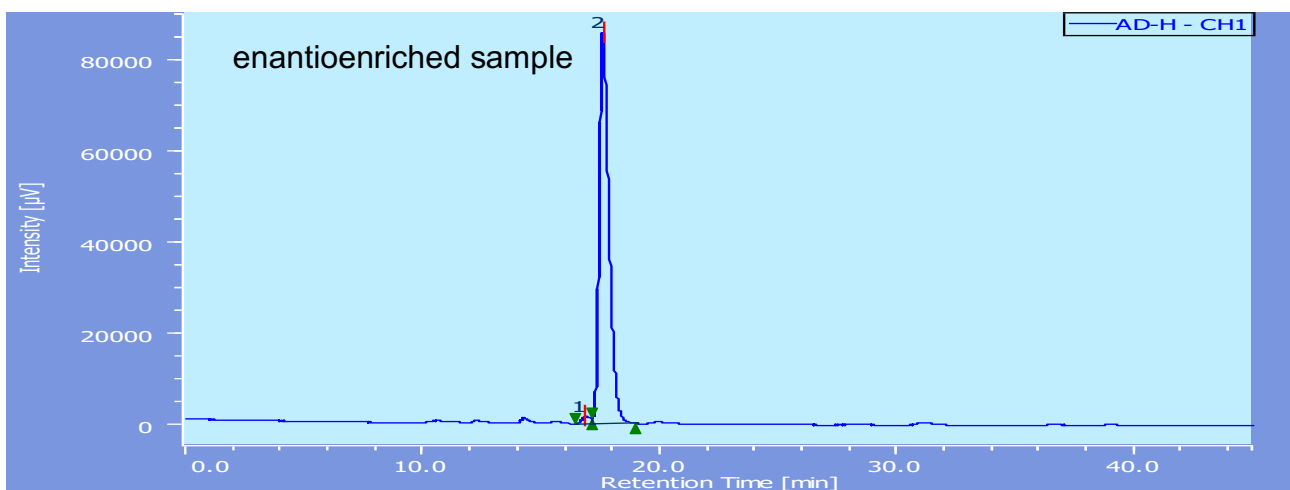
peak	retention time	area	hight	area, %	hight, %
1	23.660	28952121	772889	49.167	51.647
2	25.740	29932758	723588	50.833	48.353



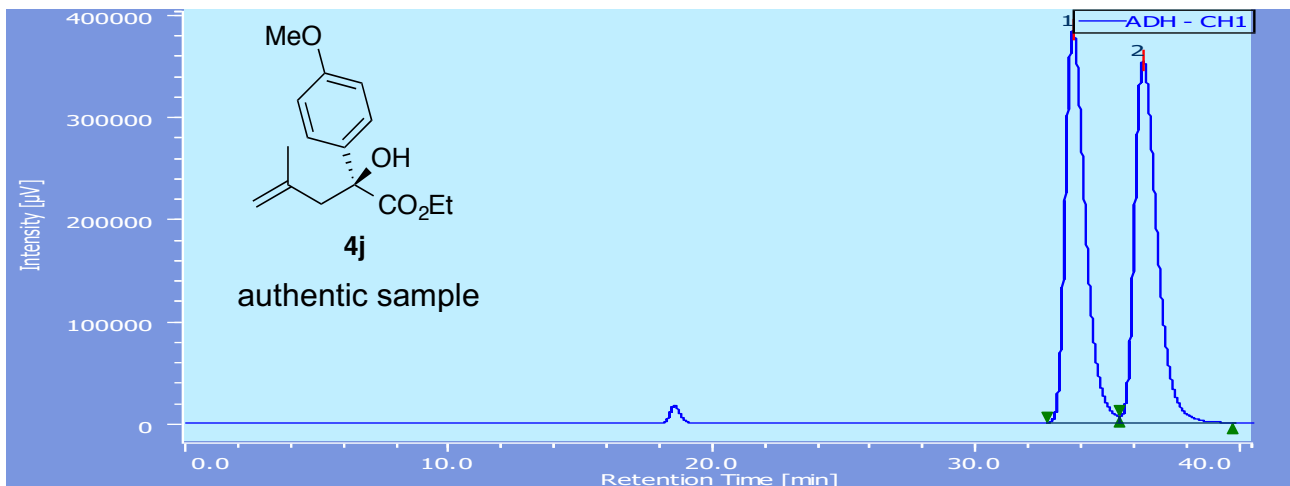
peak	retention time	area	hight	area, %	hight, %
1	22.868	62785878	1235620	98.813	97.433
2	25.043	754071	32552	1.187	2.567



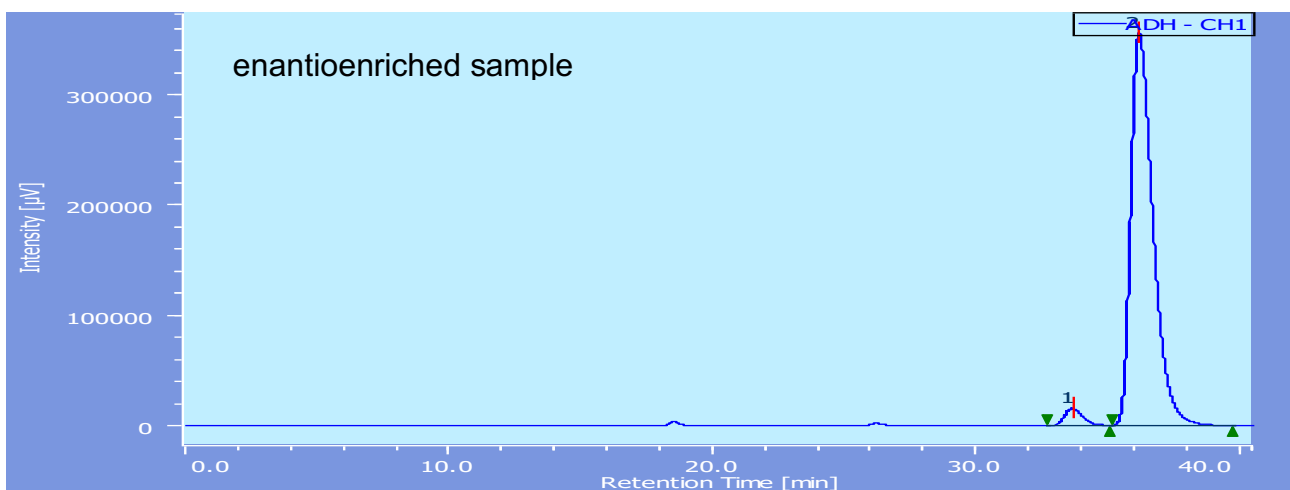
peak	retention time	area	hight	area, %	hight, %
1	17.133	1071933	39397	50.370	51.474
2	18.333	1056177	37140	49.630	48.526



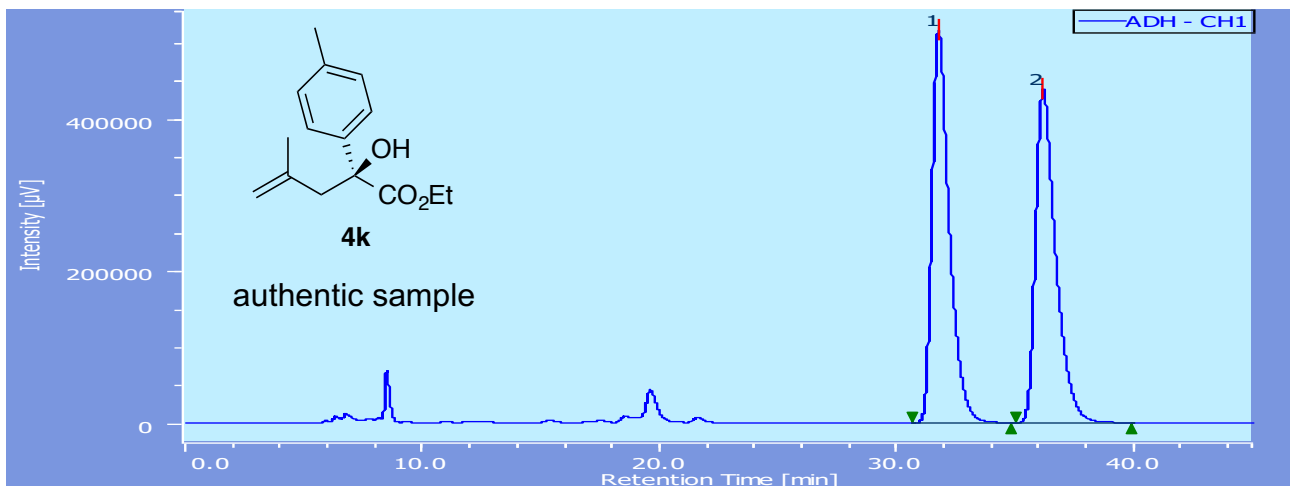
peak	retention time	area	hight	area, %	hight, %
1	16.842	39807	1655	1.595	1.893
2	17.592	2456102	85774	98.405	98.107



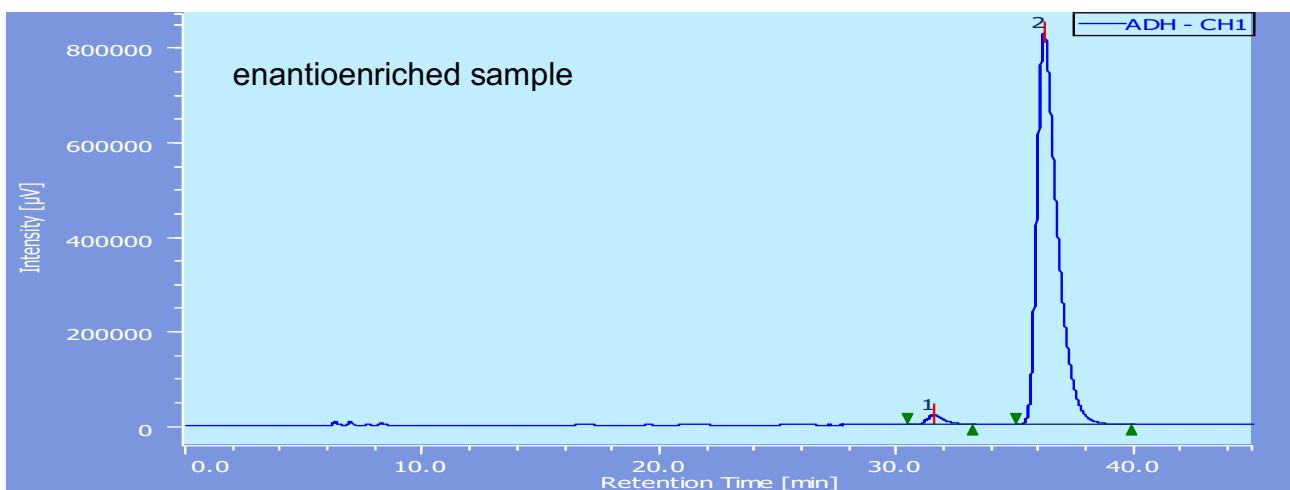
peak	retention time	area	hight	area, %	hight, %
1	33.633	20577298	383475	49.581	52.049
2	36.292	20924882	353286	50.419	47.951



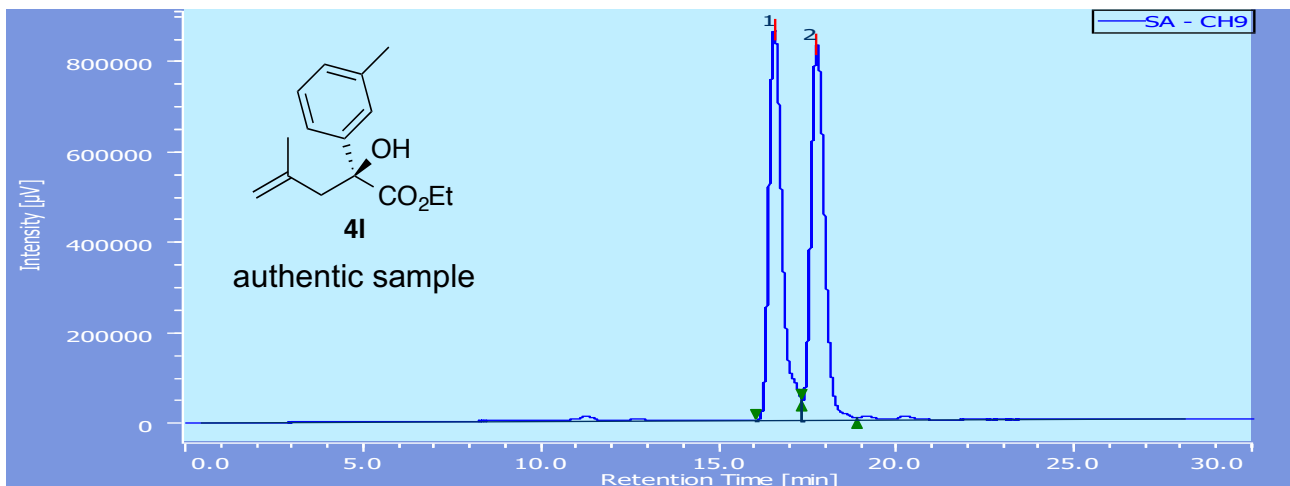
peak	retention time	area	hight	area, %	hight, %
1	33.617	770356	15957	3.577	4.298
2	36.142	20767823	355272	96.423	95.702



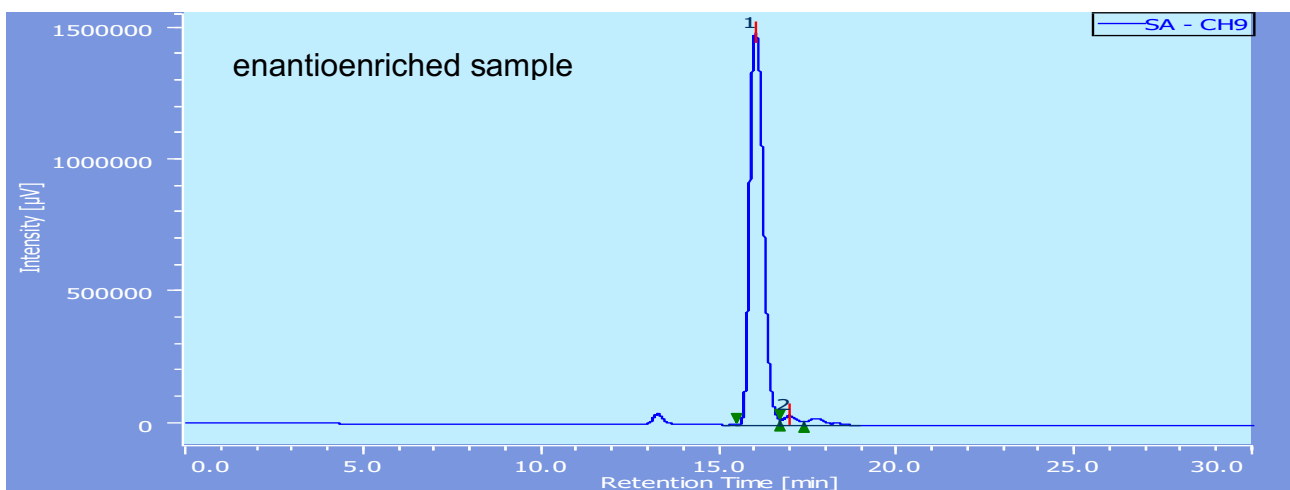
peak	retention time	area	hight	area, %	hight, %
1	31.717	26189284	514999	50.316	54.065
2	36.117	25860694	437561	49.684	45.935



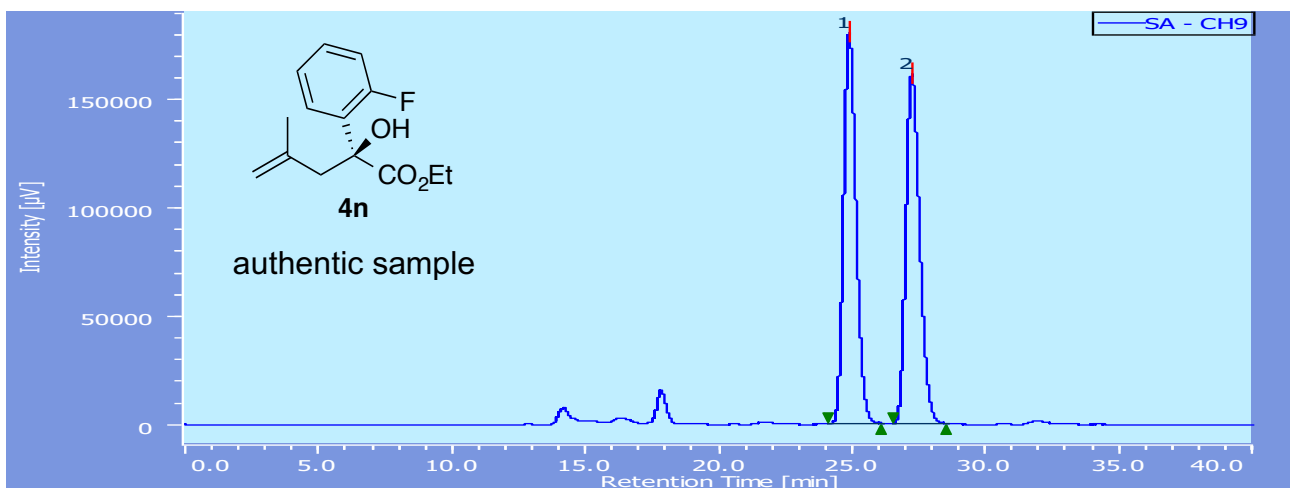
peak	retention time	area	hight	area, %	hight, %
1	31.508	1011904	19945	2.005	2.355
2	36.158	49459042	826878	97.995	97.645



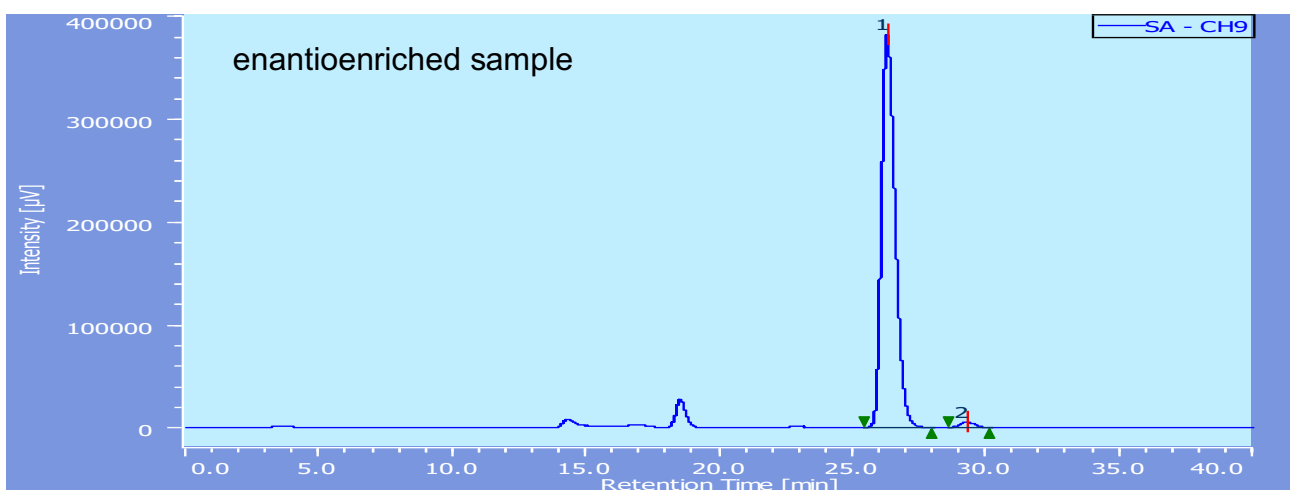
peak	retention time	area	hight	area, %	hight, %
1	16.537	22847496	862302	50.600	50.972
2	17.728	22305766	829403	49.400	49.028



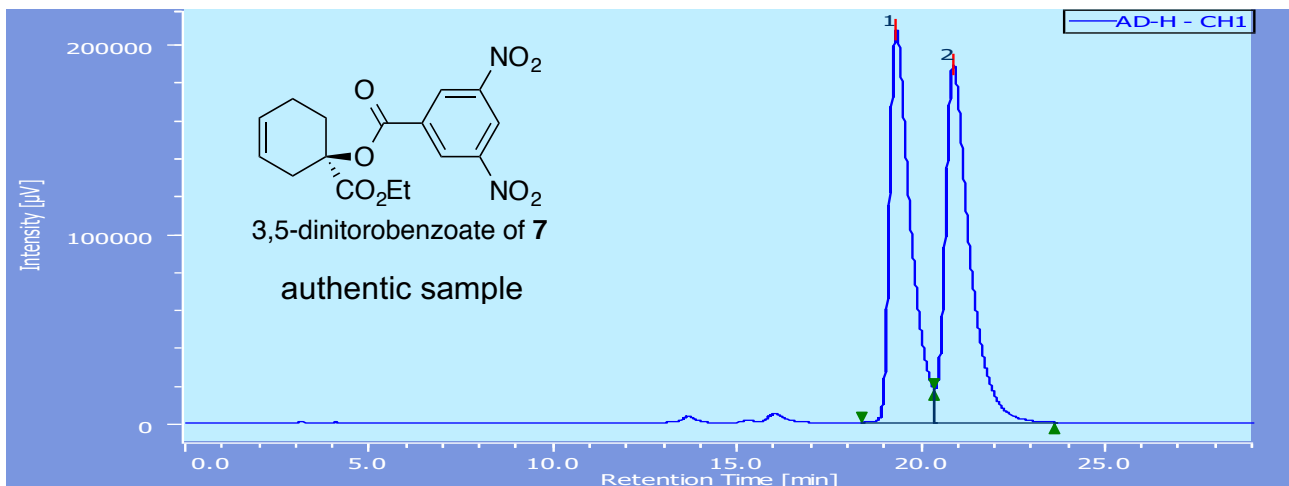
peak	retention time	area	hight	area, %	hight, %
1	16.007	39788699	1484510	97.709	97.603
2	16.950	933020	36455	2.291	2.397



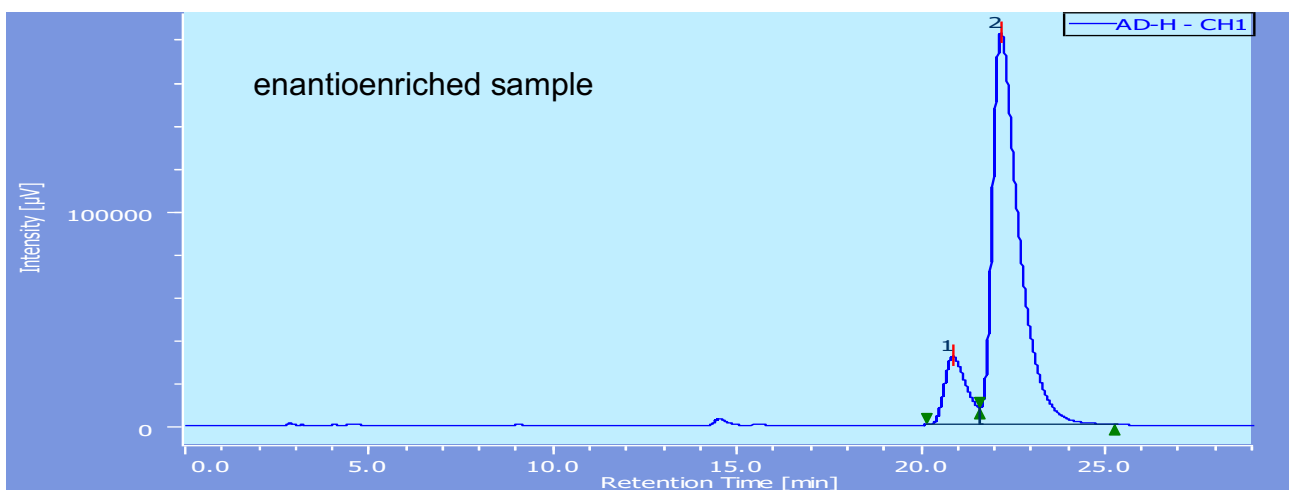
peak	retention time	area	hight	area, %	hight, %
1	24.845	5901268	180131	50.386	52.870
2	27.188	5810848	160576	49.614	47.130



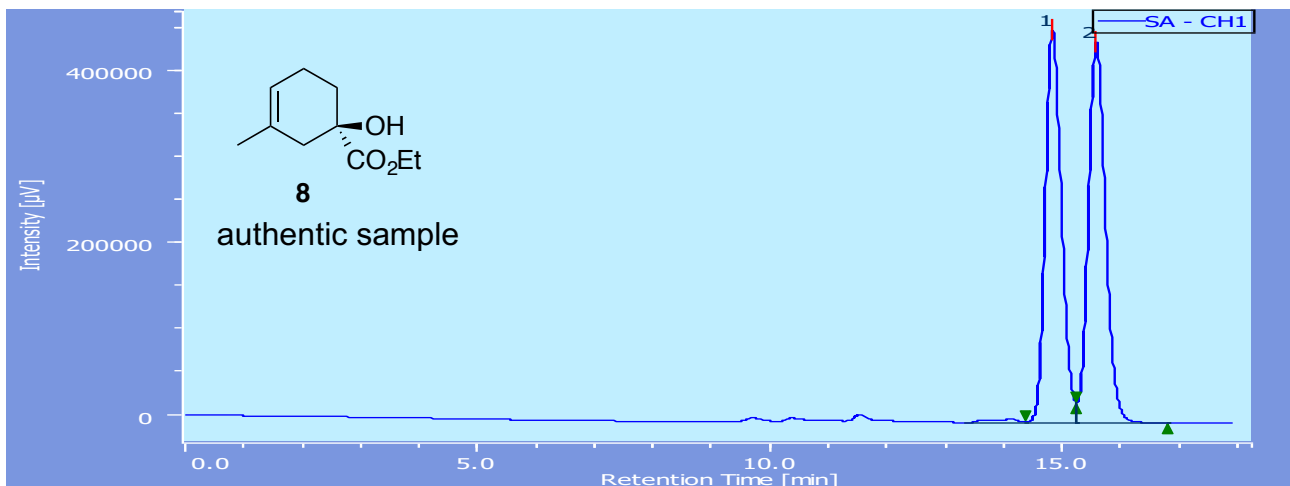
peak	retention time	area	hight	area, %	hight, %
1	26.267	13597157	381102	98.528	98.554
2	29.235	203158	5592	1.472	1.446



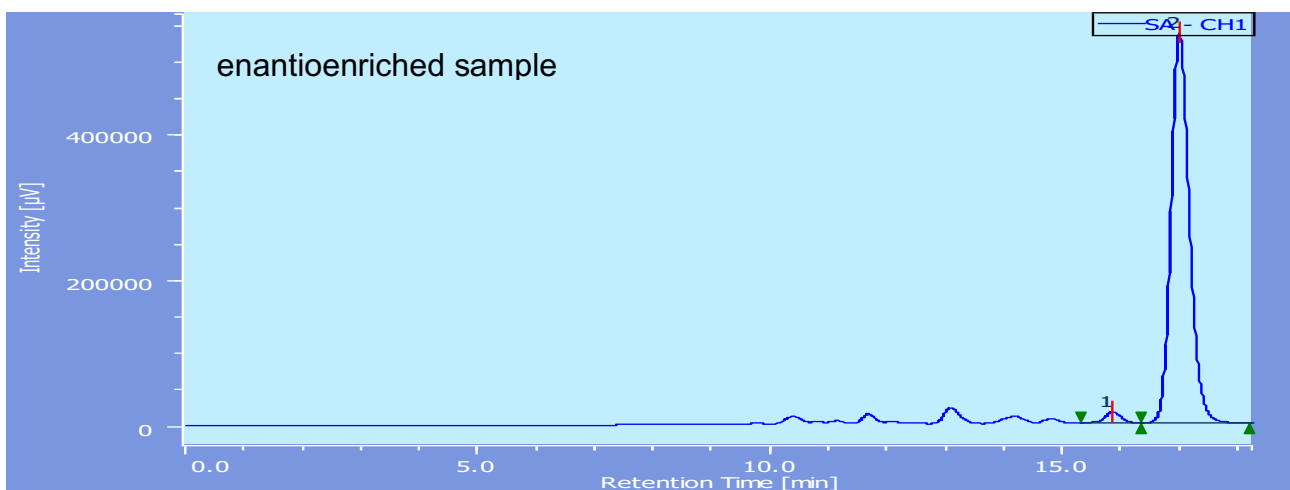
peak	retention time	area	hight	area, %	hight, %
1	19.292	8227189	206487	48.601	52.317
2	20.842	8700948	188198	51.399	47.683



peak	retention time	area	hight	area, %	hight, %
1	20.825	1329447	31711	12.687	14.836
2	22.133	9149491	182036	87.313	85.164



peak	retention time	area	hight	area, %	hight, %
1	14.808	8724701	456075	49.242	50.819
2	15.550	8993172	441371	50.758	49.181



peak	retention time	area	hight	area, %	hight, %
1	15.833	329463	15799	2.722	2.870
2	16.967	11772604	534613	97.278	97.130